An-Najah National University
Faculty of Graduate Studies

Simulation of a Hybrid Power System Consisting of Wind Turbine, PV, Storage Battery and Diesel Generator with Compensation Network: Design, Optimization and Economical Evaluation.

By
Mahmoud Salah Ismail Abdel-Qader

Supervisor
Prof. Dr. Marwan Mahmoud

Submitted in Partial Fulfillment of the Requirements for the Degree of Master in Clean Energy and Energy Conservation Strategy Engineering, Faculty of Graduate Studies, at An-Najah National University, Nablus, Palestine

2008

Simulation of a Hybrid Power System Consisting of Wind Turbine , PV, Storage Battery and Diesel Generator with Compensation Network : Design , Optimization and Economical Evaluation.

By

Mahmoud Salah Ismail

This thesis was defended successfully on 18/12/2008 and approved by:

Committee Member	Signature
1- Prof. Dr Marwan Mahmoud (Supervisor)	.....
2- Dr. Imad Ibrik (Internal Examinar)	.....
3- Dr. Abdel-Karim Daud (External Examinar)	.....

DEDICATION

To the soul of my father…….

To my mother, brothers and sisters...…….

To my wife, daughters, and son…….

To all friends and colleagues…….

To every one works in this field……

To all of them,

I dedicate this work

ACKNOWLEDGMENT

It is an honor for me to have the opportunity to say a word to thank all people who helped me to complete this study, although it is impossible to include all of them here.

My thanks and appreciations go to the staff of Clean Energy and Conservation Strategy Engineering Master Program in An-Najah National University, especially Dr. Imad Ibrik, the director of Energy Research Center, and the coordinator of this master program, for his valuable suggestions and assistance, also for Eng. Mo'ien Omar for his assistance in providing me with useful data from the center.

This project would not have been possible without the endless support and contributions from my family, especially my mother for her kindness, my wife for here encouragement and patient , my brothers and sisters for their support, also from my friends and colleagues for their useful help, and to every one who contribute to complete this effort.

Finally, and most importantly, my furthermost appreciation goes to my supervisor, Prof. Dr. Marwan Mahmoud for his exceptional guidance and insightful comments and observations throughout the duration of this project.

إقرار

أنا الموقع أدناه مقدم الرسالة التي تحمل العنوان:

Simulation of a Hybrid Power System Consisting of Wind Turbine , PV, Storage Battery and Diesel Generator with Compensation Network : Design , Optimization and Economical Evaluation

محاكاة نظام قدرة مهجن مكون من مولد طاقة رياح,خلايا شمسية,بطارية تخزين و مولد ديزل مع شبكة تعويض:تصميم,تحقيق النظام الأمثل و تقييم اقتصادي.

اقر بان ما اشتملت عليه هذه الرسالة إنما هي نتاج جهدي الخاص, باستثناء ما تمت الإشارة إليه حيثما ورد , و إن هذه الرسالة ككل , أو أي جزء منها لم يقدم من قبل لنيل أي درجة علمية أو بحث علمي أو بحثي لدى أي مؤسسة تعليمية أو بحثية أخرى.

Declaration

The work provided in this thesis, unless otherwise referenced, is the researcher's own work, and has not been submitted elsewhere for any other degree or qualification.

Student's Name: Mahmoud Salah Ismail **اسم الطالب**: محمود صلاح اسماعيل

Signature: **التوقيع:**

Date: 18/12/2008 **التاريخ:**

TABLE OF CONTENTS

LIST OF TABLES

LIST OF FIGURES

LIST OF APPENDICES

Abbreviations

ACT	Total Annual Cost
ART	Total Annual Revenue
a-Si	Amorphous-Silicon
BOS	Balance of System
CI(G)S	Copper Indium(Gallium) Diselenide
COE	Cost of Energy
DOD	Depth of Discharge
ELT	Total load Energy
EPBT	Energy Pay Back Time
HAWT	Horizontal Axis Wind Turbine
I_{SC}	Short Circuit Current
kVAR	Kilo Volt Ampere Reactive
kWh	Kilo Watt Hour
LCC	Life Cycle Cost
MPPT	Maximum Power Point
NIS	New Israeli Shekel
NOCT	Normal Operating Cell Temperature
NPV	Net Present Value
PSH	Peak Sun Hour
PV	Photovoltaic
PWF	Present Worth Factor
PWFC	Cumulative Present Worth Factor
PWV	Present Worth Value
rpm	Revolution per minute
SC-Si	Single Crystaline-Silicon
SOC	State of Charge
SOD	Self of Discharge
TSR	Tip Speed Ratio
VAWT	Vertical Axis Wind Turbine
V_{OC}	Open Circuit Voltage
W_p	Watt peak

Simulation of a Hybrid Power System Consisting of Wind Turbine , PV, Storage Battery and Diesel Generator with Compensation Network : Design , Optimization and Economical Evaluation.

By
Mahmoud Salah Ismail

Supervisor
Prof. Dr. Marwan Mahmoud

Abstract

Hybrid power systems based on new and renewable energy sources, especially photovoltaic and wind energy, are an effective option to solve the power-supply problem for remote and isolated areas far from the grids.

Microsoft Excel software programming package is used to analyze data measurements for both wind and solar radiation measurements for the two locations in Palestine (Ramallah and Nablus). Results of analysis illustrate that energy density available in wind for Ramallah site is about 2008 kWh/m^2.year, while it is 927 kWh/m^2.year for Nablus site, and the daily average of solar radiation intensity on horizontal surface is about 5.4 kWh/m^2 .day.

A Matlab software package is used to develop a simulation program to simulate different scenarios of operation of the hybrid system by making energy balance calculations on an hourly basis for each of the 8760 hours in a year and then to choose the appropriate sizes of the different components for the most optimum scenario. The optimization is based on cost of generation.

Results of the simulation illustrate that the most economic scenario is the scenario that uses a hybrid system mainly dependent on wind. Cost of

energy (COE) in this scenario is 1.28 NIS/kWh. Other scenarios dependent on wind-only hybrid system, PV-only hybrid system, wind stand-alone system, PV stand-alone system, or diesel only, give results of COE greater than this value. The amount of CO_2 produced as a result of operation of the wind-PV hybrid system is very small compared with that produced as a result of operation of the diesel only. This is a very important environmental issue that shall be considered and not ignored.

It was concluded that none of the hybrid system scenarios analyzed could presently be justified on COE basis, compared to the alternative of simply purchasing electricity from the grid where the COE is 0.70 NIS/kWh. Considering not electrified far from grid remote areas, changes in electricity prices, subsidy levels, costs for renewable energy equipment, or taking into account environmental considerations might alter the position in the future.

CHAPTER ONE

INTRODUCTION

Chapter 1

Introduction

Hybrid power systems, which combine conventional and renewable power conversion systems are the best solution for feeding the mini-grids and isolated loads in remote areas. Properly chosen renewable power sources will considerably reduce the need for fossil fuel leading to an increase in the sustainability of the power supply. At the same time, conventional power sources aid the renewable sources in hard environmental conditions, which improves the reliability of the electrical system.

Over the present years hybrid technology has been developed and upgraded its role in renewable energy sources while the benefits it produces for power production can't be ignored and have to be considered. Nowadays many applications in rural and urban areas use hybrid systems. Many isolated loads try to adopt this kind of technology because of the benefits which can be received in comparison with a single renewable system.

For the Palestinian case, the daily average of solar radiation intensity on horizontal surface is about 5.4 kWh/m^2 and day, while the total annual sunshine hours amounts to about 3000 [1]. These figures are relatively high and very encouraging to use PV generators for electrification of certain loads as it has been world wide successfully used.

The annual average of wind velocity at different places in Palestine is about 3 m/s which makes the utilization of wind energy converters surely un feasible in such places . In other places it exceeds this number and reaches up

to 5.5 m/s (Al-Mazra'a Al-sharqiyah/Ramallah is an example and it is the case under study in the thesis) which makes it feasible to be used to operate a wind turbine. At Nablus, the annual average of wind velocity reaches to about 4.5 m/s . Nablus site is also considered in this study as a comparison with Ramallah site [2] .

Technically a system which is entirely dependent only on renewable energy sources can not be a reliable electricity supply, especially for isolated loads in remote areas. This is because the availability of the renewable energy sources can not be ensured. Therefore, wind , solar PV hybrid systems, which combine conventional and renewable sources of energies, are a better choice for isolated loads.

A hybrid system using wind , solar PV, diesel generator as a back up system, and a battery as a storage system is expected to: satisfy the load demands , minimize the costs , maximize the utilization of renewable sources, optimize the operation of battery bank, which is used as back up unit , ensure efficient operation of the diesel generator, and reduce the environment pollution emissions from diesel generator if it is used as a stand alone power supply .

The high capital cost of hybrid systems is affected by technical factors such as efficiency, technology, reliability, location, as well as some non-technical factors, so the effect of each of these factors shall be considered in the performance study of the hybrid system.

One of the important factors, which directly affects the electricity cost is correct system-sizing mechanism of the system's components. Over-sizing of components in hybrid system make the system, which is already expensive, more expensive, while under-sizing makes the system less reliable. Thus optimum sizing for different components gives economical and reliable benefits to the system.

The software package developed in this thesis is used to simulate the operation of a system by making energy balance calculations for each of the 8760 hours in a year and then to choose the appropriate sizes of the different components in the system.

The first step in analyzing any hybrid system is to specify the configuration of the system. Chapter 2 in this thesis introduces a general description of the hybrid system: construction, features, and benefits and the block diagram adopted for the hybrid system.

To completely study and analyze any hybrid system, different components constructing the hybrid system shall be studied, identified, specified, and chosen appropriately. Different issues concerning operation, technology, types, specifications and data analysis of both wind and solar radiation measurements are reviewed and studied through chapters 3 and 4 respectively in this thesis . Microsoft Excel software programming package is used to make the wind data analysis required.

A simulation software is developed to analyze the operation of the hybrid system. The first step in developing the software program is to

appropriately mathematically model different components constructing the hybrid system. Chapter 5 in this thesis introduces mathematical modeling and appropriate sizing of all components constructing this hybrid system.

To appropriately analyze different scenarios of the hybrid system, and then to choose the optimal one, an evaluation based on economical analysis shall be done. Chapter 6 in this thesis introduces different economic figures used to compare the different scenarios, also introduces different costs of the components constructing the system.

An initial step in developing the software simulation program is to identify the flowcharts upon which the operation of the hybrid system under different modes and the decision of the energy flow depend. Different flowcharts determining the operation of the hybrid system are presented in chapter 7.

Tables and figures present and illustrate different results of the simulation program for the different scenarios and comparison between results are introduced and presented in chapter 8 in this thesis.

General conclusions and recommendations concerning results of the simulation are introduced and presented in chapter 9 in this thesis.

CHAPTER TWO

HYBRID SYSTEM

Chapter 2

Hybrid System

A hybrid renewable energy system is a system in which two or more supplies from different renewable energy sources (solar-thermal, solar-photovoltaic, wind, biomass, hydropower, etc.) are integrated to supply electricity or heat, or both, to the same demand. The most frequently used hybrid system is the hybrid which consists of Photovoltaic (PV) modules and wind turbines.

Because the supply pattern of different renewable energy sources intermittent but with different patterns of intermittency, it is often possible to achieve a better overall supply pattern by integrating two or more sources. Sometimes also including a form of energy storage. In this way the energy supply can effectively be made less intermittent, or more firm.

Combining renewable hybrid system with batteries as a storage system, to increase duration of energy autonomy, will make optimal use of the available renewable energy resource and this in turn can guarantee high supply reliability. To deal with different weather conditions and to make the system supplies load demand at the worst conditions, this strategy requires large storage capacity and therefore it is very expensive. It is cheaper to supply peaks or to supply demand during periods of cloudy weather or poor wind days with another back up supply (usually diesel generator), although this lowers the proportion of renewable energy used. Selecting appropriate size of the storage system is such that to minimize diesel running time and to maximize fuel savings.

Dump loads are recommended to be used in hybrid power systems as secondary loads to provide a sink for excess renewable generated power to keep power balance of the system at all times, also improve the economic return of the system by allowing excess renewable energy to meet an on-site energy needs that would otherwise have to be met with other energy source.

Optimum match design is very important for PV/wind hybrid system, which can guarantee battery bank working at the optimum conditions as possible as can be, therefore the battery bank's lifetime can be prolonged to the maximum and energy production cost decreased to the minimum. In last few years, some commercial software packages for simulating wind power, PV and hybrid generating systems have been developed. By using computer simulation, the optimum system configuration can be found by comparing the performances and energy production costs of different system configurations. To simulate the practical operating situations of renewable energy systems, many factors need to be considered [3].

2.1 Benefits of a Hybrid System

The main benefits (advantages) of a hybrid system can be summarized as :

- The possibility to combine two or more renewable energy sources, based on the natural local potential of the users.

- Environmental protection especially in terms of CO_2 emissions reduction.

- Low cost – wind energy, and also solar energy can be competitive with

nuclear, coal and gas especially considering possible future cost trends for fossil and nuclear energy.

- Diversity and security of supply.

- Rapid deployment - modular and quick to install.

- Fuel is abundant, free and inexhaustible.

- Costs are predictable and not influenced by fuel price fluctuations although fluctuations in the price of batteries will be an influence where these are incorporated.

2.2 Block Diagram of a Hybrid System

There are many possible configurations of hybrid power systems. One way to classify systems architectures is to distinguish between AC and DC bus systems. DC bus systems are those where the renewable energy components and sometimes even the back up diesel generator feed their power to a DC bus, to which is connected an inverter that supplies the loads. This is for small hybrid systems. Large power hybrid systems use an AC bus architecture where wind turbines are connected to the AC distribution bus and can serve the loads directly.

The configuration used to be evaluated in this thesis has a DC bus which combines the DC output of the PV module, the DC output of the wind turbine, and the battery bank. The AC bus of this configuration combines the output of the bidirectional inverter, the output of the back-up diesel generator

and the load. This parallel configuration, requires no switching of the AC load supply while maintaining flexibility of energy source, but the bidirectional power inverter shall be chosen to deal with this mode of operation. Figure 2.1 illustrates the block diagram of this configuration.

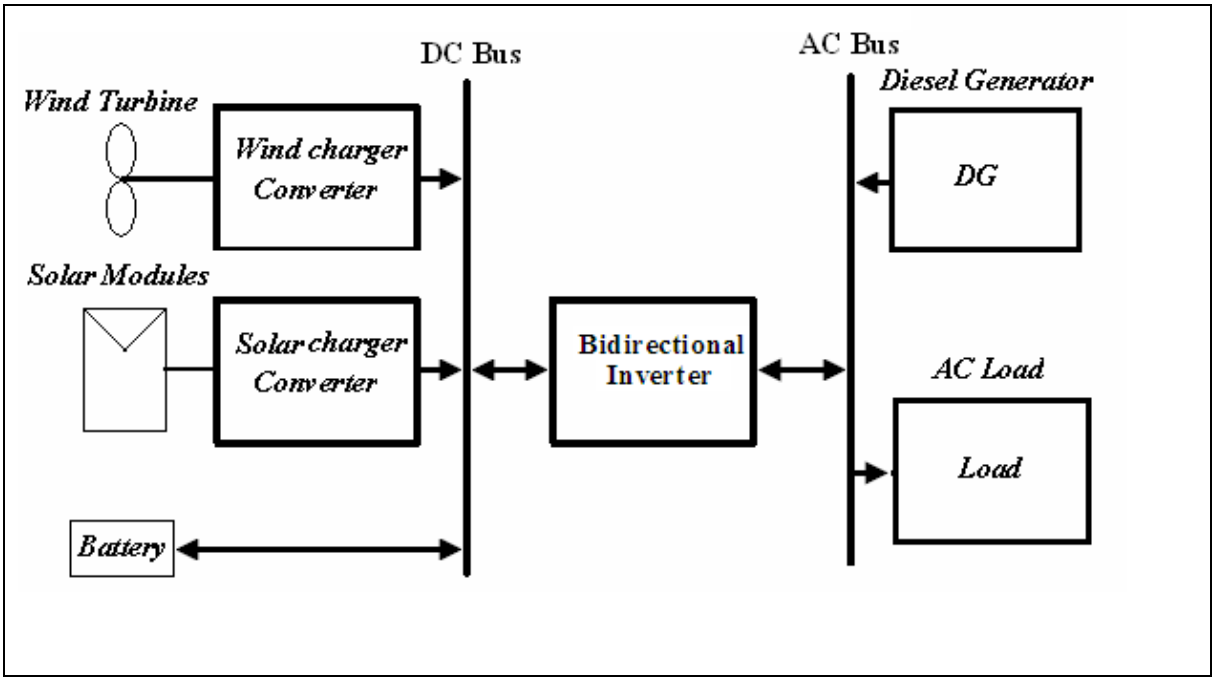

Figure(2.1): Block diagram of the hybrid system.

CHAPTER THREE

WIND ENERGY

Chapter 3

Wind Energy

All renewable energy (except tidal and geothermal power), and even the energy in fossil fuels, ultimately comes from the sun. The sun radiates 174,423,000,000,000 kilowatt hours of energy to the earth per hour. In other words, the earth receives 1.74×10^{17} W of power [4].

Wind energy has been used for thousands of years for milling grains, pumping water and other mechanical power applications . But the use of wind energy as an electrical supply with free pollution what makes it attractive and takes more interest and used on a significant scale .

Attempts to generate electricity from wind energy have been made since the end of nineteenth century . Small wind machines for charging batteries have been manufactured since the 1930s . Wind now is one of the most cost-effective methods of electricity generation available in spite of the relatively low current cost of fossil fuels. The technology is continuously being improved both cheaper and more reliable , so it can be expected that wind energy will become even more economically competitive over the coming decades [5].

3.1 The Earth's Wind Systems

The earth's wind systems are due to the movement of atmospheric air masses as a result of variations in atmospheric pressure, which in turn are the result of differences in the solar heating of different parts of the earths surface.

One square meter of the earths surface on or near the equator receives more solar radiation per year than one square meter at higher latitudes. As a result , the tropics are considerably warmer than the high latitude regions. Atmospheric pressure is the pressure resulting from the weight of the column of the air that is above a specified surface area.

Like all gases, air expands when heated, and contracts when cooled. In the atmosphere, warm air is lighter and less dense than cold air and will rise to high altitudes when strongly heated by solar radiation.

A low pressure belt is created at the equator due to warm humid air rising in the atmosphere until it reaches the top of the troposphere (approximately 10 km) and will spread to the North and the South. This air gradually cools until it reaches latitudes of about 30 degrees, where it sinks back to the surface, creating a belt of high pressure at these latitudes. The majority of the world's deserts are found in these high pressure regions.

Some of the air that reaches the surface of these latitudes is forced back towards the low-pressure zone at the equator, forming what is known "trade winds" .

However, not all of the air that sinks at the 30 degree latitudes moves toward the equator. Some of it moves toward the poles until it reaches the 60 degree latitudes, where it meets cold air coming from the poles. The interaction of the two bodies of air causes the warmer air to rise and most of this air cycles back to the 30 degree latitude regions where it sinks to the surface , contributing to high pressure belt [5].

The remaining of air that rises moves toward poles and sinks to the surface at the poles as it cools. It returns to the 60 degree latitude region.

As the earth is rotating, any movement on the Northern hemisphere is diverted to the right, if we look at it from our own position on the ground. (In the southern hemisphere it is bent to the left). This apparent bending force is known as the Coriolis force. (Named after the French mathematician Gustave Gaspard Coriolis 1792-1843). Figure 3.1 shows the overall pattern of global wind (also known as geostrophic wind) circulation.

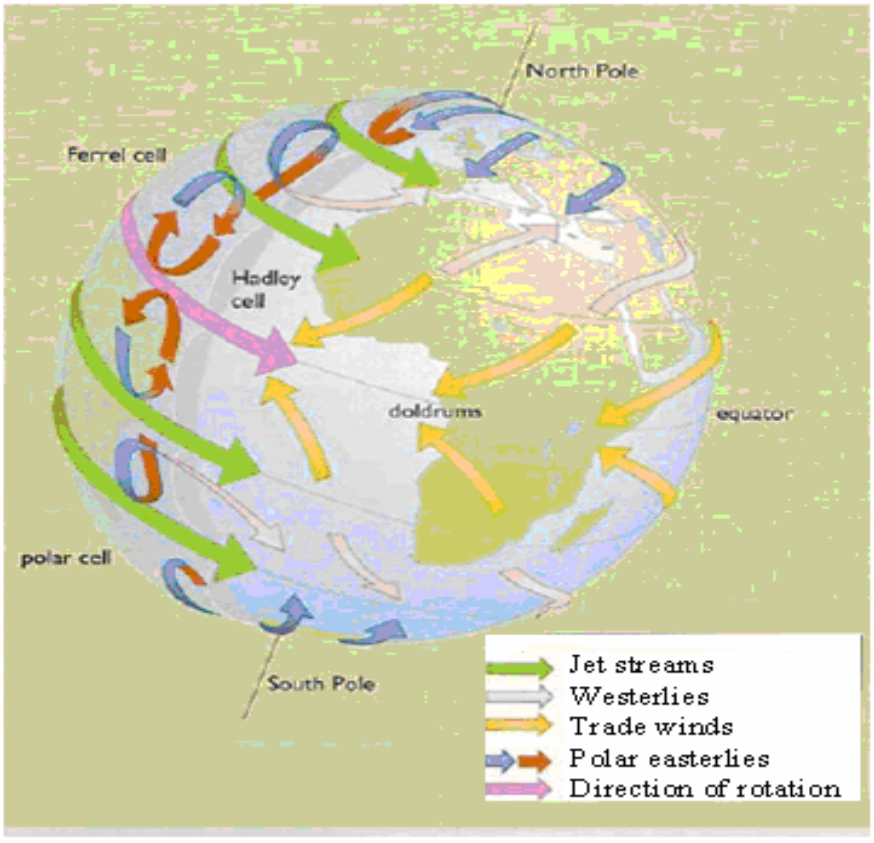

Figure (3.1) : The global wind circulation [5].

As a result of the Coriolis bending force, general results for the prevailing wind directions according to the latitude are presented in table 3.1 [4]:

Table (3.1): Prevailing wind directions**.**

Latitude	90-60°N	60-30°N	30- 0°N	0-30°S	30-90°S	60-90°S
Direction	NE	SW	NE	SE	NW	SE

The prevailing wind directions are important when siting wind turbines, since they must be placed in the areas with least obstacles from the prevailing wind directions.

In addition to the main global wind systems mentioned above there are also local wind patterns, such as sea breezes and mountain valley winds [4].

Land masses are heated by the sun more quickly than the sea in the daytime. The air rises, flows out to the sea, and creates a low pressure at ground level which attracts the cool air from the sea. This is called a sea breeze. At nightfall there is often a period of calm when land and sea temperatures are equal. At night the wind blows in the opposite direction. The land breeze at night generally has lower wind speeds, because the temperature difference between land and sea is smaller at night.

Mountain valley winds are created when cool mountain air warms up in the morning and, as it becomes lighter, begins to rise : cool air from the valley

below then moves up the slope to replace it. During the night the flow reverses, with cool mountain air sinking to the valley [5].

3.2 Wind Turbines

Modern wind turbines come in two basic configurations based on the direction of the rotating shaft (axis): horizontal axis and vertical axis. They range in size from very small machines that produce a few tens or hundreds of watts to very large turbines producing as much as 5 megawatts of power.

3.2.1 Horizontal axis wind turbines

Most wind machines being used today are the horizontal-axis type. Horizontal-axis wind machines have blades like airplane propellers. Horizontal axis wind turbines (HAWTs) predominantly have 2 or 3 blades, or a large number of blades. The later are described as high-solidity devices and include the multi blade wind turbines used for water pumping on farms. In contrast, the swept area of wind turbines with 2 or 3 blades is largely void: only small fraction of this area appears to be solid. These are referred to as low-solidity devices [5].

Rotors of modern low-solidity HAWTs generally have 2 or 3 wing-like blades. They are almost universally employed to generate electricity. Some experimental single-bladed HAWTs have also been produced. Figures 3.2 , 3.3 , 3.4 and 3.5 show different types of HAWTs.

Figure(3.2): 1-blade HAWT from Riva Calzoni, central Italy, 1998.

Figure(3.3): 2-blade HAWT,30 kW, Pitch Wind Systems AB Company (Sweden).

Figure (3.4): 3-blade HAWT,2 MW,Okinawa,New Energy Development Company-(Japan).

Figure(3.5): Multi-blade HAWT, for water pumping, Turpex company , South Africa

3.2.2 Vertical axis wind turbines

Vertical axis wind turbines (VAWTs) have blades that go from top to bottom. The most common types of these turbines are Savonius and one of the most popular in the world market, Darrieus. These turbines can harness winds from any direction without the need to reposition the rotor when the wind direction changes [5].

The blades of a Darrieus VAWT have a curved shape and this likes a shape taken by a spinning rope. This shape is a structurally efficient one, but the unusually shaped blades are difficult to manufacture, transport and install. In order to overcome these problems, straight-bladed VAWTs have been developed: these include the H-type vertical axis and V-type vertical axis wind turbines [5]. Darrieus-type VAWTs and H-type VAWTs are shown in figures 3.6 and 3.7 .

Figure (3.6): A 4 MW, Darreius-type VAWT, Cap Chat, Quebec, late 1990s.

Figure (3.7): A H- type VAWT built in Wales, rated power 130 kW.

VAWTs have a greater solidity than HAWTs, which usually results in a heavier and more expensive rotor. VAWTs are not at economically competitive with HAWTs [5].

3.2.3 Main parts of a wind turbine

A wind turbine consists of the following four main parts: the base, tower, nacelle, and blades, as shown in figure 3.8 . The blades capture the wind's energy and spin a generator in the nacelle. The tower contains the electrical circuits, supports the nacelle, and provides access to the nacelle for maintenance while the base is made of concrete and steel and supports the whole structure.

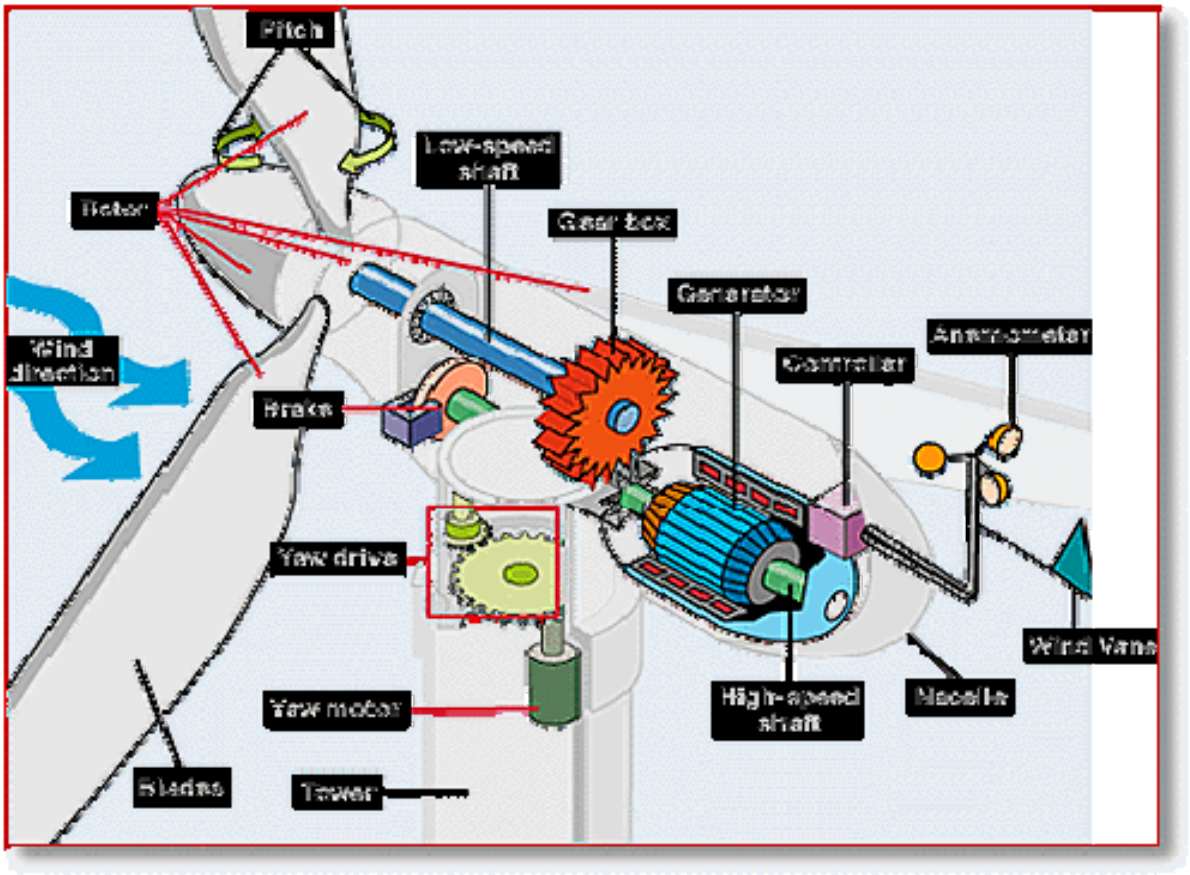

Figure (3.8): Main parts of a wind turbine [6].

3.3 Aerodynamics of Wind Turbines

Wind turbines are operating in an unconstrained air fluid. Force is transferred from air fluid to the blades of the wind turbine . This force can be considered to be equivalent to two component forces acting in two perpendicular directions, known as the drag force and the lift force. The magnitude of these drag and lift forces depends on the shape of the blade, its orientation to the direction of air, and the velocity of air [5].

The drag force is the component that is in line with the direction of air. The lift force is the component that is at right angles to the direction of the air. These forces are shown in figure 3.9.

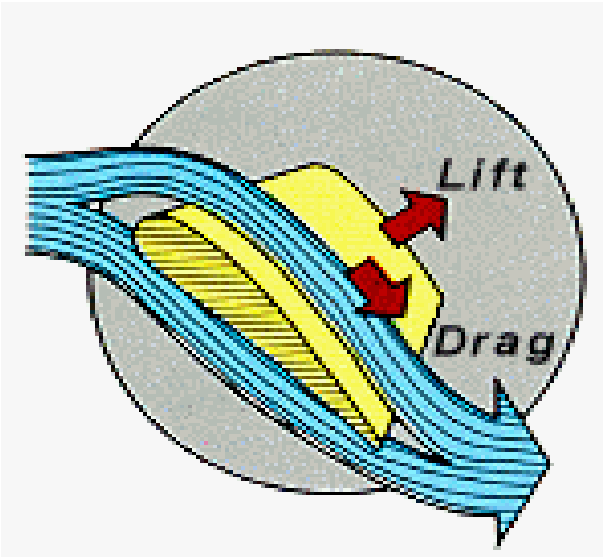

Figure (3.9): Lift and drag force components [7].

A low pressure region is created on the downstream side of the blade as a result of an increase in the air velocity on that side. In this situation, there is a direct relationship between air speed and pressure: the faster the airflow, the lower the pressure. The lift force acts as a pulling force on the blade, in a direction at right angles to the airflow.

Aerofoils:

There are two main types of airfoil section: asymmetrical and symmetrical. Both have a convex upper surface , a rounded end called the leading edge facing the direction from which the air stream is coming, and a sharp end called the trailing edge. The length from the tip of the leading edge to the tip of the trailing edge is known as the cord.

Each aerofoil has an angle of attack at which the lift force is at a maximum compared to drag force. This angle of attack results in the

maximum resultant force and is thus the most efficient setting of the blades of a HAWT.

The wind velocity as seen from a point on a moving blade is known as the relative wind velocity. It represents the resultant vector of the undisturbed wind velocity vector and the tangential velocity vector of the blade at that point on the blade [5].

Most horizontal axis wind turbines operate with their rotation axes in line with the wind direction . The rotation axis is maintained in line with wind direction by a yawing mechanism, which constantly realigns the wind turbine rotor in response to change in wind direction [5].

3.4 Wind Turbine Velocities, Power, and Energy

3.4.1 Velocities, power, and energy available in wind

The speed of rotation of a wind turbine is usually measured in either rotation speed in revolutions per minute (N in rpm) or angular velocity in radians per second (ω in rad/s) **.** The relation ship between the two is given by**:**

$$\omega = 2*\pi*N/60 \qquad (3.1)$$

Another measure of a wind turbine's speed is its tip speed, ν, which is the tangential velocity of the rotor at the tip of the blades measured in meter per second and it equals to:

$$\nu = \omega*r \qquad (3.2)$$

where r is the tip radius in meters.

A non dimensional ratio known as the tip speed ratio (TSR) is obtained by dividing the tip speed, ν, by the undisturbed wind speed, V_o. This ratio which provides a useful measure can be used to compare wind turbines of different characteristics.

$$TSR = \omega * r / V_o \quad (3.3)$$

A wind turbine of a particular design can operate over a range of tip speed ratios, but will usually operate with its best efficiency at a particular tip speed ratio. The optimum tip speed ratio for a given wind turbine rotor will depend upon both the number of blades and the width of each blade [5].

A term describes the percentage of the area of the rotor, which contains material rather than air is known as solidity. Wind turbines with large number of blades have high solidity, but wind turbines with small number of narrow blades have low solidity. Multi blade wind pumps have high solidity rotors and modern electricity generating wind turbines (with one, two or three blades) have low solidity rotors. The turbines with low solidity have to turn much faster than the high solidity turbines in order to interact with all the wind passing through. Optimum tip speed ratios for modern low solidity wind turbines range between about 6 and 20 [5].

The energy contained in the wind is its kinetic energy (E_{Kin}) and it is equal to [5]:

$$E_{Kin} = 0.5 * m * V^2 \quad (3.4)$$

where (m) is the mass of air in kilograms and (V) is speed of air in meters per second. Mass of air flowing through a certain area (A) per second ($\dot{m}$) is:

$$\dot{m} = \rho * A * V \quad (3.5)$$

where ρ is the density of air in kilograms per cubic meter.

So, kinetic energy in the wind per second which is equal to power (P) in the wind in watts is equal to:

$$P = 0.5 * \rho * A * V^3 \quad (3.6)$$

As it is appeared from the power relation, wind speed has a strong influence on power output.

The power contained in the wind is not in practice the amount of power that can be extracted by a wind turbine. This is because losses are incurred in the energy conversion process , also because some of the air is pushed aside by the rotor and by passing it without generating power.

3.4.2 Power and energy produced by a wind turbine

Each wind turbine has its own characteristic known as wind speed power curve. The shape of this curve is influenced by the blades area, the choice of airfoil, the number of blades, the blade shape, the optimum tip speed ratio, the speed of rotation, the cut-in wind speed, the shutdown speed, the rated speed, and gearing and generator efficiencies. The power output of a wind turbine varies with wind speed and wind turbine power curve. An example of such curve is shown in figure 3.10.

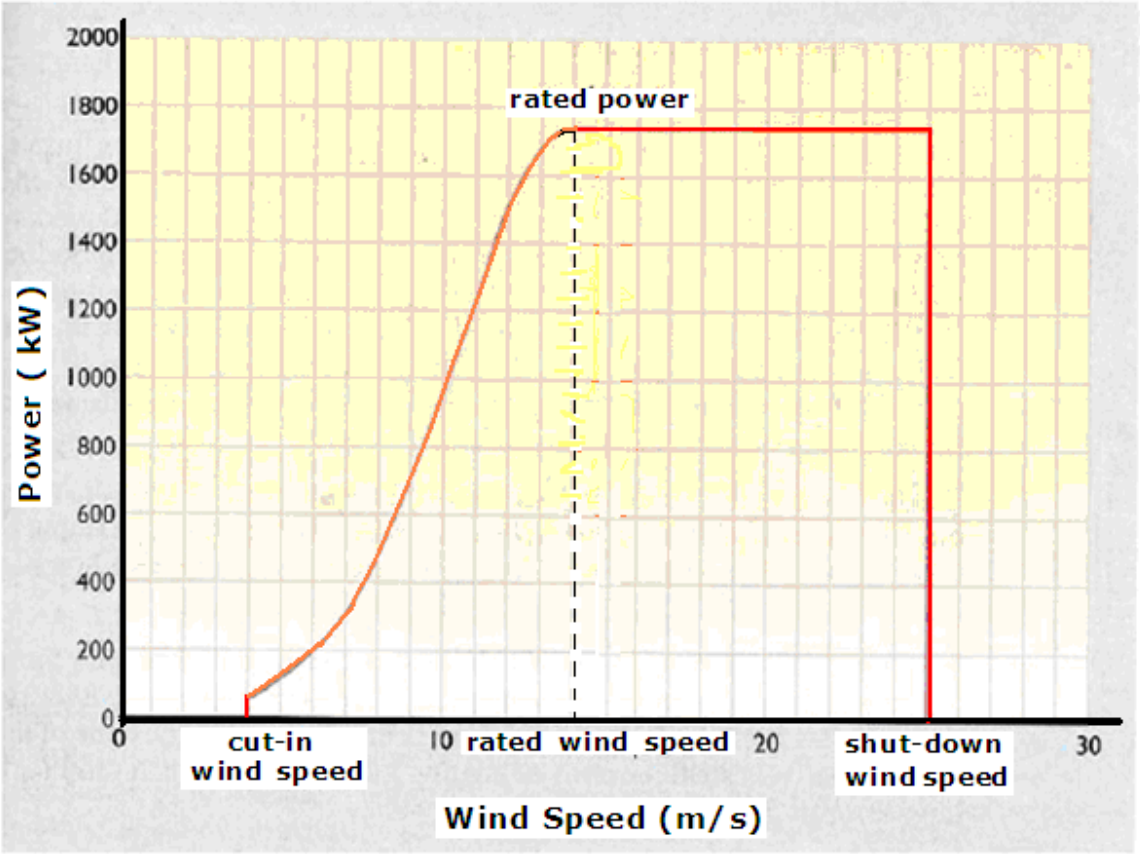

Figure (3.10) : Typical wind turbine power curve [5].

The energy that a wind turbine will produce depends on both its power curve and the wind speed frequency distribution at the site. Wind speed frequency distribution is a graph showing the number of hours for which the wind blows at different wind speeds during a given period of time.

Energy produced at any wind speed can be obtained by multiplying the number of hours of its duration by the corresponding turbine power at this wind speed obtained by the turbine's power curve. The total energy produced is calculated by summing the energy produced at all the wind speeds within the operating range of the turbine.

The best way to determine the wind speed distribution at a sight is to carry out wind speed measurements including record of duration for which the wind speed lies within each wind speed band.

Availability of the turbine is one of the factors that affect the total energy generation. Availability is an indication of the reliability of the turbine installation and is the fraction of a given period of time for which a wind turbine is available to generate, when the wind is blowing within the turbine's operating range. Typical values of annual availabilities exceed 90% [5].

A rough initial estimate of electricity production (in kWh / m²- year) at a certain site is [5] :

$$E_{gen} = K_{WT} * (V_{av})^{3} \quad (3.7)$$

where:

E_{gen} is the annual electrical energy generated by a wind turbine (kWh),

K_{WT} = 3.2 (kg/m/s) is a factor based on typical turbine performance, and

V_{av} is the site average annual wind speed in m/s.

3.4.3 Effect of height on wind speed

The height at which the speed of wind is measured affects the value of the wind speed. As height increases the speed of wind increases, so it is more valuable to increase the height of wind turbine in respect of power that can be captured, but as height increases the initial capital cost of the tower

increases also the maintenance and operation costs increases, so it is a compromise issue.

So when calculating the output of wind generator, the measured data of average hourly wind speed must be converted to the corresponding values at the hub height. The most commonly used formula is power law, expressed as:

$$\frac{V}{V_R} = \left(\frac{Z}{Z_R}\right)^{\alpha} \tag{3.8}$$

where V is wind speed at desired height (Z) ; V_R is wind speed at the reference height (Z_R); α is the ground surface friction coefficient, the one-seventh-power law ratio is used corresponds to most common surfaces[3].

3.5 Wind Speed Distribution

Average value for wind speed for a given location does not alone indicate the amount of energy a wind turbine could produce there. To assess the climatology of wind speeds at a particular location, a probability distribution function is often fit to the observed data. Different locations will have different wind speed distributions. The distribution model most frequently used to model wind speed climatology is a two-parameter Weibull distribution because it is able to conform a wide variety of distribution shapes, from Gaussian to exponential. The Rayleigh model is a specific form of the Weibull function in which the shape parameter(defined later in this section)

equals 2, and very closely mirrors the actual distribution of hourly wind speeds at many locations.

Weibull distribution

The measured wind speed variation for a typical site throughout a year indicates that the strong gale force winds are rare, while moderate and fresh winds are quite common, and this is applicable for most areas. Figure 3.11 shows the Weibull distribution describing the wind variation for a typical site .

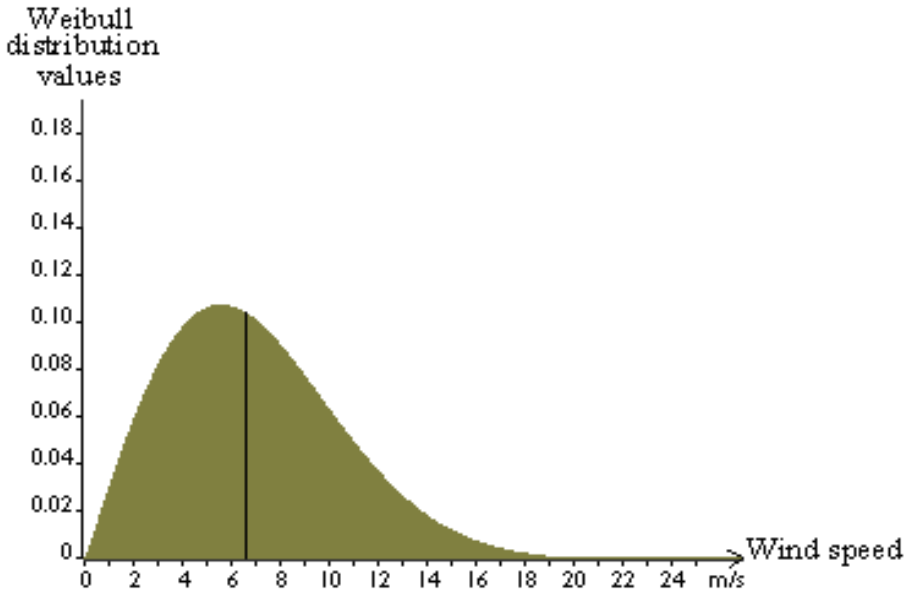

Figure (3.11): Weibull probability density distribution [7].

The area under the curve is always exactly 1, since the probability that the wind will be blowing at some wind speeds including zero must be 100 per cent. The distribution of wind speeds is skewed, i.e. it is not symmetrical. Sometimes there is very high wind speeds, but they are very rare. The statistical distribution of wind speeds varies from place to place around the

globe, depending upon local climate conditions, the landscape, and its surface. The Weibull distribution may thus vary, both in its shape, and in its mean value.

The Weibull probability density distribution function is given by

$$F(v) = K * \frac{v^{(K-1)}}{C^{K}} * e^{-\left(\frac{V}{C}\right)^{K}} \quad \text{.....(3.9)}$$

where

K is the Weibull shape factor, it gives an indication about the variation of hourly average wind speed about the annual average,

C is the Weibull scale factor [7].

Each site has its own K and C , both can be found if the average wind speed V and the available power in wind (flux) are calculated using the measured wind speed values. Graph shown in figure 3.12 gives a relation between the Weibull scale parameter C and average wind speed V as a function of shape parameter K, and the graph shown in figure 3.13 which gives a relation between Weibull scale parameter C and the available power in wind (flux) as a function of shape parameter K . Using these two graphs, beginning from K=2, and manipulating the number of iterations until certain tolerance is achieved, the values of both K and C can be found. The coefficient R is given by the following relation

$$R = \frac{\text{Flux}}{0.5 * \rho * C^{3}} \qquad (3.10)$$

where ρ is the density of air in (kg /m^3).

The following illustrates the way to find values of both C and K:

- For K=2 and from graph in figure (3.12) the corresponding coefficient (V/C) can be read , the scale parameter C is calculated .
- The value of C calculated in the previous step is used to find the coefficient R , and from graph in figure (3.13) , the corresponding new value of K is read .
- For this value of new K the two previous steps are repeated until certain tolerance for both C and K is reached [8] .

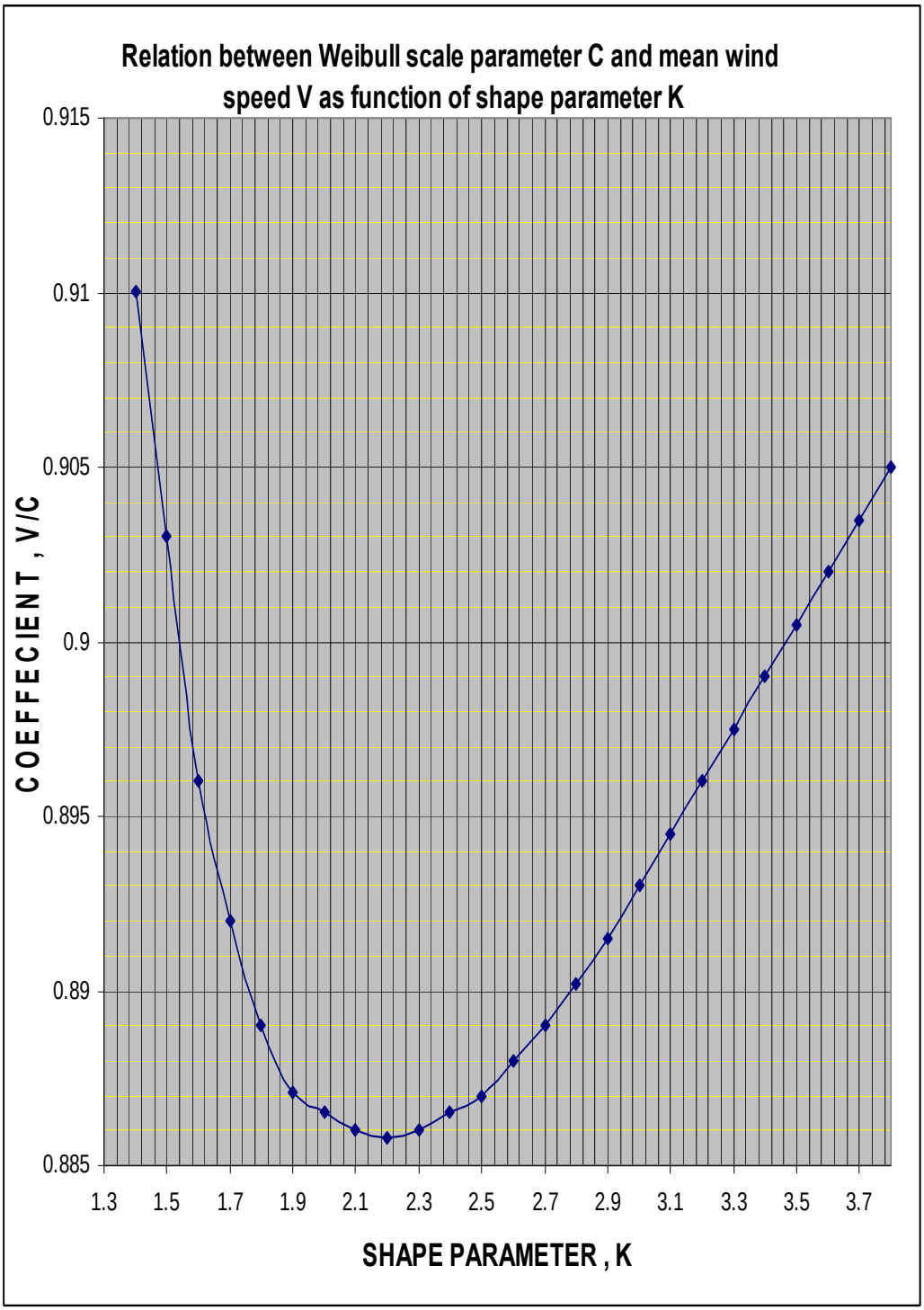

Figure (3.12): Relation between the coefficient V/C and shape parameter K [8] .

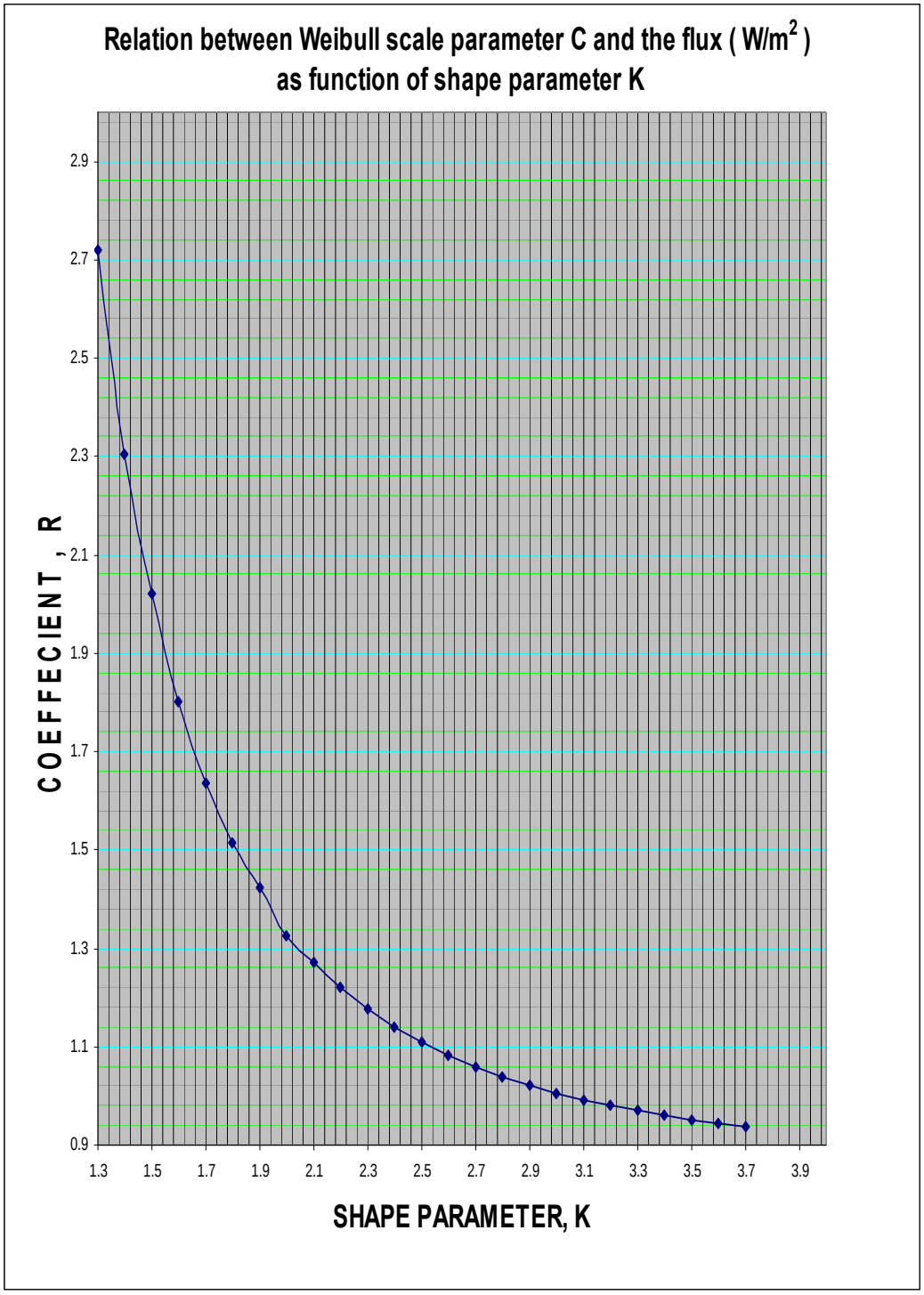

Figure(3.13): Relation between coefficient R and shape parameter K [8].

3.6 Wind Data Calculations for Ramallah & Nablus Sites

Different wind measurements were carried for each month through the year 2006. The wind data obtained includes hourly average wind speeds for each hour in the month [2]. Calculations were performed on these data for each month to obtain the duration in hours for each 1 m/s speed range selected. The total wind speed range was divided into 1 m/s speed ranges taking the ranges: 0-1, 1-2, 2-3, 3-4, and so on.

For each month, average wind speed, percentage of occurrence of each wind speed, power density for each wind speed, Weibull values for each wind speed, energy available in the wind for each wind speed, and the total energy available in wind are calculated. Table 3.2 shows the average wind speed for each month, energy available in the wind for each month. Table 3.3 shows in detail values for percentage of occurrence for each wind speed range , power available in the wind for each range per unit area using equation 3.6, power density by multiplying percentage of occurrence with power available in wind for each range, Weibull values using equation 3.9, energy available in wind by multiplying power density for each range , Weibull value for this range and total hours in year , and finally energy available in wind by multiplying power density for each range , occurrence percentage for this range and total hours in year.

Table (3.2) : Average wind speed for each month/Ramallah

Month	Average wind speed	Energy available in wind(kWh/m²) Using data	Energy available in wind(kWh/m²) Using Weibull
1	**6.74**	**361.71**	**234.71**
2	**6.56**	**229.85**	**164.44**
3	**6.49**	**283.66**	**173.04**
4	**6.75**	**254.52**	**252.30**
5	**4.90**	**100.23**	**200.06**
6	**5.58**	**132.88**	**162.76**
7	**5.83**	**145.49**	**200.49**
8	**5.33**	**104.14**	**126.30**
9	**4.90**	**80.90**	**119.10**
10	**5.21**	**96.46**	**129.33**
11	**3.90**	**125.41**	**145.16**
12	**4.52**	**92.76**	**121.54**
Sum		**2008.02**	**2029.25**

Table (3.3) : Yearly wind calculations/Ramallah

Speed range (m/s)	Mid range (m/s)	Duration (hours)	Occurrence percentage (%)	Power (W/m^2)	Power density (W/m^2)	Weibull values	Energy (kWh/m^2) (using Weibull)	Energy (kWh/m^2) (using data)
0-1	**0.5**	**82**	**0.936**	**0.08**	**0.001**	**0.03601**	**0.02**	**0.01**
1-2	**1.5**	**589**	**6.724**	**2.04**	**0.137**	**0.08230**	**1.47**	**1.20**
2-3	**2.5**	**1058**	**12.078**	**9.45**	**1.142**	**0.11133**	**9.22**	**10.00**
3-4	**3.5**	**1209**	**13.801**	**25.94**	**3.580**	**0.12520**	**28.45**	**31.36**
4-5	**4.5**	**1242**	**14.178**	**55.13**	**7.816**	**0.12616**	**60.93**	**68.47**
5-6	**5.5**	**1240**	**14.155**	**100.66**	**14.248**	**0.11736**	**103.48**	**124.81**
6-7	**6.5**	**961**	**10.970**	**166.15**	**18.227**	**0.10235**	**148.96**	**159.67**
7-8	**7.5**	**728**	**8.311**	**255.23**	**21.211**	**0.08443**	**188.76**	**185.81**
8-9	**8.5**	**563**	**6.427**	**371.55**	**23.879**	**0.06626**	**215.66**	**209.18**
9-10	**9.5**	**390**	**4.452**	**518.71**	**23.093**	**0.04968**	**225.75**	**202.30**
10-11	**10.5**	**218**	**2.489**	**700.36**	**17.429**	**0.03569**	**218.98**	**152.68**
11-12	**11.5**	**159**	**1.815**	**920.13**	**16.701**	**0.02463**	**198.50**	**146.30**
12-13	**12.5**	**103**	**1.176**	**1181.64**	**13.894**	**0.01635**	**169.22**	**121.71**
13-14	**13.5**	**60**	**0.685**	**1488.53**	**10.195**	**0.01046**	**136.34**	**89.31**
14-15	**14.5**	**56**	**0.639**	**1844.42**	**11.791**	**0.00645**	**104.24**	**103.29**
15-16	**15.5**	**28**	**0.320**	**2252.94**	**7.201**	**0.00384**	**75.86**	**63.08**
16-17	**16.5**	**15**	**0.171**	**2717.74**	**4.654**	**0.00221**	**52.70**	**40.77**
17-18	**17.5**	**14**	**0.160**	**3242.42**	**5.182**	**0.00123**	**35.02**	**45.39**
18-19	**18.5**	**10**	**0.114**	**3830.63**	**4.373**	**0.00066**	**22.30**	**38.31**
19-20	**19.5**	**9**	**0.103**	**4486.00**	**4.609**	**0.00035**	**13.64**	**40.37**
20-21	**20.5**	**4**	**0.046**	**5212.15**	**2.380**	**0.00018**	**8.02**	**20.85**
21-22	**21.5**	**7**	**0.080**	**6012.72**	**4.805**	**0.00009**	**4.54**	**42.09**
22-23	**22.5**	**7**	**0.080**	**6891.33**	**5.507**	**0.00004**	**2.47**	**48.24**
23-24	**23.5**	**8**	**0.091**	**7851.61**	**7.170**	**0.00002**	**1.30**	**62.81**
Sum		**8760**	**100%**		**229.225**	**1.00328**	**2025.85**	**2008.01**

Yearly average wind speed V= 5.521 m/s
Weibull shape factor K = 1.81(calculated using graphs in figures 3.12,3.13)
Weibull scale factor C = 6.35 m/s(calculated using graphs in figures 3.12,3.13)
Density of air ρ = 1.21 kg/m^3

Figure 3.14 shows a graphical representation of monthly average wind speed for each month in the year, while figure 3.15 shows a graphical representation of the distribution of hourly duration for different ranges of wind speed.

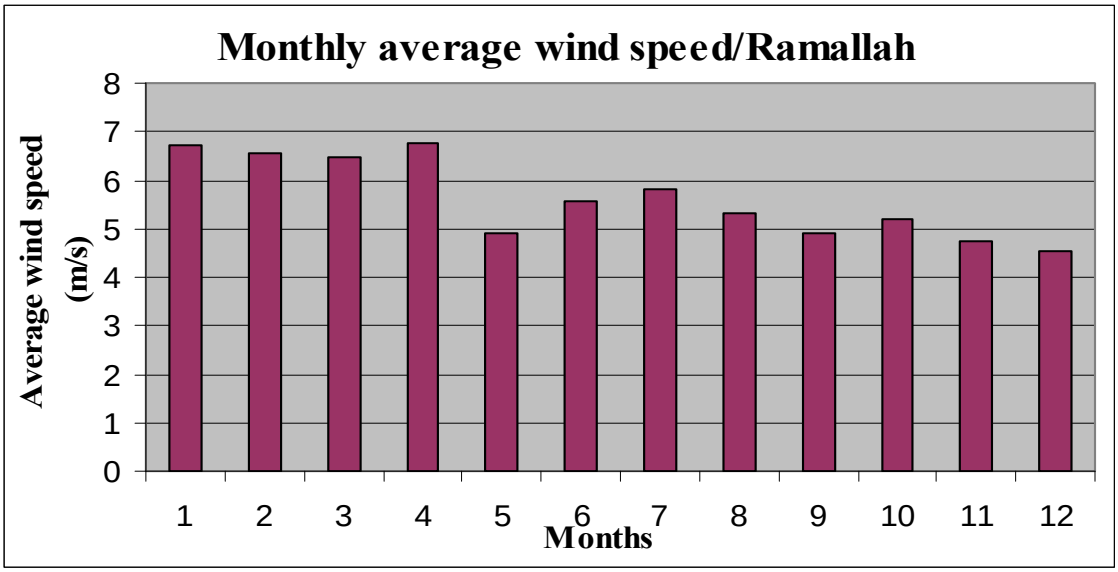

Figure (3.14): Monthly average wind speed for Ramallah site

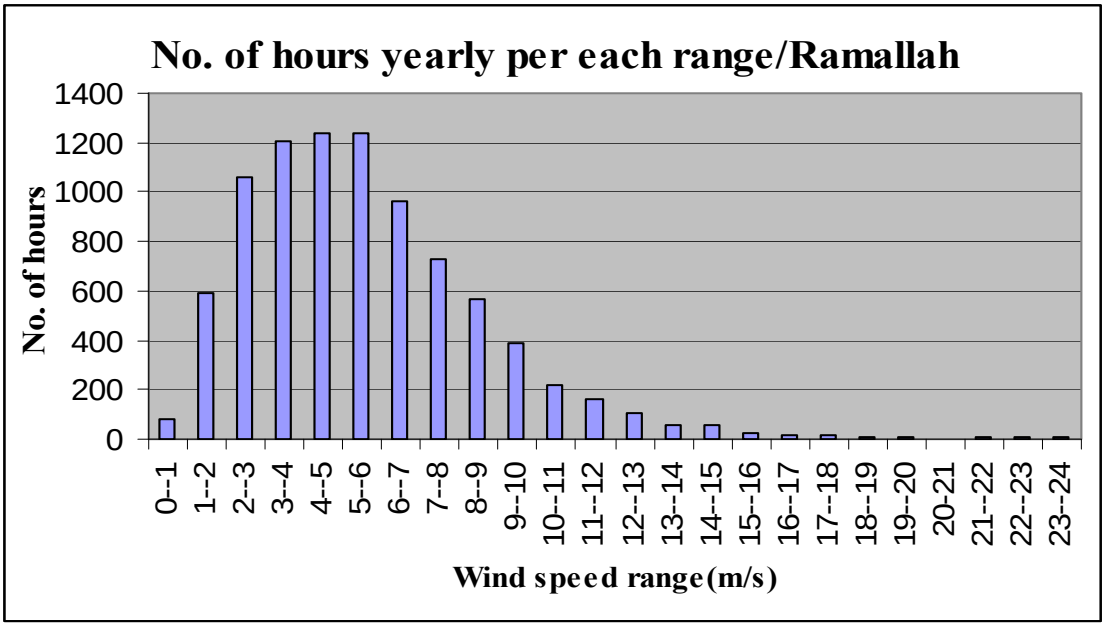

Figure (3.15): Number of hours per year for each wind speed range/Ramallah

Figure 3.16 shows the distribution of energy and Weibull distribution for the wind measurements.

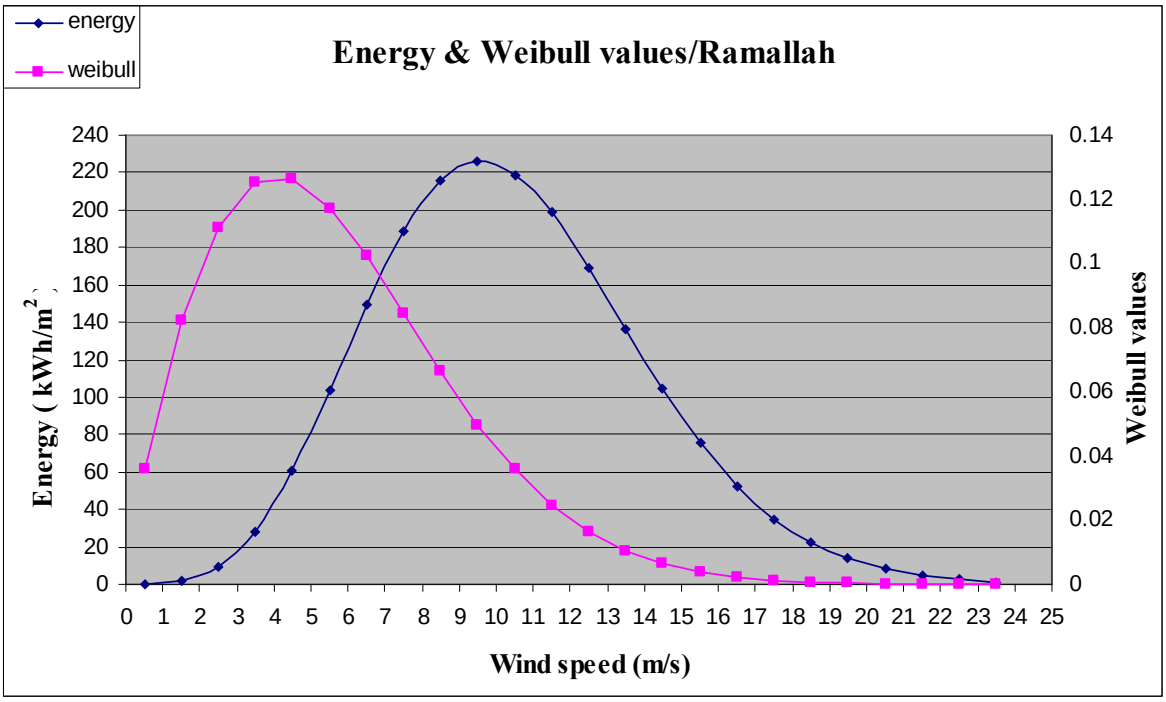

Figure (3.16): Yearly energy and Weibull distributions/Ramallah site

Figure 3.17 shows the wind duration curve for Al-Mazra'a Al-Sharqiyyah site. It is a cumulative frequency diagram, its horizontal axis represents the cumulative time duration in hours as wind speed group decreases starting at the highest wind speed group. It can be used to calculate graphically the energy produced by a certain wind turbine if its power curve is known.

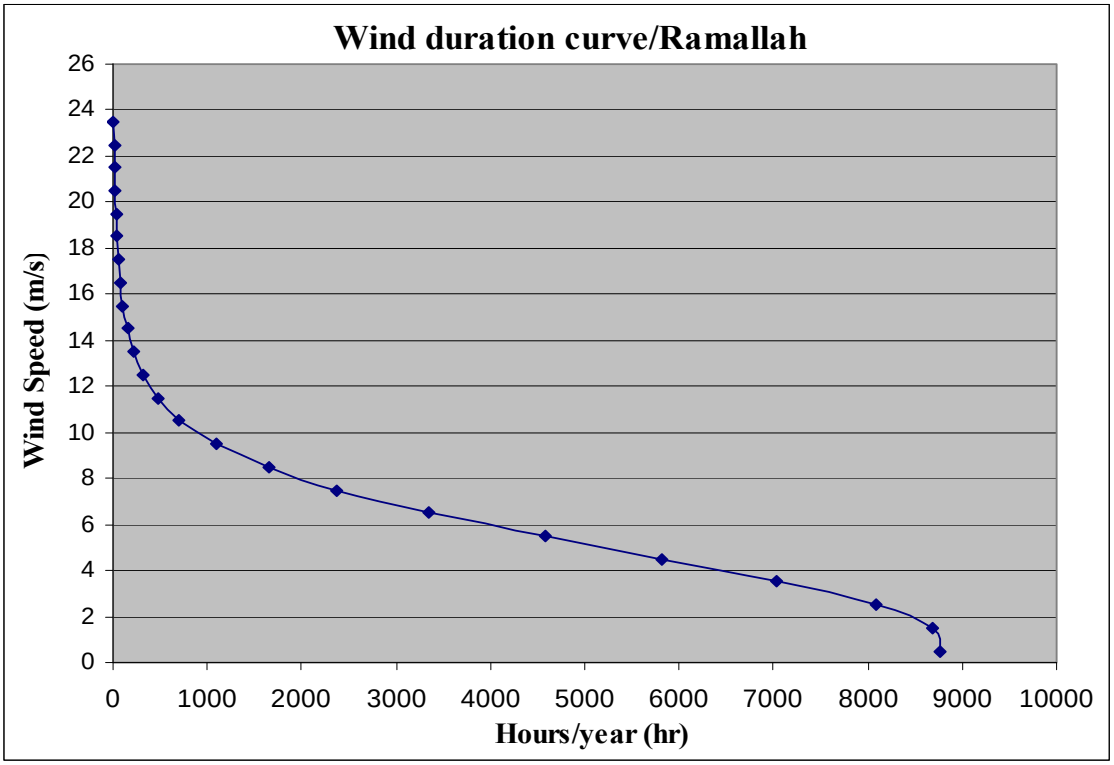

Figure (3.17) : Wind duration curve for Ramallah site

Figures (3.18) , (3.19) show yearly energy , Weibull values and yearly wind duration curve for Nablus site respectively. For Nablus site, table 3.4- as table 3.3 before - shows: percentage of occurrence for each wind speed range , power available in wind for each range per unit area, power density, Weibull values, energy available in wind using Weibull values , and finally energy available in wind using wind data available.

Table (3.4): Yearly wind calculations/Nablus

Speed range (m/s)	Mid range (m/s)	Duration (hours)	Occurrence percentage (%)	Power (W/m²)	Power density (W/m²)	Weibull values	Energy (kWh/m²) (using Weibull)	Energy (kWh/m²) (using data)
0-1	**0.5**	**733.68**	**8.375**	**0.08**	**0.006**	**0.05334**	**0.03**	**0.06**
1-2	**1.5**	**376.64**	**4.300**	**2.04**	**0.088**	**0.12065**	**2.08**	**0.77**
2-3	**2.5**	**1105.78**	**12.623**	**9.45**	**1.193**	**0.15541**	**12.90**	**10.45**
3-4	**3.5**	**1786.15**	**20.390**	**25.94**	**5.289**	**0.16174**	**37.70**	**46.33**
4-5	**4.5**	**1802.06**	**20.572**	**55.13**	**11.341**	**0.14702**	**73.62**	**99.35**
5-6	**5.5**	**1285.92**	**14.679**	**100.66**	**14.776**	**0.12044**	**110.12**	**129.44**
6-7	**6.5**	**788.24**	**8.998**	**166.15**	**14.950**	**0.09039**	**135.01**	**130.97**
7-8	**7.5**	**440.14**	**5.024**	**255.23**	**12.824**	**0.06274**	**141.05**	**112.34**
8-9	**8.5**	**205.65**	**2.348**	**371.55**	**8.723**	**0.04054**	**128.66**	**76.41**
9-10	**9.5**	**101.65**	**1.160**	**518.71**	**6.019**	**0.02450**	**104.17**	**52.73**
10-11	**10.5**	**55.81**	**0.637**	**700.36**	**4.462**	**0.01389**	**75.74**	**39.09**
11-12	**11.5**	**25.93**	**0.296**	**920.13**	**2.724**	**0.00741**	**49.87**	**23.86**
12-13	**12.5**	**9.67**	**0.110**	**1181.64**	**1.304**	**0.00372**	**29.94**	**11.42**
13-14	**13.5**	**5.17**	**0.059**	**1488.53**	**0.878**	**0.00177**	**16.47**	**7.69**
14-15	**14.5**	**2.83**	**0.032**	**1844.42**	**0.597**	**0.00079**	**8.33**	**5.23**
15-16	**15.5**	**8.17**	**0.093**	**2252.94**	**2.100**	**0.00034**	**3.89**	**18.40**
16-17	**16.5**	**3.83**	**0.044**	**2717.74**	**1.189**	**0.00014**	**1.68**	**10.42**
17-18	**17.5**	**0.83**	**0.010**	**3242.42**	**0.308**	**0.00005**	**0.67**	**2.70**
18-19	**18.5**	**0.67**	**0.008**	**3830.63**	**0.292**	**0.00002**	**0.25**	**2.55**
19-20	**19.5**	**0.50**	**0.006**	**4486.00**	**0.256**	**0.00001**	**0.09**	**2.24**
20-21	**20.5**	**1.00**	**0.011**	**5212.15**	**0.595**	**0.00000**	**0.03**	**5.21**
21-22	**21.5**	**7.83**	**0.089**	**6012.72**	**5.377**	**0.00000**	**0.01**	**47.10**
22-23	**22.5**	**0.67**	**0.008**	**6891.33**	**0.524**	**0.00000**	**0.00**	**4.59**
23-24	**23.5**	**11.17**	**0.127**	**7851.61**	**10.009**	**0.00000**	**0.00**	**87.68**
Sum		**8760**	**100.00**		**105.824**	**1.00490**	**932.33**	**927.02**

Yearly average wind speed V= 4.346 m/s
Weibull shape factor K = 1.9(calculated using graphs in figures 3.12,3.13)
Weibull scale factor C = 6 m/s(calculated using graphs in figures 3.12,3.13)
Density of air ρ = 1.21 kg/m³

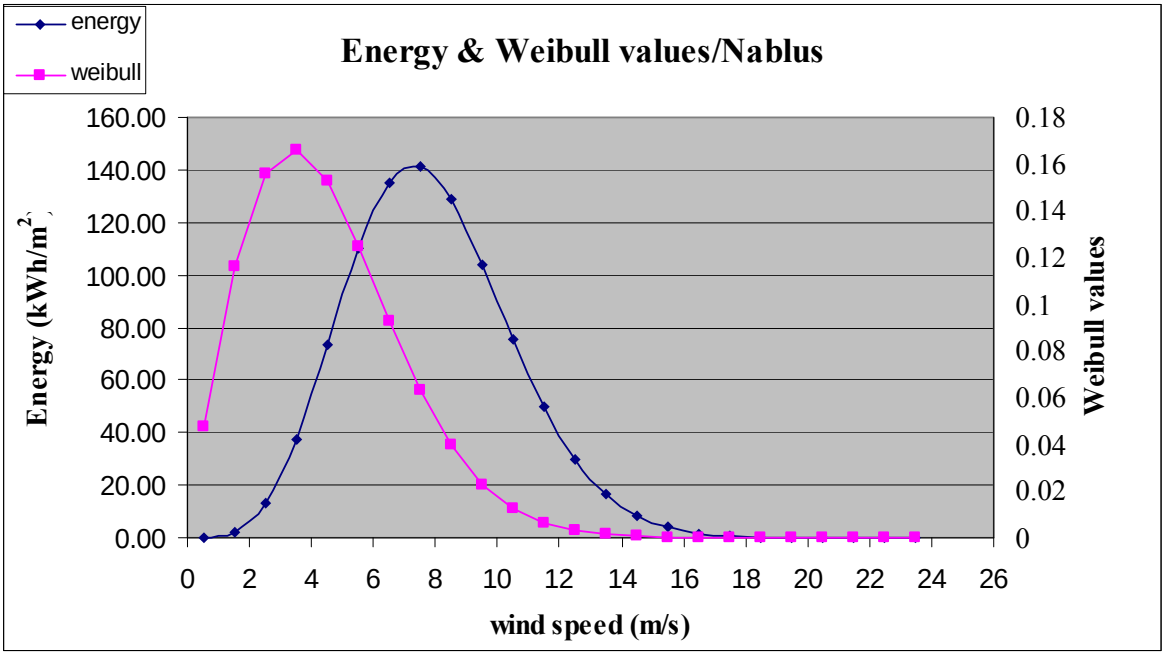

Figure (3.18): Yearly energy and Weibull distributions for Nablus site

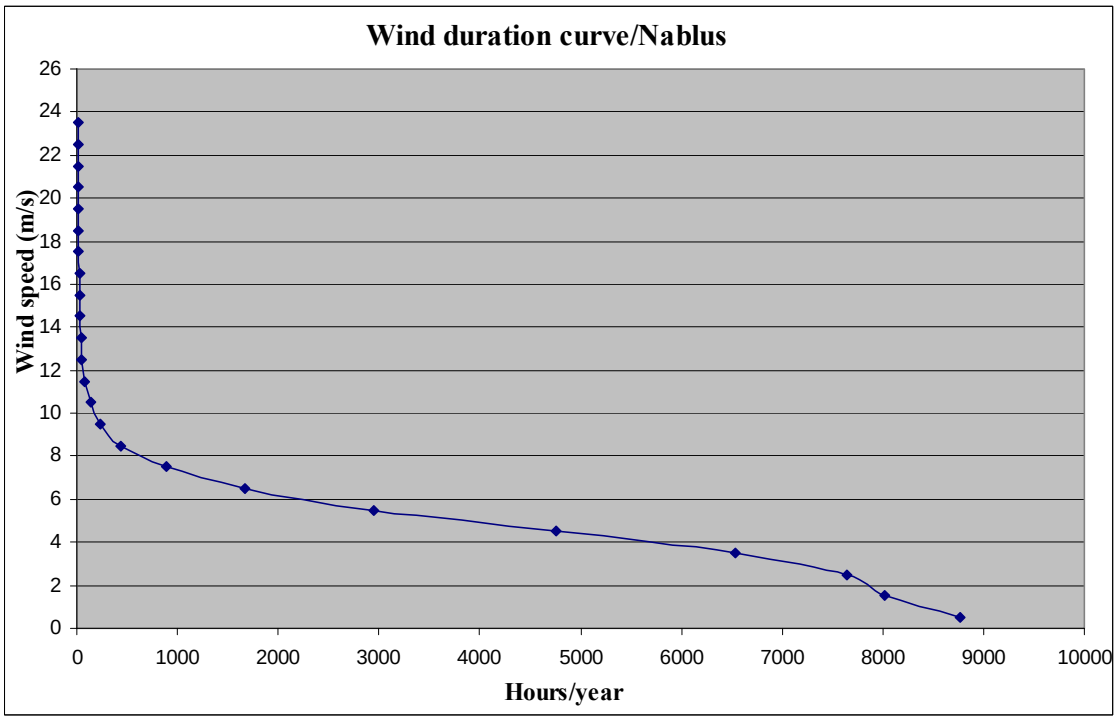

Figure (3.19) : Wind duration curve for Nablus site

CHAPTER FOUR

PHOTOVOLTAIC TECHNOLOGY

Chapter 4

Photovoltaic Technology

The sun is the largest energy source of life while at the same time it is the ultimate source of most of renewable energy sources. Solar energy can be used to generate electricity in a direct way with the use of photovoltaic modules. Photovoltaic is defined as the generation of electricity from light where the term photovoltaic is a compound word and comes from the Greek word for light, photo, with, volt, which is the unit of electromotive power. The technology of photovoltaic cells was developed rapidly over the past few decades. Nowadays the efficiency of the best crystalline silicon cells has reached 24% for photovoltaic cells under laboratory conditions and for that used in aerospace technology and about 14-17% overall efficiency for those available commercially while modules costs dropped to below 4$ per watt peak (4$/$W_P$) [5].

4.1 Solar Cells: Construction and Operation

4.1.1 Photovoltaic construction

A solar cell is considered the basic part in the photovoltaic system, it is a device that converts light energy into electrical energy by the photovoltaic effect. Solar cells are often electrically connected and encapsulated as a module. PV modules often have a sheet of glass on the front (sun up) side , allowing light to pass while protecting the semiconductor wafers from the elements (rain, hail, etc.). Solar cells are also usually connected in series in

modules, creating an additive voltage. Connecting cells in parallel will yield a higher current. Modules are then interconnected, in series or parallel, or both, to create an array with the desired peak DC voltage and current.

PV cells consist basically of a junction between two thin layers of semi conducting materials, known as p (positive) type semiconductors and n (negative) type semiconductors. The p-type semiconductor is created when some of the atoms of the crystalline silicon are replaced by atoms with lower valence like boron which causes the material to have a deficit of free electrons. The n-type semiconductor is created when some of their atoms of the crystalline silicon are replaced by atoms of another material which has higher valence band like phosphorus in such a way that the material has a surplus of free electrons.

The photovoltaic cell consists of 6 different layers of materials as shown in figure 4.1 .

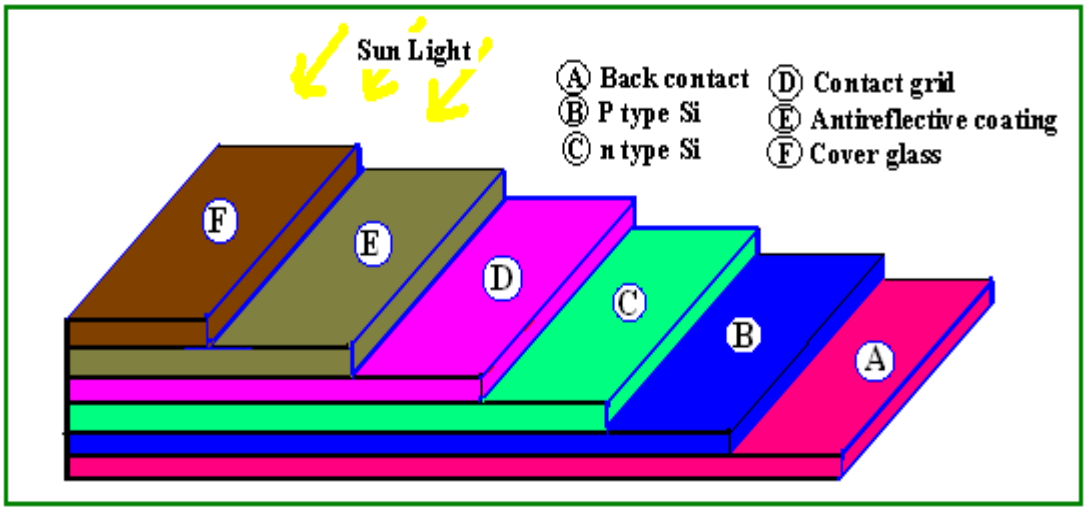

Figure(4.1): Silicon PV cell construction

4.1.2 Photovoltaic operation

When the photovoltaic cell becomes exposed to the light beam which consists of photons, the electrons are stimulated. The electrons start moving rapidly, jump into the conduction band and they leave holes in the valence band. Some of the electrons are attracted from n-side to combine with holes on the nearby p-side. Similarly, holes on the near p-side are attracted to combine with the electrons on the nearby n-side. The flow of the electrons from one semiconductor to the other creates the electric current into the photovoltaic cell.

If a variable load is connected through the terminals of the PV cell, the current and the voltage will be found to vary. The relationship between the current and the voltage is known as the I-V characteristic curve of the PV cell. The I-V curve for a typical silicon PV cell under standard conditions is shown in figure 4.2.

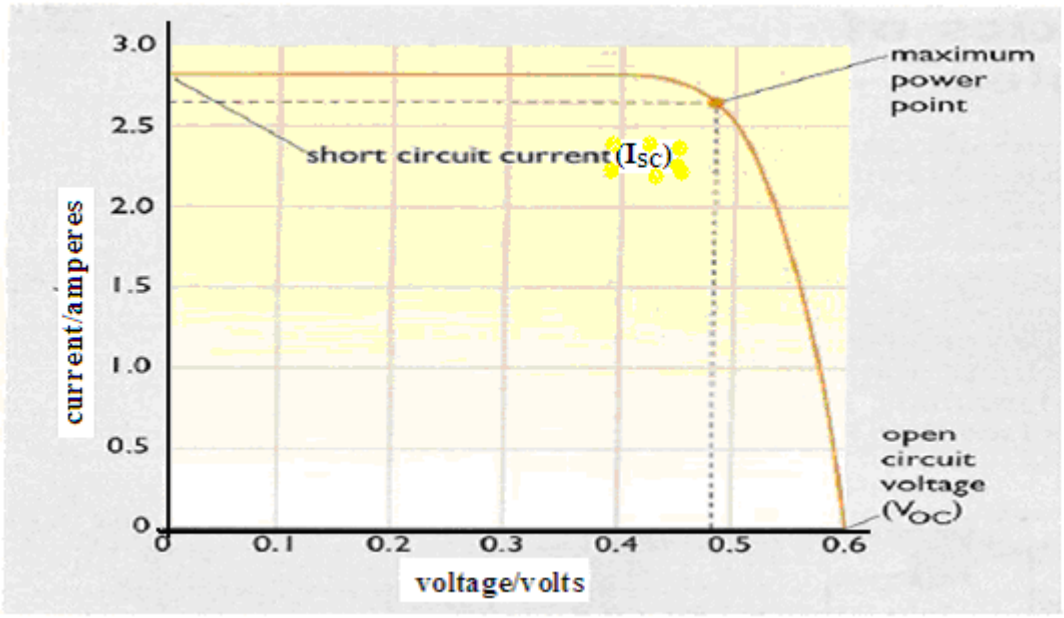

Figure (4.2): I-V characteristic curve of a typical Si cell [5].

To measure the I-V characteristic of a PV cell and to find the maximum power point, an international standard conditions shall be fulfilled. These standard conditions are: irradiance level that shall be 1000 W/m², the reference air mass that shall be 1.5 solar spectral irradiance distribution, and cell or module junction temperature that shall be of 25°C [5].

Open circuit voltage (V_{OC}) is the voltage appears across the terminals of the PV cell when it is open circuited, while short circuit current (I_{SC}) is the current passes through the short circuit when the terminals of the PV cell are short circuited. The term fill-factor is defined as the ratio between the maximum power delivered by the PV cell and the product of open circuit voltage and the short circuit current of the cell.

The cell will deliver maximum power at maximum power point (MPPT) on the I-V characteristic curve which represents the largest area of the rectangular under the I-V characteristic. A technique to utilize effectively the photovoltaic is known as a maximum-power- point tracking (MPPT) method, which makes it possible to acquire as much power as possible from the photovoltaic, this is accomplished by a built in circuit in the charger controller or in the inverter circuit following the PV module.

The efficiency of a solar cell is defined as the power P_{max} produced by the cell at MPPT divided by the power of radiation incident upon it [8].

4.1.3 Photovoltaic mathematical modeling

The equivalent circuit diagram of an ideal solar cell is shown in Figure 4.3.

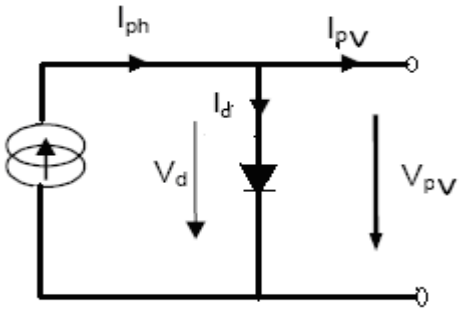

Figure (4.3): Equivalent circuit of an ideal solar cell

The mathematical function of an ideal illuminated solar cell is given in the following equation [9] :

$$I_{PV} = I_{Ph} - I_d = I_{Ph} - I_o * \left(e^{\frac{q V_d}{K_B T}} - 1 \right) \qquad (4.1)$$

where:

I_{PV} : load current [A]

I_{Ph} : photon current which represents the short circuit current I_{sc} [A]

I_o : saturation current [A]

q : electron charge [$e = 1.602*10^{-19}$ C]

$\mathbf{V_d}$: which represents the PV voltage (V_{PV}) [V]

$\mathbf{K_B}$: Boltzmann constant [$1.38*10^{-23}$ J/K]

T : diode absolute temperature [°K]

4.1.4 Temperature and solar radiation effects on PV performance

The two most important effects that must be considered are due to the variable temperature and solar radiation. The effect of these two parameters must be taken into account while sizing the PV system.

Temperature effect: This has an important effect on the power output from the cell. The temperature effect appears on the output voltage of the cell, where the voltage decreases as temperature increases. This decrease for silicon cell is approximately 2.3 mV per 1°C increase in the solar cell temperature.

The solar cell temperature T_c can be found by the following equation [9]:

$$T_C = T_{amb} + \left(\frac{NOCT-20}{800}\right)*G \qquad (4.2)$$

where:

T_{amb} : ambient temperature in °C

G : solar radiation in W/m²

NOCT : Normal Operating Cell Temperature which is defined as the cell temperature when the module operates under the following conditions at open circuit:

Solar radiation : 800 W/m²

Spectral distribution : AM1.5

Ambient temperature : 20 °C

Wind speed : > 1 m/s

Solar radiation effect: The solar cell characteristics are affected by the variation of illumination. Increasing the solar radiation increases in the same proportion the short circuit current. The following equation illustrates the effect of variation of radiation on the short circuit current:

$$I_{sc}(G) = I_{sc}(\text{at } 1000 \text{ W/m}^2) * (G \text{ (in W/ m}^2) / 1000) \quad (4.3)$$

The output power from the PV cell is affected by the variation of cell temperature and variation of incident solar radiation. The maximum power output from the PV cell can be calculated using the following equation [8]:

$$P_{out\text{-}pv} = P_{r\text{-}pv} * (G/G_{ref}) * [\, 1 + K_T (T_c - T_{ref}) \,] \quad (4.4)$$

where :

$P_{out\text{-}pv}$: output power from the PV cell

$P_{r\text{-}pv}$: rated power at reference conditions

G : as defined before

G_{ref} : solar radiation at reference conditions (G_{ref} =1000 W/ m²)

T_c : cell temperature, calculated using equation (4.2)

T_{ref} : cell temperature at reference conditions (T_{ref} = 25 °C)

K_T : temperature coefficient of the maximum power

($K_T = -3.7 * 10^{-3}$ / 1°C for mono and poly crystalline Si)

The following equation can be used to calculate the cell temperature approximately if the NOCT is not given by the manufacturer [8]:

$$T_C = T_{amb} + 0.0256 * G \quad (4.5)$$

where T_c, T_{amb}, and G are as defined before.

4.1.5 Effect of tilting the PV panels on the total solar radiation collected

Measurements of solar radiation usually occur on a horizontal plane. PV panels are usually fixed making a tilt angle (β) with the horizontal. This is done to make the PV panels facing the sun to collect more solar radiation. Value of this tilt angle depends mainly on latitude value of the location (L) and seasonal changes. PV panels may be fixed with a not changing tilt angle or may be changed seasonally to collect more solar radiation. These changes are as follows [10]:

- $\beta = L + 20^{o}$ during winter season.
- $\beta = L$ during spring and autumn seasons.
- $\beta = L - 10^{o}$ during summer season.

If these changes are made, a yearly increase in solar radiation by a value of 5.6% can be obtained [10]. For Palestine (especially Ramallah & Nablus sites) latitude (L) is about 32^{o} .

PV panels can be fixed facing directly geographic south or fixed so that the normal of the tilted panel makes an angle with the geographical south. This angle is called azimuth angle (a_w). This will also affect the collected solar radiation.

The value of solar radiation is not only affected by the previous mentioned factors but also affected by the solar time (t_s) during a day and the number of this day during the year(N) .

A mathematical model developed by Liu & Jordan in 1960 is used to calculate the total instantaneous or hourly solar radiation on a tilted surface at certain location (G_T) if solar radiation on a horizontal surface (G_H) is measured at this location. This model is as follows [8]:

$$G_T = G_b * \cos(i) + G_d * \cos^2(\beta/2) + G_H * \rho_r * \sin^2(\beta/2) \quad (4.6)$$

where ρ_r is effective diffused ground reflection index, G_b is beam radiation collected by the PV module and can be calculated as follows:

$$G_b = 1800 * K_H - 520 \quad \text{if} \quad 0.3 \leq K_H \leq 0.85 \text{ and otherwise } G_b = 0 \quad (4.7)$$

where K_H can be calculated as follows:

$$K_H = (G_H / G_{Ho}) \quad (4.8)$$

where G_{Ho} can be calculated as follows:

$$G_{Ho} = 1353 * [\ 1 + 0.034 * \cos(\ N * 360 / 365\ )\ ] * \sin(\alpha\ ) \quad (4.9)$$

where α is the solar altitude angle that describes the angle measured between a line from the observer's position to the sun and the horizon, and can be calculated as follows:

$$\alpha = \sin^{-1}[\ \sin(\delta_s) * \sin(L) + \cos(\delta_s) * \cos(L) * \cos(H_s)\ ] \quad (4.10)$$

where δ_s is the solar declination angle that represents the angular position of the sun north or south of the earth's equator and H_s is the solar hour angle that takes zero value when the sun is straight overhead,

negative before local noon and positive in the afternoon. δ_s and H_s can be calculated as follows:

$$\delta_s = 23.45 * \sin [360 * (N + 284)/ 365] , \quad (4.11)$$

$$H_s = 15 * (t_s - 12) \quad (4.12)$$

where t_s as indicated before is solar time in military hours.

In equation (4.6) , the angle i is the angle of incidence that represents the angle between the solar radiation beam and the normal to a surface and can be calculated as follows:

$$i = \cos^{-1}[\cos (a_s - a_w) * \cos (\alpha) * \sin (\beta) + \cos (\beta) * \sin(\alpha)] \quad (4.13)$$

where a_s is the azimuth angle of the sun that represents the angle between the true south and the horizontal projection of the line from the observer's position and the sun and can be calculated as follows:

$$a_s = \sin^{-1}[-1 * \sin(H_s) * \cos(\delta_s) / \cos(\alpha)] \quad (4.14)$$

In equation (4.6) , the diffused radiation part G_d that collected by the PV module can be calculated as follows:

$$G_d = G_H - G_b * \sin(\alpha) \quad (4.15)$$

4.2 Solar Radiation in Palestine

Solar radiation data during a year are very important and essential for design and sizing of PV power systems. Solar radiation measurements in

addition to temperature measurements are necessary to calculate the output power of the PV system. Solar radiation and temperature measurements shall be available on hourly basis to be used by the simulation program for the evaluation process. Solar radiation and temperature measurements are complete and available for Nablus site. For Ramallah site the temperature measurements are not available, so Nablus data are used by the simulation program to evaluate both Nablus and Ramallah sites.

Table 4.1 presents the monthly average of daily solar radiation for different months for Nablus site, while figure 4.4 illustrates a graphical representation for these averages.

Table(4.1): Monthly average of daily solar radiation for Nablus site [2].

Month	**Monthly average solar radiation (kWh/m^2-day)**
1	2.89
2	3.25
3	5.23
4	6.25
5	7.56
6	8.25
7	8.17
8	8.10
9	6.30
10	4.70
11	3.56
12	2.84

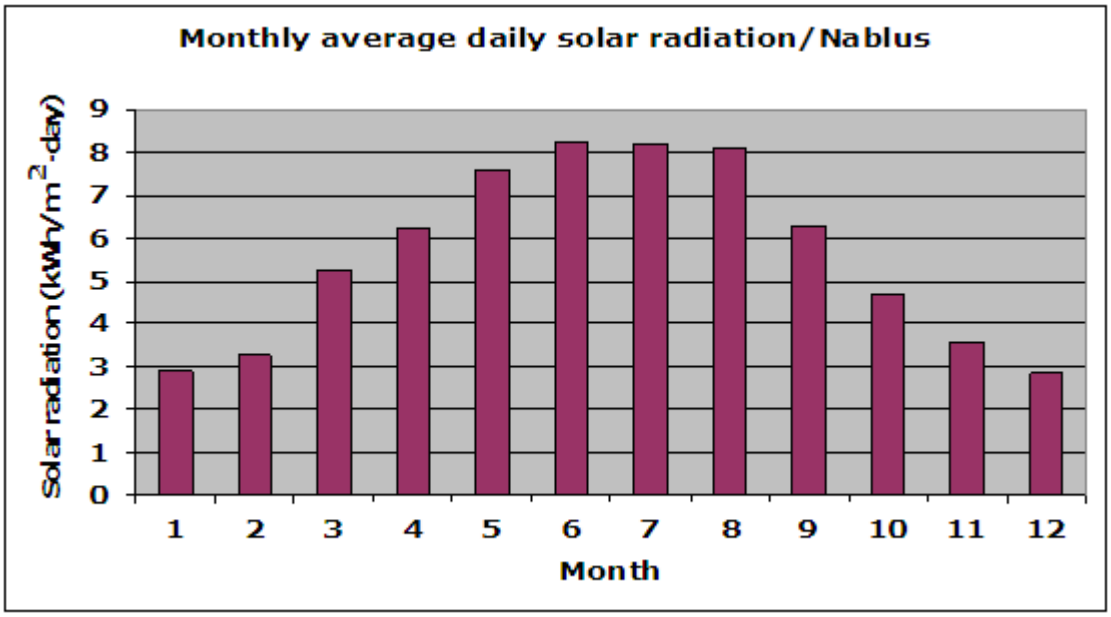

Figure (4.4): Monthly average daily solar radiation for Nablus site [2].

4.3 Main PV Cell Types

The material that is widely used in the industry of PV cells is silicon. Silicon can be found inside the sand in the form of silicon oxide (SiO2). Depending on the structure of the basic material from which PV cells are made and the particular way of their preparation, PV cells can mainly be categorized as follows [11]:

1. Mono-crystalline: The efficiency of a single crystal silicon cell varies between 13-16% and it is characterized by a high cost for its manufacture and has a dark blue color.

2. Poly-crystalline: Its efficiency varies between 10-14% and it is characterized by lower cost silicon which is used for its manufacture and has light blue color.

3. Amorphous (non crystalline) silicon: This type of photovoltaic cells achieves maximum efficiency not more than 10%. Production cost is much cheaper than what is for the previous two types. Its efficiency degrades with time.

Other types of PV cells use other materials or compounds rather than silicon. Other innovative PV technologies use multi-junction, silicon spheres, or photo electrochemical in manufacturing the PV cells [5].

4.4 PV Solar Cell Technology

In contrast to widely-used electricity generation technologies, photovoltaic (PV) systems produce little or no environmental pollution at the point of use. However, there are numerous materials and energy inputs that go into the fabrication of the components of PV systems that may carry significant environmental burdens.

4.4.1 Recent technology in manufacturing PV modules

Crystalline silicon was the original materials technology used by the PV industry to manufacture solar cells. First widely used in space satellites, conventional crystalline silicon solar cells are fabricated in a step-and-repeat, batch process from small wafers of single crystal or polycrystalline silicon semiconductor materials. Although, substantial advances have been made in the development of this technology, the cost of crystalline PV modules is still high because of materials costs and numerous processing steps that are needed

to manufacture the modules. Crystalline silicon solar modules are bulky, break easily, and consume more energy in manufacturing.

A major cost limitation of the current dominant silicon solar cell technologies, which are fabricated using traditional crystalline and polycrystalline silicon based processes, is with the large volume of material used and the associated expensive assembly and interconnection methods required to produce the large area products required for substantial power generation.

For the past 15 years a new kind of PV has emerged based on thin-film semiconductors deposited on a variety of substrates. The most common of these thin films currently in use is amorphous silicon (a-Si). The PV cells built from it are invariably less efficient than crystalline PV, but thin film PV counters this with a host of advantages including relatively low cost of manufacture, flexibility and savings on materials. The last of these factors has proved especially importance, since there has been an ongoing shortage of silicon that has plagued the industry [12].

Silicon is not the only thin-film material that can be used for PV. Other materials that have been researched or actually deployed include gallium arsenide (GaAs), copper indium (gallium) diselenide (CIS or CIGS) , and cadmium telluride (CdTe) where each has its advantages and disadvantages. Although these materials are typically being used in conjunction with relatively complex manufacturing processes with deposition at its core, there is also growing interest in creating lower cost thin film PV using printing technology combined with silicon or organic inks [12].

Amorphous silicon PV modules were the first thin-film PV modules to be commercially produced and are presently the only thin-film technology that has had an impact on the overall PV markets. However, the efficiencies of these modules have not yet reached levels that were predicted in the 1980's. To a significant degree this is due to the intrinsic degradation of a-Si under illumination. The amount of light-induced degradation can be limited to 20% in modules operating under outdoor conditions. Both material processing schemes and device design schemes have been developed to improve the stabilized solar cell efficiency of a-Si solar cells. The use of multi-band gap multi junction devices (allowing the use of thinner absorber layers in the component cells) and the use of light-trapping appear to be the most powerful device design techniques to improve stabilized device performance. Presently, champion cells have stabilized efficiencies of 12% and champion modules have stabilized efficiencies of over 10% [13].

The industry is currently using two approaches to build a-Si-based modules. Substrate type devices are built on stainless steel foil while superstrate type devices are built on glass coated with transparent conductors. However, the goal for all high efficiency a-Si device designs is maximizing the optical enhancement (light trapping) and minimizing the light-induced degradation [13].

4.4.2 Energy payback of PV cells

There is a significant energy input needed for manufacturing PV equipment. This manufacturing energy input has been reduced during the

research and development (R&D) efforts of the past decades, although there is still room for considerable improvements.

A common method used to express economic costs of electricity-generating systems is to calculate a price per delivered kilowatt-hour (kWh). The solar cell efficiency in combination with the available irradiation has a major influence on the costs, but generally speaking the overall system efficiency is important. Using the commercially available solar cells and system technology leads to system efficiencies between 5 and 19%. According to publications in 2005,[14], photovoltaic electricity generation costs ranged from ~0.60 US$/kWh (central Europe) down to ~0.30 US$/kWh in regions of high solar irradiation. This electricity is generally fed into the electrical grid on the customer's side of the meter .

Another approach to look on the energy cost production of PV modules, the environmental effects while manufacturing PV modules, the amount of energy required during manufacturing PV modules, and comparison between different technologies in manufacturing PV modules, is to calculate the energy payback time of a module. The energy payback time is one standard of measurement adopted by several analysts to look at the energy sustainability of various technologies. It is defined as the time necessary for a photovoltaic module to generate the amount of energy used to produce it.

The energy payback time of a photovoltaic cell is an indication about the energy required to make a cell compared to how much it could generate in its lifetime. The energy payback time of a modern photovoltaic module is anywhere from 1 to 20 years (usually under five) depending on the type and

where it is used . This means that solar cells can be net energy producers, meaning that they generate more energy over their lifetime than the energy expended in producing them [15].

Parameters determine the energy payback time for a PV module are: manufacturing technology used to produce PV panel, the amount of illumination that the system received, and the conversion efficiency of the PV system. The energy needed to produce a product includes both the energy consumed directly by the manufacturer during processing, and the energy embodied in the incoming raw materials.

How a PV module is used is primarily a question of location and module efficiency. Location determines the solar solar radiation, and combined with efficiency, determines the electrical output of the PV module. But installation details are important too (fixed tilt or tracking, grid-connected or stand-alone, etc.), as are balance of system requirements such as mounting structure, inverter, and batteries [16].

The module energy payback time (EPBT) is computed using this formula [16] :

$$EPBT = \frac{E_S}{E_g} \qquad (4.16)$$

where E_S : Specific energy (kWh_e / kW_p) for production of PV module.

$\dot{E}_g$: Energy generation rate (kWh / kW_p- year), this corresponds to peak sun hours (PSH) of the location where the PV module is installed multiplied by number of days in a year.

As it is obvious from equation (4.16) , a location with higher solar radiation , or a module with lower energy requirements or higher efficiency, reduces the payback time.

Payback for crystalline-silicon PV systems:

Most solar cells and modules sold today are crystalline silicon. Both single-crystal and multicrystalline silicon use large wafers of purified silicon. Purifying and crystallizing the silicon are the most energy-consumptive parts of the solar-cell manufacturing process. Other aspects of silicon cell and module processing that add to the energy input include: cutting the silicon into wafers, processing the wafers into cells, assembling the cells into modules (including encapsulation), and overhead energy use for the manufacturing building.

One of the key contributors to the energy payback field is the Dutch researcher Eric Alsema, whose work is recent, comprehensive, and clear on methodology and data. To calculate payback, Alsema reviewed previous energy analysis and did not charge for the energy that originally went into crystallizing microelectronics scrap. His best estimates of energy used to make near-future, frameless PV were 600 kWh/m^2 for single crystal- silicon modules and 420 kWh/m^2 for multicrystalline silicon. Assuming 12%

conversion efficiency (at standard conditions) and 1700 kWh/m^2 per year of available sunlight energy, Alsema(1998) calculated a payback of about 4 years for current multicrystalline-silicon PV systems. Projecting 10 years into the future, he assumes a solar grade silicon feedstock and 14% efficiency, dropping energy payback to about 2 years [17].

Other recent calculations generally support Alsema's figures. Based on a solar-grade feedstock, Japanese researchers Kazuhiko Kato calculated a multicrystalline payback of about 2 years. Palz and Zibetta also calculated energy payback of about 2 years for current multicrystalline silicon PV. In (2000) Knapp and Jester studied an actual manufacturing facility and found that, for single-crystal-silicon modules, the energy payback time was 3.3 years. This includes the energy to make the aluminum frames and purify and crystallize the silicon, but does not appear to include the energy input for the BOS components such as inverters, wiring and mounting structures. The additional energy payback time for the BOS is estimated to be about a half a year [17].

For single-crystal silicon - which Alsema did not calculate - Kato calculated payback of 3 years when he did not charge at all for off-grade feedstock.

Payback for thin-film PV systems:

Thin-film PV modules use very little semiconductor material. The major energy costs for manufacturing are the substrate on which the thin films are deposited, the film-deposition process, and facility operation. These

energy costs are similar for all thin-film technologies (copper indium deselenide, cadmium telluride, amorphous silicon), varying only in the film deposition processes themselves, so amorphous silicon is a representative technology [17].

Alsema estimated that it takes 120 kWh/m^2 to make near-future, frameless, amorphous silicon PV modules. He added another 120 kWh/m^2 for a frame and a support structure for a rooftop-mounted, grid-connected system. Assuming 6% conversion efficiency (standard conditions) and 1700 kWh/m^2 per year of available sunlight energy, Alsema calculated a payback of about 3 years for current thin-film PV systems. Kato and Palz calculated shorter paybacks for amorphous silicon, each ranging from 1-2 years [17].

Deleting the frame, reducing use of aluminum in the support structure, and assuming a conservative increase to 9% efficiency and other improvements, Alsema projected the payback for thin-film PV ten years from now to drop to just 1 year [17].

These figures are for rooftop systems. Support structures for ground-mounted systems-as might be found more advantageous for central utility generation-would add about another year to the payback period [17].

A study carried out by Alsema (2000) to find the energy requirement for different types of PV modules led to the results as shown in table 4.2. Estimates for module efficiencies and energy consumption in frameless module production for the future years are also presented in this table. The energy requirement per watt will be reduced also as the module efficiencies

rise . Aluminum frames would add another 400 MJ/m^2 (corresponds to 111.1 kWh/ m^2),which represents some 10-25% of the total energy investment [18].

Of the estimated 1200 MJ/m^2 (corresponds to 333.3 kWh/ m^2)required for the production of frameless amorphous silicon modules, the cell material represents only 4% [18].

With a typical lifetime of 25 to 30 years, this means that modern solar cells are net energy producers, i.e they generate much more energy over their lifetime than the energy expended in producing them.

Table (4.2) : Module efficiencies and energy consumption for (frameless) PV module manufacturing (source Alsema 2000).

Present		2010	2020
Single crystal silicon (Sc-Si)			
Module efficiency (%)	14	16	18
Energy consumption (MJ/m^2)	5700	3200	
Energy consumption (MJ/Wp)	41	20	
Energy consumption (kWh/Wp)	11.4	5.55	
Multi-crystalline silicon (Mc-Si)			
Module efficiency (%)	13	15	17
Energy consumption (MJ/m^2)	4200	2600	
Energy consumption (MJ/Wp)	32	17	13
Energy consumption (kWh/Wp)	8.9	4.7	3.6
Thin-film			
Module efficiency (%)	7	10	15
Energy consumption (MJ/m^2)	1200	900	
Energy consumption (MJ/Wp)	17	9	5-6
Energy consumption(kWh/Wp)	4.7	2.5	1.4-1.7

For Palestinian case where total solar radiation is 5.4 kWh/m^2-day which corresponds to 1971 kWh/m^2-year, and according to the information in table 4.2 at year 2000, the EPBT for single crystal silicon – by using equation 4.16 - is about 5.78 year, the EPBT for multi-crystalline silicon is about 4.5 year, and the EPBT for thin-film is about 2.4 year.

According to information presented in this table, module efficiency will increase , specific manufacturing energy and therefore the EPBT will decrease for the next years from year 2000. These figures are predicted because of advance in technology and manufacturing processes in this field. A recent study – that presented later in this chapter - carried by Alsema (2006) illustrates this.

Figure 4.5 below shows lines of constant energy payback for both crystalline and thin-film technologies at different locations (different solar radiations). For the two types of Siemens PV modules—single-crystalline silicon (SC-Si) and thin film copper indium diselenide (CIS) examined, the results are indicated by horizontal lines on this graph. For crystalline silicon (SC-Si) module which has a specific energy (E_S) about 5600 kWh_e /kW_p and indicated by a horizontal line and at a location with 1700 kWh/m^2-year solar radiation that indicated by a vertical line, the two lines crosses at a point located on approximately the 3.3-year constant energy payback line. This means that EPBT for these types of modules is about 3.3 years. Following the same procedure the EPBT for thin film copper indium diselenide (CIS) module in full production which has a specific energy (E_S) about 3100 kWh_e /kW_p is just under two years and it about 1.8 years [16] .

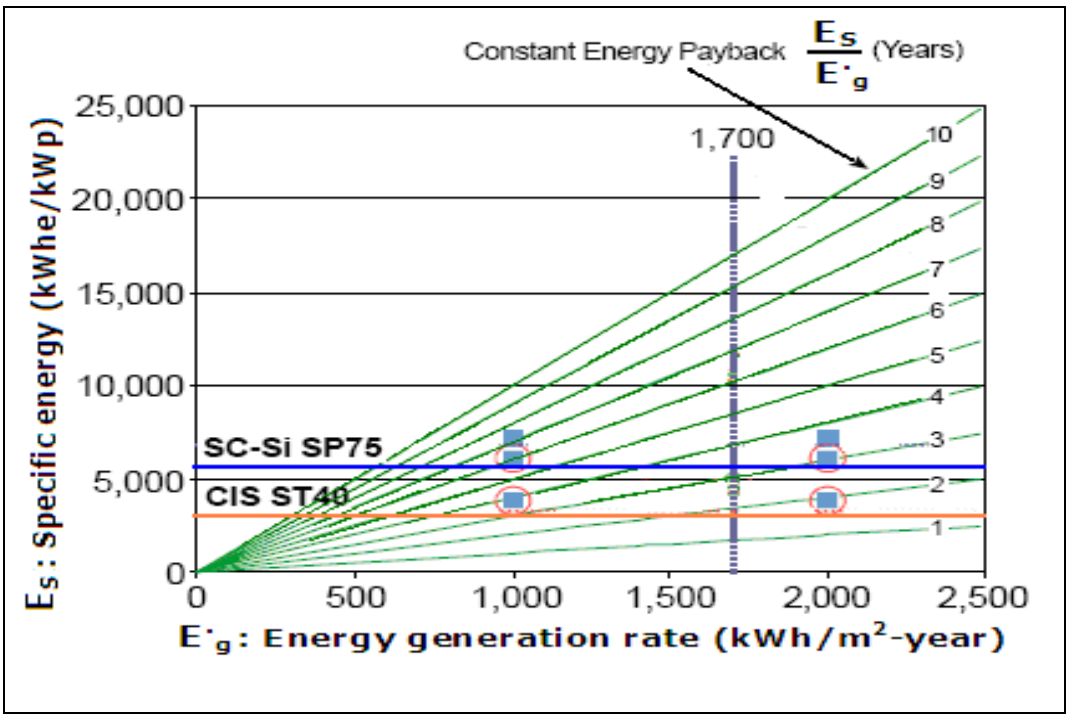

Figure (4.5) : Energy payback time for different production & different locations [16].

Figure 4.6 below shows a detailed description for the energy requirement to manufacture the two types of PV modules under test and the total energy required for the manufacturing. For crystalline silicon (SC-Si) module which has a specific energy (E_S) about 5600 kWh_e /kW_p and an EPBT of 3.3 year as indicated before, 51% of the total energy required for manufacturing is for preparing the materials required for the manufacturing. These materials include direct materials that are part of the finished product, such as silicon, glass, and aluminum. They also include indirect materials that are used in the process but do not end up in the product, such as solvents, argon, or cutting wire. The remaining energy required which constitutes 49% of the total required energy is for processes that begin with poly silicon preparation, crystal growing and ingot shaping , then slicing the ingot into wafers and processing into solar cells, and end up with framing, IV

measurement & labeling, and packaging for the module. Part of the total energy which constitutes about 59% of the total required energy is for preparing the ingot (include materials and processes), 22% is for preparing the cell, and the remaining is for preparing the module. The same is for copper indium diselenide (CIS) module that 44% of the total required energy is for preparing the embodied materials and the remaining which constitutes 56% is for the manufacturing processes.

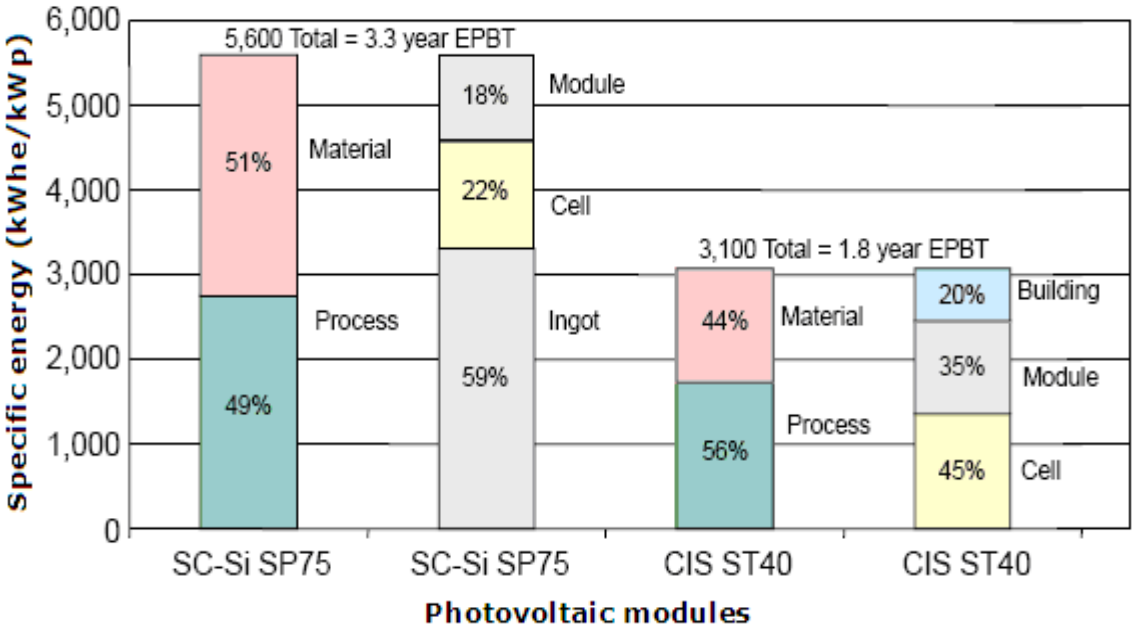

Figure (4.6): Energy requirements details for manufacturing PV modules.[16]

According to this study the payback times for today's SC-Si and CIS photovoltaic technologies are substantially less than their expected lifetimes. With a module lifetime of thirty years, a SC-Si SP75 module which has a 3.3 EPBT will produce nine times the energy used in its production and a

CIS-ST40 module which has a 1.8 EPBT will produce seventeen times. These results are based on solar radiation of 1700 kWh / m^2 - year.

Unfortunately, the EPBT for PV systems is not easy to determine. It depends on a variety of factors . As a result, values given for EPBT in the literature vary considerably, EPBT is very site-specific, as it does not only depend on the PV system itself but also on where the module is used, with the regional differences in solar irradiation.

A recent study carried by Alsema (2006) for both crystalline silicon and thin film technologies led to the results for energy payback time as given in a graphical representation as shown in figure 4.7 .

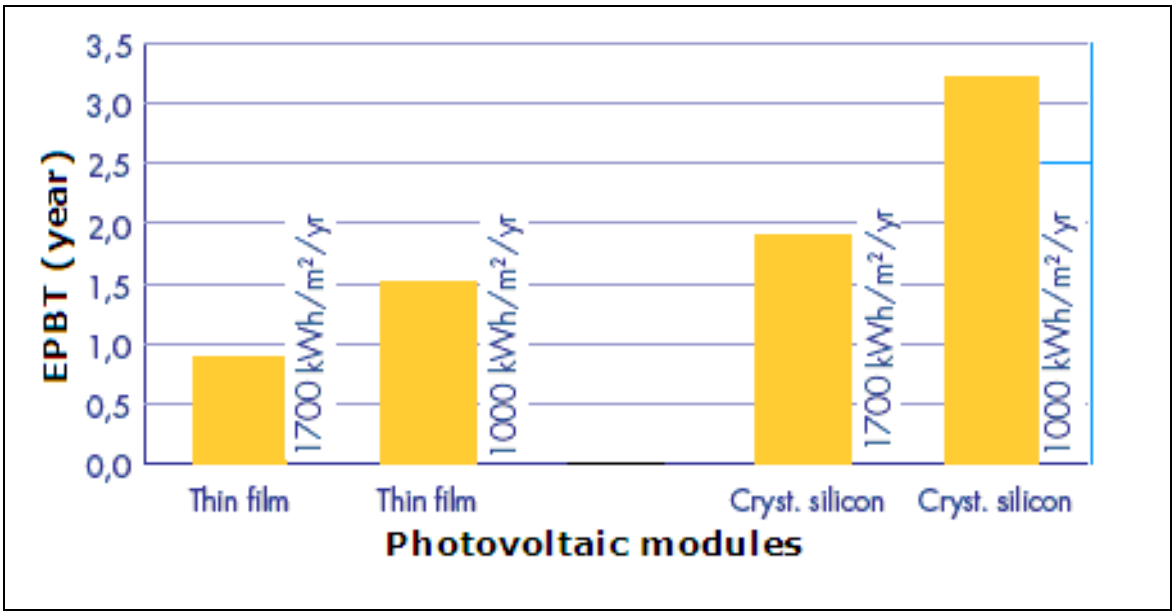

Figure (4.7) :Energy pay back times for crystalline & thin film PV modules .Source: Alsema, De Wild, Fthenakis, 21st European Photovoltaic Energy Conference, Dresden, 2006.

Another important issue which affects considerably the EPBT is the balance-of-system (BOS) elements, which often include support structures for

the actual PV modules, wiring, charge controllers, and batteries. These components vary between PV systems, depending on the individual circumstances.

In rural electrification, the PV systems are mainly based on crystalline silicon and placed on rooftops. This reduces the importance of BOS in the EPBT for two reasons. First of all, generally rooftop systems require less material for supports than ground mounted systems, and it is the production of module and array supports where the energy requirements of BOS are highest. Secondly, in systems using crystalline silicon, the share of the BOS in EPBT is only some 10-30% of the total, depending on the type of installation, because the production of silicon crystal cells is very energy-intensive. Also, in stand-alone applications some energy storage has to be used. The production of commonly used lead-acid batteries is energy-intensive, and as batteries have to be replaced several times during the lifetime of the system, their impact on EPBT is considerable [18] .

Until now the silicon cells in the photovoltaic industry have mostly been made from material that has been rejected by the micro-electronics industry for impurities. This silicon is of unnecessarily high quality for PV and it is believed that to use lower-grade silicon would substantially reduce the energy input. On the other hand, it could be argued that as long as the PV industry uses “waste” of an another industry, the energy input to silicon production should not be included in the EPBT calculations for PV. This approach would reduce the energy input requirements and EPBT by more than two thirds [18] .

CHAPTER FIVE

HYBRID SYSTEM COMPONENTS MODELING AND SIZING

Chapter 5

Hybrid System Components Modeling and Sizing

The most frequent combination of renewable energy sources for electric power supply is wind and solar photovoltaic . The components and subsystems of a stand alone power supply system based on renewable sources are interconnected to optimize the whole system. The design of a hybrid system will depend on the requirements of the load (isolated or not isolated , rural or urban , DC or AC) and on the power supply system.

Off-grid hybrid systems can also incorporate energy storage in batteries to increase duration of energy autonomy. If a permanent electric power supply is required , a back up diesel generator can be connected to the system to provide electric energy for peak loads which can't be covered by the hybrid system.

It is so important to determine the appropriate size of hybrid system components. The system shall not be oversized (expensive without increasing performance) or undersized (not capable to operate load).

5.1 Load Profile

Load profile study and determination is the first step for design of any electric power system . Nature of operation of loads and behavior of consumers are the parameters that determine the load profile . In Palestinian case most of loads are lighting fixtures , radio/TV , domestic appliances (washing machines , fans , refrigerators , and others). Nature of operation of these loads , ON and OFF of these loads between day and night which make

the load profile as shown in figure (5.1). The hybrid system is designed to supply this Palestinian case study daily load curve.

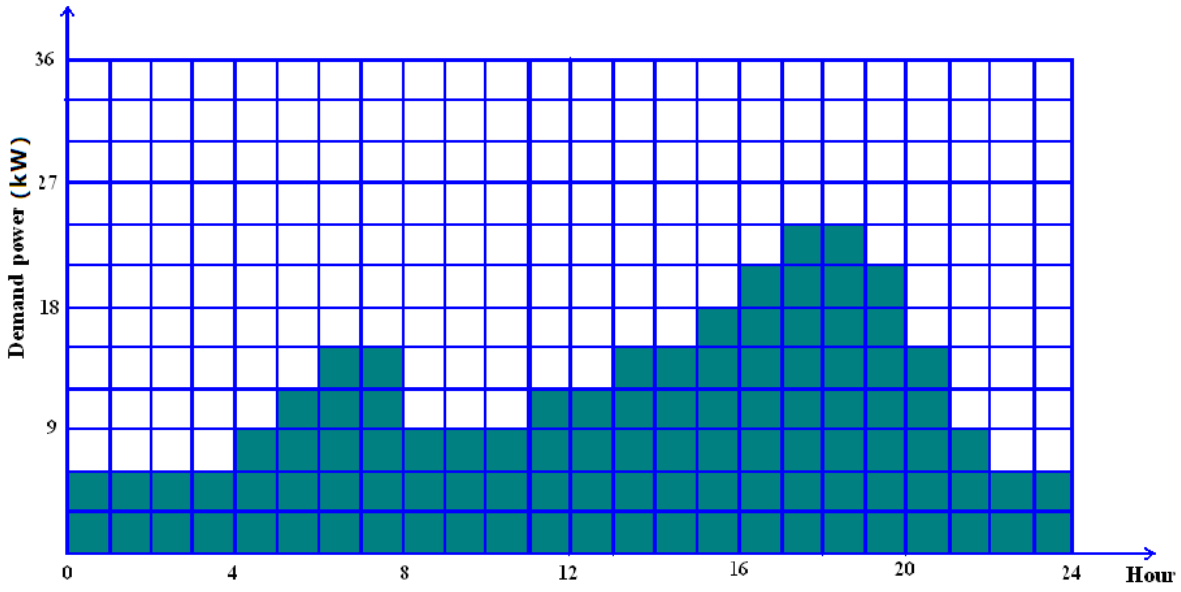

Figure (5.1) : A typical daily load curve

5.2 Wind Turbine Modeling and Sizing

The power output of a wind turbine is determined by its power curve and the instantaneous wind speed at the sight of installing this wind turbine. A mathematical model for the power curve of a wind turbine taking into account these parameters is as follows [19] :

$$P_W = \begin{cases} 0 & V < V_{ci} \\ a * V^3 - b * P_r & V_{ci} < V < V_r \\ P_r & V_r < V < V_{co} \\ 0 & V > V_{co} \end{cases} \qquad (5.1)$$

where,

P_W (in W/m^2) : is the output power density generated by a wind turbine ,

$$a = \frac{P_r}{V_r^{\,3} - V_{ci}^{\,3}} \quad . \tag{5.2}$$

$$b = \frac{V_{ci}^{\,3}}{V_r^{\,3} - V_{ci}^{\,3}} \tag{5.3}$$

and , P_r , V , V_{ci} , V_r , V_{co} are rated power (w) , instantaneous , cut-in , rated and cut-out wind speeds in (m /s) respectively.

The real electrical power delivered is calculated as

$$P_{wout} = P_w * A_w * \eta_G \tag{5.4}$$

where A_w is the total swept area of the wind turbine in (m^2) , η_G is the electrical efficiency of the wind generator and any other electrical components connected to the generator.

Verification of this wind turbine mathematical model

For a wind turbine its wind speed power curve is shown in figure 5.2, table 5.1 shows values of power generated by this 30 kW rated power wind turbine calculated using either mathematical model given in equation (5.1) or by a direct read of power for any speed from the power curve. The values of quantities read from the curve and used by mathematical model are: P_r = 30 kW, V_{ci} = 2 m/s, V_r = 9.5 m/s. The difference in values of power is

small (gives more accurate results than using linear model between the V_{ci} and V_r), so using the given mathematical model will yield an accurate results. This power curve is for the wind turbine chosen to be used by the simulation program for the evaluation process. [www.iig.com.au/wind/powercurve.htm]

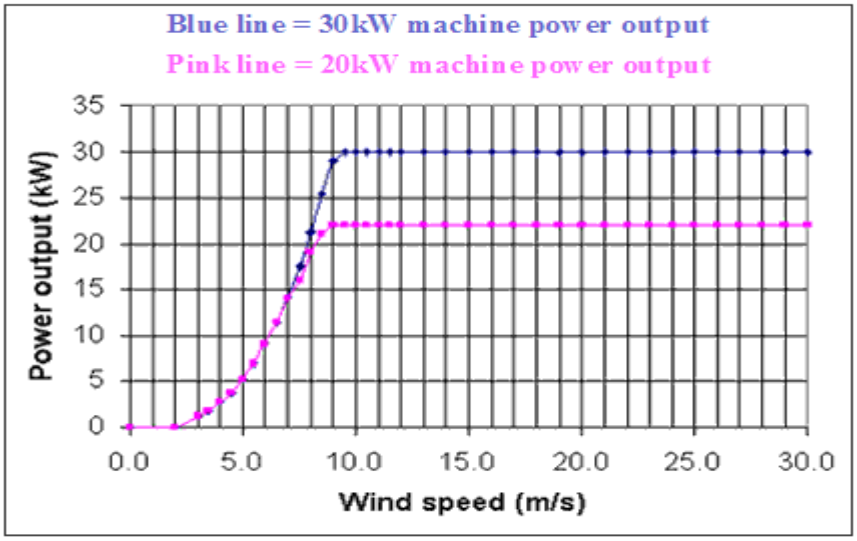

Figure(5.2) :Wind speed power curve

Table (5.1): Values of generated wind turbine power using either modeling equation or curve .

V (m/s)	P_w (kW/m^2) Using equation	P_w (kW/m^2) Using curve
4	2.0	2.4
5	4.1	5
6	7.3	9
7	11.8	14
8	17.8	21.5
8.5	21.4	25.5

5.3 PV Panel Modeling and Sizing

The total peak power of the PV generator required to supply certain load depends on load , solar radiation , ambient temperature , power temperature coefficient , efficiencies of solar charger regulator and inverter and on the safety factor taken into account to compensate for losses and temperature effect. This total peak power is obtained as follows :

$$P_{r\text{-}pv} = \frac{E_L}{\eta_{PVR} * \eta_V * PSH} * S_F \quad . \qquad (5.5)$$

where E_L is the daily energy consumption in kWh , PSH is the peak sun hours (in Palestinian case PSH = 5.4) and as a figure it represents the yearly average of daily solar radiation intensity on horizontal surface in (kWh/m^2 – day), η_{PVR} , η_V are efficiencies of solar charger regulator and inverter and S_F is the safety factor [1] .

The output power of the PV panel taking into consideration the solar radiation variation and temperature variation effects is given by equation (4.4) and it is rewritten below :

5.4 Battery Bank Modeling and Sizing

The output power from the wind turbine varies with wind speed variations through the day. Also the maximum power output of the PV generator varies according to variations in solar radiation and temperature. So the PV generator and the wind turbine may not be able to meet the load

demands at all times . A battery between the DC bus of the hybrid system and the load will compensate and act as a power supply during these times.

Excess energy during times when the output power from the wind turbine and the PV generator exceed the load requirement is stored in the battery to supply load at times when the wind turbine and the PV generator are not able to supply load.

The two main types of batteries used in hybrid systems are nickel-cadmium and lead-acid . Nickel-cadmium batteries are restricted in use for few systems due to higher cost , lower energy efficiency and limited upper operating temperature. Lead-acid batteries is still the most common type for the hybrid systems [20] .

5.4.1 Lead acid battery construction and performance

A lead acid battery in its basic construction is made of more than one electrochemical cells interconnected in such a way to provide the required voltage and current. Lead acid battery is constructed of two electrodes , the positive one consists of lead dioxide PbO_2 and the negative consists of pure lead (Pb). The empty space between the two electrodes is filled with diluted sulphuric acid (H_2SO_4). The voltage of the battery depends on cell temperature and the density of the acid solution, also its density changes with temperature and charge state. A battery with a 12V nominal voltage is constructed of $6*2$V lead acid cells. The upper and lower limits of charging and discharging open circuit voltage at 25 C^o are 14.4V and 10.5V respectively [20] .

The depth of discharge (DOD) is the state of charge of the battery. The relation between battery voltage and its depth of discharge is almost linear until a cut-off-voltage point is reached. Operating battery beyond this point will result in increasing the internal resistance of the battery and may result in damaging of it. A charge controller (regulator) is used to control operation of battery within its design limits so that not to exceed its cut-off point, also not to exceed overcharge limit.

A lead acid battery loses some of its capacity due to internal chemical reaction. This phenomenon is called self of discharge (SOD) of the battery and it increases with increasing in battery temperature. Providing batteries with lead grid or lead-calcium grid will minimize its SOD [20] .

Long life-time, cycling stability rate and capability of standing very deep discharge are the main design points shall be taken into account when choose a battery for certain application.

5.4.2 Lead acid battery rating and model

Battery rating is commonly specified in terms of its Ampere-hour (Ah) or Watt-hour (Wh) capacity. The ampere-hour capacity of a battery is the quantity of discharge current available for a specified length of time at a certain temperature and discharge rate. High discharge current would result in reduction of the battery capacity and will decrease its life time.

The ampere-hour efficiency of a battery (η_{Ah}) is the ratio of amount of total Ampere-hours the battery provides during discharge to that required to charge it back to its original condition. The battery efficiency can be specified

as Watt-hour efficiency (η_{Wh}) , its definition is in the same manner as η_{Ah}. η_{Wh} has values lower than η_{Ah} because the variation in voltage is taken into account [20] .

When the power generated from the renewable system (wind and PV in the case under study) exceeds the load requirement, energy is stored in the battery. A minimum storage level is specified for a battery so that should not be exceeded it. This level is a function of battery DOD so that

$$E_{min} = E_{BN*}(1- DOD) \qquad (5.6)$$

where

E_{min}: minimum allowable capacity of the battery bank,

$E_{BN:}$ is the nominal capacity of battery bank,

DOD : is the depth of discharge.

Energy stored in the battery at any time during charging mode can be expressed as [3]:

$$E_b(t) = E_b(t-1) * (1-\sigma) + (E_W(t) + E_{PV}(t) - E_L(t)/ \eta_v) * \eta_{Wh} \qquad (5.7)$$

Energy stored in the battery at any time during discharging mode can be expressed also as [3]:

$$E_b(t) = E_b(t-1) * (1-\sigma) - (E_L(t)/ \eta_v - (E_W(t) + E_{PV}(t))) \qquad (5.8)$$

where $E_b(t)$ and $E_b(t-1)$: are the charge capacity of battery bank at the time t and (t-1) respectively,

σ : is hourly self discharge rate,

$E_W(t)$: is the energy from wind turbine during the time interval,

$E_{PV}(t)$: is the energy from PV system during the time interval,

$E_L(t)$: is the load requirement during the time interval,

η_v and η_{wh} : are the efficiency of inverter and battery bank respectively as stated before.

5.4.3 Battery bank sizing

The two types of lead-acid batteries available at high capacities are the regular and the block types. The block type has long life time (>10 years), high cycling stability-rate (> 1000 times) and capability of standing very deep discharge, but has higher price than regular batteries [1] .

The ampere-hour capacity (C_{Ah}) and watt-hour capacity (C_{Wh}) of a battery bank required to supply a load for a certain period (day) when an energy from renewable resources is not available can be specified as follows [1] :

$$C_{Wh} = \frac{E_L * AD}{\eta_v * \eta_{Wh} * DOD} \qquad (5.9)$$

where AD : is the daily autonomy.

It is obvious from relation (5-9) that total capacity of the battery depends on daily autonomy which represents number of days that battery will be capable to supply the load in case of shortage of the renewable sources.

5.5 Diesel Generator Ratings and Fuel Consumption

A back up diesel generator can be connected to the hybrid system to provide electric energy for peak loads which can't be covered by this hybrid system if a permanent electric power supply is required or in case of incapability of the renewable sources to supply the load .

5.5.1 Diesel generator rating

Diesel generator is used in the system for following tasks: To supply load when the output power from wind and PV is not enough to operate this load, as well as to bring the SOC of batteries to an acceptable level. The diesel generator rating shall be large enough to achieve these tasks. Optimal unit sizing of a diesel generator requires careful consideration of several factors including detailed analysis of daily and seasonal load fluctuations, annual load growth, and incorporation of practical constraints for feasible and reliable diesel operation. If diesel units are only sized based on peak and/or average load values, on an annual base, with some safety margins and additional capacity for future expansion, the diesel plant will generally be very oversized. The reason is that remote community loads are normally characterized as being highly variable, with the peak load as high as many times the average load.

Number of hours of operation depends on the size of wind turbine and PV system, size of diesel generator and the climate conditions.

Type of diesel generator - according to its number of poles - shall be selected considering the expected number of hours of operation per year. For applications require less than about 400 hours of operation per year, 2-pole generators are recommended since these generators have higher rpm. Otherwise 4-pole generators are selected [9].

5.5.2 Diesel generator sizing

The diesel generator should be selected to cover the load so its ratings are determined according to load specifications. The optimum selection of the generator rating is such that the generator with other sources shall provide load with power it needs at all cases. A practical approach for large loads is to employ multiple units, e.g. a set of two or three diesels, with various sizes and apply a diesel cycling and dispatch strategy to optimize the loading of each unit to achieve maximum fuel efficiency.

5.5.3 Diesel generator fuel consumption

In a hybrid system the diesel fuel consumption would be proportional to the power generated by this generator. Thus the fuel use would be proportional to the load.

In actual practice the specific (diesel) fuel consumption (kWh/liter) is never in exact proportion to the load and reduces non-linearly with reducing load. Figure 5.3 indicates maximum energy production occurring at the rated capacity and the production rate reducing with the load. At idling conditions,

i.e., at no load, the diesel engine consumes approximately 2.5 times more fuel to produce a unit of energy (or generates only 40% of the energy for a liter of diesel) than when operating at the rated capacity. At a loading of 40%, the fuel consumption is 23% higher than at full load or the energy generation is 19% less than at the rated capacity. Thus efficiency of diesel generator always reduces with the decrease in load [21].

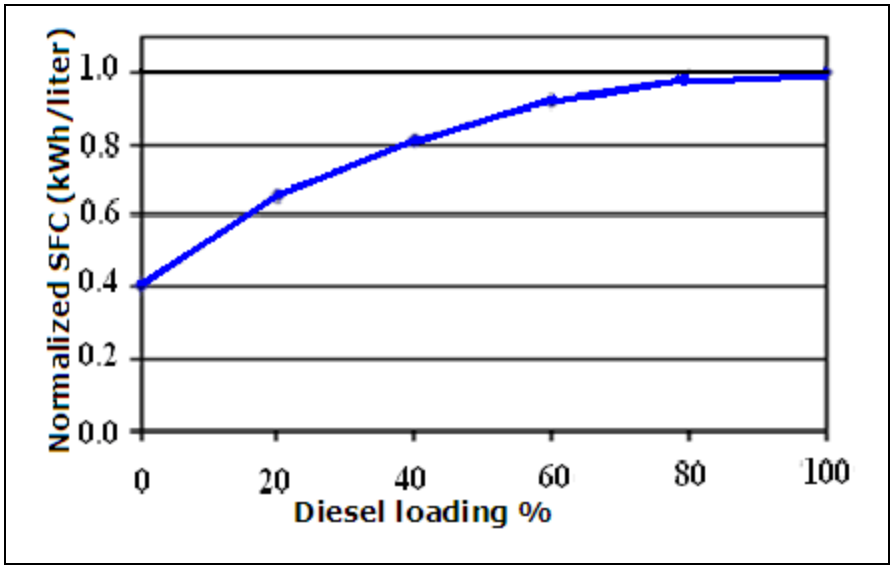

Figure (5.3) : Specific diesel consumption curve

An approximation linear model for fuel consumption and its relation with rated power of the diesel generator and the actual power provided by this diesel generator is developed by Skarstein and Uhlen (1989) [22].

$$F=0.246 * P_{Gout} + 0.08415 * P_{Gr} \quad (5.10)$$

where F : is fuel consumption (L/h),

P_{Gout} : is the actual operating output power (kW),

P_{Gr} : is the rated electric power of diesel generator (kW),

0.246 : is an empirical factor and it is in (liters/kWh), and

0.08415: is also an empirical factor and it is in (liters/kWh).

5.5.4 Effect of power factor of the load on diesel generator fuel consumption

As it is obvious from equation (5-10), diesel generator fuel consumption is function of real rated power of the electrical generator turned by the diesel engine and the actual output power of the load supplied by the generator. Also, different manufactures of diesel generators give specific curves of their products relating the diesel fuel consumption with the load real power supplied by the diesel generator rather than load apparent power.

As power factor of the load changes, the real power output from the generator would be the same. However, improving (increasing) power factor of the load will reduce current output of the alternator ,so this will give less internal losses (generator windings and other circuits). Thus a lower kW is drawn from the engine, although this will not equate to a large difference since a reasonable size generator is high efficient one.

Thus, theoretically, and based on the previous discussion, improving power factor will not end up with a reasonable saving in fuel consumption, although it may save some liters of fuel since this will reduce current drawn from the generator and this in turn will reduce power losses. This small saving will depend on rating of the generator, running time, amount of load, and the value of power factor before and after the correction.

The conclusion stated before is emphasized by results of a practical experiment done by T. L. Pryor from Murdoch University- Australia and his colleagues from University of New South Wales- Australia and Australian CRC for Renewable Energy-Australia, on a diesel generator under different modes of operation (Diesel Only: DO , diesel-battery- inverter: DBI, and diesel- battery-inverter-PV: DBIPV) and at different power factors (0.7 and 1.0) for each mode of operation. Diesel fuel consumption (L/day) is measured for each case and the results of their experiment are rewritten and presented in table 5.2.[www.acre.ee.unsw.edu.au/acrelab/Assets/Papers/ISES2001_Acrelab .pdf by TL Pryor]

Table (5.2): Diesel fuel consumption at different cases of operation and different power factors.

System	Power factor	Load (kWh/day)	Load (kVA/day)	Diesel fuel consumption (L/day)
DO	1	228.7	228.7	81.9
DO	0.7	231.5	331	83.8
DBI	1	224.6	224.6	76.6
DBI	0.7	224.8	320.6	77.8
DBI	1	102.6	102.6	35.5
DBI	0.7	101.1	144	34.8
DBIPV	1	102.6	102.6	26.5
DBIPV	0.7	100.9	143.9	26.5

From these results it can be seen that the load power factor has a minimal effect on the system performance when measured in terms of diesel fuel consumed.

Installing compensation network to improve power factor of the load to reduce fuel consumption only is not economically feasible since it needs long time to payback the price and cost of installing this network.

Installing compensation networks to improve power factor can achieve the following purposes: reduction of electrical losses, reduction of voltage drop, void of penalties, and increase capability of elements. So, installation of compensation networks in load circuits supplied by a diesel generator to achieve one or more of the previous purposes will consequently save in fuel consumption and this will enhance in reduction of time required to payback the cost of this compensation networks.

The value of the reactive power (Q) in (kVAR) required by the compensation network to improve power factor from cos(θ1) to cos(θ2) is given by the following equation:

$$Q = P * (\tan(\theta 1) - \tan(\theta 2)) \qquad (5.11)$$

where P is the real power of the load (kW) , θ1 and θ2 are angles of the load before and after installation(resp.) of the compensation network.

5.6 Charge Controller (Regulator) Modeling and Sizing

Charge controller is an essential component in hybrid systems where a storage system is required. It protects battery against both excessive overcharge and deep discharge. Charge controller shall switch off the load when a certain state of discharge is reached, also shall switch off battery from

the DC bus when it is fully charged. Charge controller can be adjusted to deal with different charge and discharge conditions.

Charge controller act as interface between each of wind turbine and PV panel and the DC bus where the battery is connected. So charge controller is modeled by its efficiency where its output is

$$P_{WR} = P_{wout} * \eta_{WR} \quad (5.12)$$

and

$$P_{PVR} = P_{PVowt} * \eta_{PVR} \quad (5.13)$$

where P_{WR} : is the output power of the wind charge controller,

P_{wout} : is the wind turbine output power,

η_{WR} : is the efficiency of the wind charge controller,

P_{PVR} : is the output power of the PV charge controller,

P_{PVout} : is the PV panel output power, and

η_{PVR} : is efficiency of the PV charge controller.

The charge controller ratings are chosen according to the battery voltage and the output power from each of wind turbine and PV panel.

5.7 Bidirectional Inverter Modeling and Sizing

A bidirectional inverter is essential in the hybrid system where a storage system and a backup diesel generator are involved in the system. It can transfer power simultaneously in both directions. The inverter can supply DC and charge the batteries so it provides a path from the AC bus to the DC bus, in this case it acts as rectifier circuit which changes AC diesel generator voltage to DC voltage. In the other way, it provides path from DC bus to the AC load so it acts as an inverter which changes DC voltage to AC voltage needed by the load.

Shape of the output waveform, power rating and efficiency are the parameters shall be considered when choose a certain bi-directional inverter to a certain application.

In a charger(rectifier) mode a bidirectional inverter can be modeled as follows:

$$P_{dicm}=P_{Gout} * \eta_{dicm} \quad (5.14)$$

where P_{dicm} : is output power of bidirectional inverter in its charge mode,

P_{Gout} : is diesel generator output power, and

η_{dicm} : is the efficiency of bidirectional inverter in its charge mode.

In this mode of operation (charger mode) the charger is characterized by its nominal AC voltage and voltage range , nominal DC output voltage that shall matched with DC bus voltage and its charging current .

In an inverter mode a bidirectional inverter can be modeled as follows:

$$P_{invm} = P_{DCB} * \eta_{invm} \quad (5.15)$$

where P_{invm} : is output power of directional inverter in its inverter mode,

P_{DCB} : is the DC bus power ,and

η_{invm} : is efficiency of bidirectional inverter in its inverter mode (usually equals the efficiency of bidirectional inverter in its rectifier mode (η_{dicm}) and thus called η_v) .

In this mode of operation(inverter mode) an inverter is characterized by its nominal voltage and voltage range that shall be matched with the DC bus voltage , nominal output voltage and its output power that shall fulfill the load power.

5.8 Dump Load

The dump load is a set of parallel load resistances. Each parallel resistance can be turned on or off upon command. In a real application, the dump load may take the form of an electric heater to heat air or water or electrical pump used to store water.

The main purpose of the dump load is to guarantee the inverter working normally. It is used to consume the surplus energy generated by the system.

5.9 Plant Management Unit

The purpose of the plant management unit is to control start and stop operation of the diesel generator, control start and stop operation of chargers, and storage and analyze data . It includes all connection and interfaces required.

CHAPTER SIX

ECONOMIC EVALUATION OF THE HYBRID SYSTEM

Chapter 6

Economic Evaluation of the Hybrid System

The costs of a hybrid system include acquisition costs, operating costs, maintenance costs and replacement costs. At end of the life of the system, the system may have a salvage value. An economic analysis is done based on life cycle costing method, which accounts for all costs associated with the system over its life time, taking into account the value of money. Life cycle costing is used in the design of the hybrid system that will cost the least amount over its lifetime. Cost annuity(cost required to generate 1 kWh of energy) is an indication on the cost of the system so that the system with the least cost annuity is selected.

6.1 Life Cycle Cost

6.1.1 Time value of money

The life cycle cost of an item consists of the total cost of procurement and operating this item over its lifetime. Some costs involved in the procurement and operating of an item are incurred at the time of an acquisition (includes costs of purchasing equipments and installation them) , and other costs are incurred at later times (includes costs of fuel if exists, operation and maintenance). The later costs may occur at regular basis or/and at irregular basis. In order to compare two similar items, which may have different costs at different times, it is convenient to refer all costs to the time of acquisition.

Two phenomena affect the value of money over time and shall be considered when evaluating economically the hybrid systems:

- The inflation rate (i) is a measure of decline in value of money. The inflation rate of any item need not necessarily follow the general inflation rate.

- The discount rate (d) relates to the amount of interest that can be earned on the principal that is saved in a certain account.

6.1.2 Present worth analysis [9]

A future amount of money for an item converted into its equivalent present value is called the present worth (PW) of this item. For an item to be purchased (n) years later with a value of (C_0) , the present worth value (PWV) is given by

$$PWV = PWF * C_0 \tag{6.1}$$

where PWF is the present worth factor, and is given by

$$PWF = \left(\frac{1+i}{1+d}\right)^n \quad . \tag{6.2}$$

where i, d and n as defined before.

Some times it is necessary to determine the present worth of a recurring expense, such as maintenance cost or fuel cost. In this case

$$PWV=PWFC * C_a \tag{6.3}$$

where C_a is the annual payment(cost) and PWFC is the cumulative present worth factor, and is given by

$$PWFC = \left(\frac{1 - X^{n}}{1 - X} \right) . \qquad (6.4)$$

where

$$X = \left(\frac{1 + i}{1 + d} \right)$$

6.2 Costs of Hybrid System Components

Costs of hybrid system include: components initial costs, components replacement costs, system maintenance costs, fuel and/or operation costs, and salvage costs or salvage revenues.

Initial costs include purchasing the following equipments required by the hybrid system: wind turbine, PV modules, batteries, diesel generator, charge controllers, bidirectional inverter, management unit, cables, and other accessories used in the installation including labors .

6.2.1 Costs of the wind turbine

Wind turbines are available in many different types in term of manufacturing process and materials used. Wind turbines require tower constructions and often difficult installation procedures. The cost of the tower and control equipment and the installation contribute a large percentage to the

wind turbine capital costs. Table 6.1 shows different types of wind turbines with different power rating and the price of each [www.folkercenter.net] .

As it is obvious, the prices presented in the table vary widely. This is because prices presented for some of the turbines include tower price, other prices include besides the price of power electronic conditioning devices, other prices include the installation cost, other prices are only for the price of the wind turbine only. But, in general, it is obvious that as rated power of the wind turbine increases the initial cost ($/kW) decreases and this is applicable for the different types.

Different research contributors in this field give an estimate installation cost for different ratings of wind turbines that include tower, wiring, utility interconnection or battery storage equipment, power conditioning unit, etc.) plus delivery and installation charges, in the ranges as follows [23]:

- A residential-scale system (1-10 kW) generally costs between $2,400 and $3,000 per installed kilowatt.

- Commercial turbines (larger than 500 kW) cost in the range of $1,000 to $2500 per kilowatt, with the lowest costs achieved when large multiple units are installed at one location.

Wind turbine operating costs comprise maintenance and replacement costs. The maintenance schedule includes lubrication of certain points on the turbine, visual inspection of major components, and checking the tightness of the various bolts on the tower and turbine. Maintenance is carried out after a certain amount of operation time. Maintenance costs for wind turbines can

vary depending on the application, type of maintenance and wind turbine sizes and increase as turbine age increases. A rule of estimation for annual operating expenses is 1.5% to 2.5% of the initial system cost. Another estimate is based on the system's energy production and is equivalent 1 to 2 cents per kWh generated from the wind turbine. For smaller wind turbine sizes, they can sometimes be assumed to be roughly in the range of PV maintenance costs. The wind turbine life is often assumed to be more than 20 years. According to the manufacturers, overhauls of the wind machines are not necessary for the life of the system (assumed to be 25 years); therefore, overhaul costs were not included in the analysis[23].

Table (6.1): Prices and costs in ($/kW) for different types of wind turbines.

Wind turbine rated power (kW)	Turbine price ($)	Cost ($/kW)	Company
5	24300	4860	WESTWIND
10	50300	5030	WESTWIND
20	77500	3875	WESTWIND
1	7041	7041	ENERGOTECH(e)
3	14376	4792	ENERGOTECH(e)
6	20244	3374	ENERGOTECH(e)
20	30807	1540	JONICA IMPIANTI(e)
.5	2288	4576	FORTIS WIND(e)
0.8	2919	3649	FORTIS WIND(e)
1.4	3889	2778	FORTIS WIND(e)
5	11009	2202	FORTIS WIND(e)
10	23772	2377	FORTIS WIND(e)
0.6	4489	7482	J. Bornay(e)
1.5	6610	4407	J. Bornay(e)
3	10201	3400	J. Bornay(e)
6	17595	2932	J. Bornay(e)
0.3	666	2220	Navitron(G)
.5	878	1756	Navitron(G)
1	1248	1248	Navitron(G)
2	2960	1480	Navitron(G)
5	8676	1735	Navitron(G)
10	15262	1526	Navitron(G)
20	26825	1341	Navitron(G)

For the case study under consideration, the installation cost of the wind turbine is considered about 3000 $/kW. The operation and maintenance cost is considered about 2.0% of the initial cost yearly.

6.2.2 Costs of PV modules

Any PV module is characterized by its peak watt (W_p)at standard test conditions. Price of PV module depends mainly on its rated power (peak power) and its type**.** Table 6.2 shows different types of PV modules according to their rated power and manufacturer, price of each module, and the cost in ($/$W_p$ **)** for each module. It is obvious that as rated power of a module increases, the cost ($/$W_p$ **)** decreases. For high rated power it can be considered about 5 ($/$W_p$ **)** [www.affordable-solar.com] .

The values of installation costs vary for different applications and projects and depend mainly on the location of installation and mounting structures. For domestic applications, it can be considered about 16% of capital costs.

Table (6.2): The cost ($/$W_p$) for different types of PV modules.

Module peak power (W_p)	Module price ($)	Cost ($/$W_p$)	Company
10	119	11.9	Sunwize
40	279	6.97	Sunwize
50	309	6.18	Sunwize
50	284	5.68	Solar world
55	340	6.18	Sunwize
60	382	6.37	Sunwize
100	552	5.52	Sunwize
165	799	4.84	Solar world
170	799	4.7	Sunwize
170	810	4.76	Suntech
173	829	4.79	GE energy
175	805	4.6	Sharp
200	999	4.99	GE energy

PV maintenance costs are often collected in monthly payments that cover system inspection by a maintenance person. The PV panels are in many cases assumed to have life times of more than 20 years. During its lifetime, no PV panel replacement costs occur.

6.2.3 Costs of batteries

Any battery is characterized by its nominal voltage and its rated Ah capacity. The 2V cell block batteries are the most common ones in the hybrid systems. Their prices are higher than the prices of regular batteries, but as mentioned before they are characterized by their high cycling rate and capability to stand very deep discharge. Table 6.3 shows different types of batteries according to their capacity and manufacturer, price of each one, and

cost in ($/kWh) for each. As it is obvious, these cost values vary in the range 250-290 ($/kWh) [www.affordable-solar.com] .

Battery operation costs comprise expenses for maintenance and replacement. Maintenance includes checking the battery electrolyte levels. Battery maintenance costs are often included in the maintenance costs of the over all system.

Battery lifetime is rated on the charge-discharge cycles that it attains at the specified DOD. Number of cycles decreases as DOD percentage assumed during system operation increases. During real system operations, batteries are to a large extent partially cycled and this affects the actual battery life time [24].

Table(6.3): Cost ($/kWh) for different types of batteries.

Voltage (V)	Capacity (Ah)	Capacity (Wh)	Price ($)	Cost ($/kWh)	Company
2	1766	3532	893	252.83	2-KS-33PS
4	546	2184	617	282.51	4-CS-17PS
4	1104	4416	1132	256.34	4-CS-17PS
4	1350	5400	1413	261.67	4-CS-17PS
6	246	3276	921	281.13	4-CS-17PS
6	683	4098	1049	266.96	4-CS-17PS
6	820	4920	1267	257.52	4-CS-17PS
8	546	4368	1277	292.35	4-CS-17PS
8	820	6560	1690	257.62	4-CS-17PS
12	357	4284	1137	265.41	12-CS-11PS
12	255	3060	862	281.7	PVX-1040T
12	210	2520	711	282.14	PVX-1040T
12	104	1248	359	287.66	PVX-1040T

6.2.4 Costs of diesel generators

Diesel generator initial costs vary with size, model and design. Table 6.4 shows different types of diesel generators according to their rated power and manufacturer, price of each one, and the cost in ($/kW) for each. It is obvious that cost ($/kW) depends on the design(method of cooling) and rated power and for the same design it decreases as rated power increases. For the range of power taken in this case study analysis, this cost can be considered about 500 ($/kW) [www.generatorjoe.net] .

Table(6.4): Cost ($/kW) for different types of diesel generators.

Diesel generator rated power(KW)	Price($)	Cost($/kW)	Company
11.7	11887.68	1016	Kohler
16.7	9213.12	551.68	GeneratorJoe
17.5	7784	444.8	GeneratorJoe
25	10244.64	409.8	GeneratorJoe
28	8671.04	309.68	GeneratorJoe
28	11894.4	424.8	GeneratorJoe
33	10725.12	325	GeneratorJoe
38	10264.8	270.1	GeneratorJoe
38	13546.4	356.5	GeneratorJoe
38	8968.96	236	GeneratorJoe
50	13920.48	278.4	GeneratorJoe
54	25238.08	467.37	Kohler
83	30651.04	369.3	Kohler

Installation costs which include transportation costs, fuel tank mounting, bedding, exhaust, and intensive labor costs can be taken as percentage of diesel generator capital costs. These costs are country specific

and as a percentage it decreases as rated power of diesel generator increases. It take values in the range (3-7) % of capital cost. For the range of power taken in this case study analysis, this installation cost can be considered about 6% of initial capital cost [24].

Regular maintenance of the diesel generator is an important factor affecting the diesel generator life. Regular maintenance includes[22] :

- Oil change which recommended to take place every 250 hour of operation.
- Oil filter replacement which recommended to take place every 500 hour of operation.
- Air filter replacement which recommended to take place every 3000 hour of operation.
- Fuel filter replacement which recommended to take place every 750 hour of operation.
- Overhaul which recommended to take place every 6000 hour of operation.

The diesel generator life time is expressed as a function of the operating hours. It varies between roughly 20000 to 30000 hours of runtime [24] .

One of the important issues concerning operation of diesel generators and its economics, is the environmental effect of carbon dioxide (CO_2) generated as a result of diesel combustion. Amount of CO_2 produced depends

upon the characteristics of the diesel generator and the fuel used and takes values in the range 2.4-2.8 Kg CO_2 / L diesel [22].

Using hybrid systems with renewable resources will reduce number of operating hours of diesel generator and also fuel consumption and consequently the amount of CO_2 generated. This issue will save money according to Koyotto agreement.

6.2.5 Costs of charging controllers (regulators)

Charging regulators are used both at output of wind turbine and PV modules. The price of charging controller depend mainly on its rated power and voltage range.

6.2.6 Cost of bidirectional inverter

Bidirectional inverter is used between the DC bus and the AC bus. Its price depends mainly on its rated power and voltage range at both input and output.

6.3 Present Worth of Different Hybrid System Costs

6.3.1 Present worth of initial costs

Costs of : wind turbine, PV modules, diesel generator, battery, charging controllers, and bidirectional inverter also installation cost of: wind turbine, PV modules, diesel generator all are summed to obtain the overall initial cost.

6.3.2 Present worth of fuel, operation, and maintenance costs

All operation and maintenance costs over the life time of the system which include maintenance cost of: wind turbine, PV modules, diesel generator, and batteries are summed and the present worth of the sum is calculated using equation (6.3) where C_a represents the summation of all annual maintenance costs. Part of operation and maintenance costs such as inspection and monitoring, test, regular check for different parts of the system, cleaning, and measurements are included in the labor cost of the system which is paid to a specialized technician .

The present worth of fuel cost is also calculated using equation (6.3) but (C_a) here represents the annual fuel cost and

$$X = \left(\frac{1 + i_f}{1 + d} \right)$$

where i_f represents fuel inflation rate and d - as stated before - represents the discount rate.

6.3.3 Present worth of replacement costs

Replacement costs include: replacement of batteries at their end of life, replacement of oil, fuel and air filters of the diesel engine, oil change, overhaul of the diesel engine, and replacement of diesel engine at its end of life.

Part of the previous mentioned replacement costs is recurring at certain periods, so to calculate the present worth of these costs, equation (6.3) shall be

used. The other part of the replacement costs is non recurring that occurs at changing intervals, so to calculate the present worth of these costs equation (6.1) shall be used where C_o represents the replacement cost of the item and the variable n in the present worth factor (PWF) relation represents the replacement year.

6.4 Economic Rates and Life Cycle Periods of Different Components

As mentioned before two economic rates affect the value of money over time and shall be considered when evaluating economically the hybrid systems: discount rate and inflation rate. Typical values of discount rate are in the range 7-15% and it is a country dependent. In this analysis a typical value of 8% is considered for discount rate. Typical values of general inflation rate are in the range 3-8% and it is also a system ,component, and country dependent. In this analysis a typical value of 4% is considered for general inflation rate. Fuel costs have their own inflation rate. Typical values of fuel inflation rate are in the range 5-10%. In this analysis a typical value of 5% is considered for fuel inflation rate [22].

The life cycle period of the system is taken to be the life cycle period of the component that has a maximum life time. In this analysis, it is for the PV system and the wind turbine, and it is 24 years. The life time of the diesel generator is described in terms of number of hours of operation and it is a manufacturer and percentage of loading dependent. In this analysis a typical value of 24000 hour of operation is considered . The life time of the battery- as mentioned before- is dependent mainly on number of charge-discharge cycles which in turn depends on value of DOD assumed. In this analysis a

typical value of 12 years is considered as a life time of battery where a DOD is assumed to be 80%.

The life times of the other components of the hybrid system such as inverter, charge controllers, and management system generally take values greater than 20 years. Because the cost of each is small in comparison with the other components, in this analysis a 24 years life time is considered for each.

6.5 Cost of Electricity Production (COE)

Comparison of different scenarios considered in the hybrid system analysis is based on calculating the cost of electricity production in ($/kWh) for each scenario. Cost of electricity production (COE) includes all different costs : initial capital costs, recurring and nonrecurring costs due to operation, maintenance, repair, component replacement, and the fuel costs.

COE is the ratio between the total annual cost(ACT) and the total energy required by the load (ELT) . So,

$$\text{COE} = \frac{\text{ACT}}{\text{ELT}} \tag{6.5}$$

where ACT is in $/year and ELT is in kWh/year. Total annual cost is calculated using equation (6.3) where C_a here represents the required ACT and PWV here represents total life cycle cost (LCC) in $ calculated on present

worth basis. Equation (6.3) here becomes:

$$ACT = \frac{LCC}{PWFC} \tag{6.6}$$

The scenario which achieves the technical requirement and with the lowest COE is selected among other scenarios.

6.6 Tariff and the Net Present Value

Tariff is the rate at which electrical energy is supplied to a consumer. Tariff shall recover: initial capital costs, operation and maintenance costs, transmission and distribution costs, besides tariff shall achieve a suitable profit. So for a strictly commercial venture the service tariff should be equal to the COE plus appropriate profit. Different types of tariff systems can be used in electrical power systems. One of the simplest types is the single tariff type. In this type a fixed rate is charged per kWh of energy consumed.

Assuming certain tariff ($/kWh), the total annual revenue (ART) as a result of energy sold can be calculated using the following equation:

$$ART = Tariff * ELT \tag{6.7}$$

The present worth of this annual revenue, which represents the total income can be calculated using equation (6.3) where C_a here represents the

ART.

Net present value (NPV) of any scenario can be calculated by subtracting the LCC from the present worth of the income, so in order to calculate the NPV the following equation is used:

$$NPV = PWV \text{ of income} - LCC \quad (6.8)$$

Linking equation (6.3) with equation (6.8) will yield

$$NPV = (PWFC * ART) - LCC \quad (6.9)$$

For a project to be profitable the NPV must have a positive value. The greater the NPV the more profitable is the system.

6.7 Sensitivity Analysis

The results of the design process are only as good as the quality of the data that can be fed to the model. Some of the assumed input parameters might be different as the system is installed and used. Costs of components or labor might change, the level of demand can be higher or lower than expected.

In order to decide for what ranges and type of changes the designs remain good choices it needs to be analyzed how sensitive the recommended designs are to such changes.

Sensitivity analysis has been given to explore the system comparisons with base-case assumptions. The analysis has been carried out for the energy demand and effect on the COE is calculated for different key parameters,

such as discount rate, diesel fuel cost, fuel escalation rate, solar radiation, PV module cost.

CHAPTER SEVEN

HYBRID SYSTEM SIMULATION SOFTWARE

Chapter 7

Hybrid System Simulation Software

A software program using Matlab was developed to simulate the hybrid system behavior. An hourly time step is used through this simulation. By using computer simulation, the optimum system configuration can be found by comparing the performances and energy production costs of different system configurations.

7.1 Simulation Approach and Power Flow Strategy

The system simulation is performed by considering the system reliability as 100%, so no interruption is assumed during operation of the system.

The developed optimization software enables to change the variables of the hybrid system model in terms of sizing and operation. In such a way the life cycle cost of the hybrid system while respecting the demand requirements are minimized .

In this approach the renewable energy sources (wind & PV) plus the energy stored in the battery are used to cover the demand. The diesel generator is switched on as a back-up source when the battery is discharged to a certain level. For each hour step the simulation program compares the required energy demand and the supplied energy, and according to the

difference a decision to operate the diesel generator or to charge the battery or discharge it will be taken.

The following cases will be considered with the illustrated priority while developing the simulation software:

Case1: Sufficient generated energy by renewable sources(wind & PV).The use of this energy to supply load has priority over using batteries or diesel generator. The extra energy is used to charge batteries, figure 7.1.

Case 2: As case 1 but surplus energy is generated by the system greater than the need to supply the load and the batteries. In this case the surplus energy is consumed by the dump load, figure 7.2.

Case 3: The generated energy by the renewable sources is not sufficient to supply the load. The priority here is to use the stored energy in the batteries in addition to the generated energy by the renewable sources rather than operating the diesel generator, figure 7.3.

Case 4: The generated energy by the renewable sources is not sufficient to cover the load demands and the battery is also discharged to its minimum value. In this case the diesel generator is switched on, and in addition to the generated energy by the renewable sources, it supplies the load and charge the batteries. The hybrid system still in this mode of operation until the batteries are recharged to their full capacity, figure 7.4.

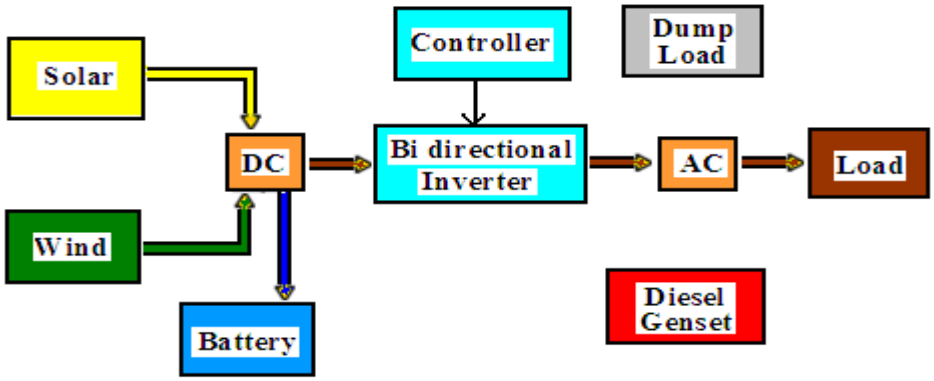

Figure(7.1) : Sufficient energy to supply load & charge batteries case.

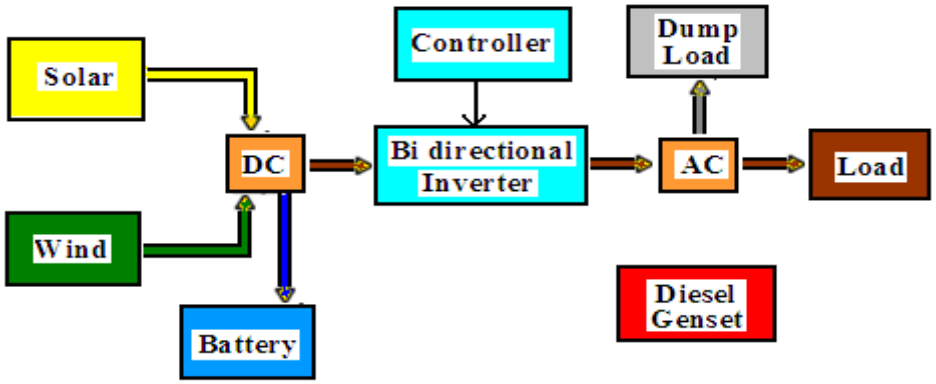

Figure(7.2) : Sufficient energy to supply load & charge batteries but the extra energy is consumed by the dump load case.

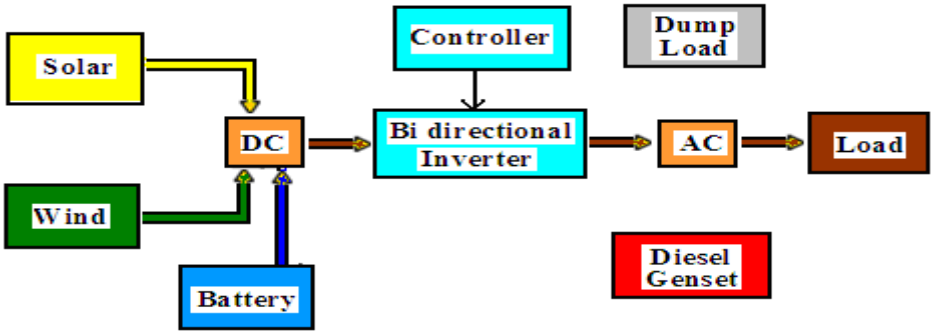

Figure(7.3) : Not sufficient energy to supply load, batteries are also used to supply load case.

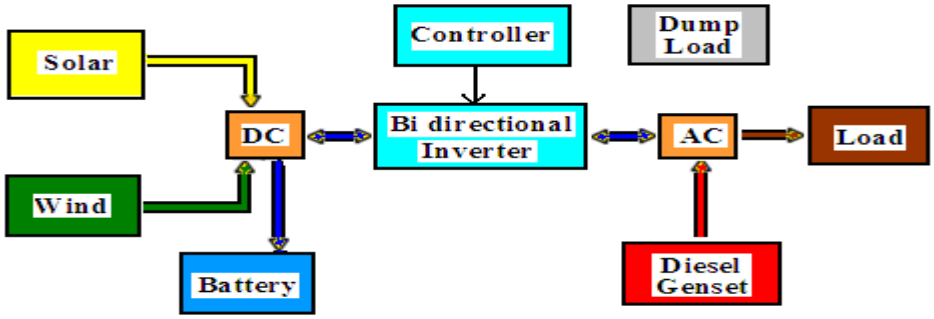

Figure(7.4) : Not sufficient energy to supply load & charge batteries, diesel generator is switched-on and do this case.

7.2 Software Inputs and Outputs

The Input variables and parameters to the simulation program are: Load demand, measured solar radiation averaged on hour basis over a year, measured temperature averaged on hour basis over a year, measured wind speeds averaged on hour basis over a year, latitude of the location, tilt angle of the PV arrays, azimuth angle of the tilted PV arrays, ground reflection index, PV contribution, number of autonomy days, height at which wind measurements are performed, height of wind turbine tower, ground surface friction coefficient, rated power of wind turbine, cut-in, rated, and cut-off wind speeds of the wind turbine, component costs, and economical factors.

The outputs from the simulation program are : PV generator rated power, battery storage capacity, yearly energy contributed by wind turbine, PV modules, and diesel generator, operating hours of diesel generator, diesel fuel consumption, dump energy, state of charge of battery, CO_2 generated as a result of operation of diesel generator, cost of energy production, and net

present value. In addition to numerical results , graphs of different variables can be obtained.

Wind speeds input to the program shall be corrected to take into account the height of the wind turbine tower. In addition to this, solar radiation input to the simulation program is measured on a horizontal plane and shall be corrected to take into account the tilted and azimuth angles of the tilted modules. Simulation program shall do that.

7.3 Simulation Program Flow Charts

The following flow charts illustrate modes of operation of the hybrid system under different conditions: flow chart shown in figure 7.5 illustrates the decision strategy for system operation , flow cart shown in figure 7.6 illustrates the charge mode of operation, flow chart shown in figure 7.7 illustrates the discharge mode of operation, and flow chart shown in figure 7.8 illustrates the diesel mode of operation.

Different abbreviations in the flow charts are as follows:

- Pw(t), Ppv(t) and Pl(t) are wind turbine , PV and load powers respectively.
- Eb(t) and Eb(t-1) are battery energies at time t and time t-1.
- Pch(t) is the charging power.
- Ech(t) is the amount of energy to be stored in the battery.
- Ebmax is the maximum energy can be stored in the battery.
- Pdch(t) is the discharging power.
- Edch(t) is the amount of energy to be discharged from the battery.
- Ebmin is the minimum energy stored in the battery not to go below.
- Pg is the diesel generator power.
- tg is the amount of time the diesel generator is on.
- Dump(t) is the dump energy.

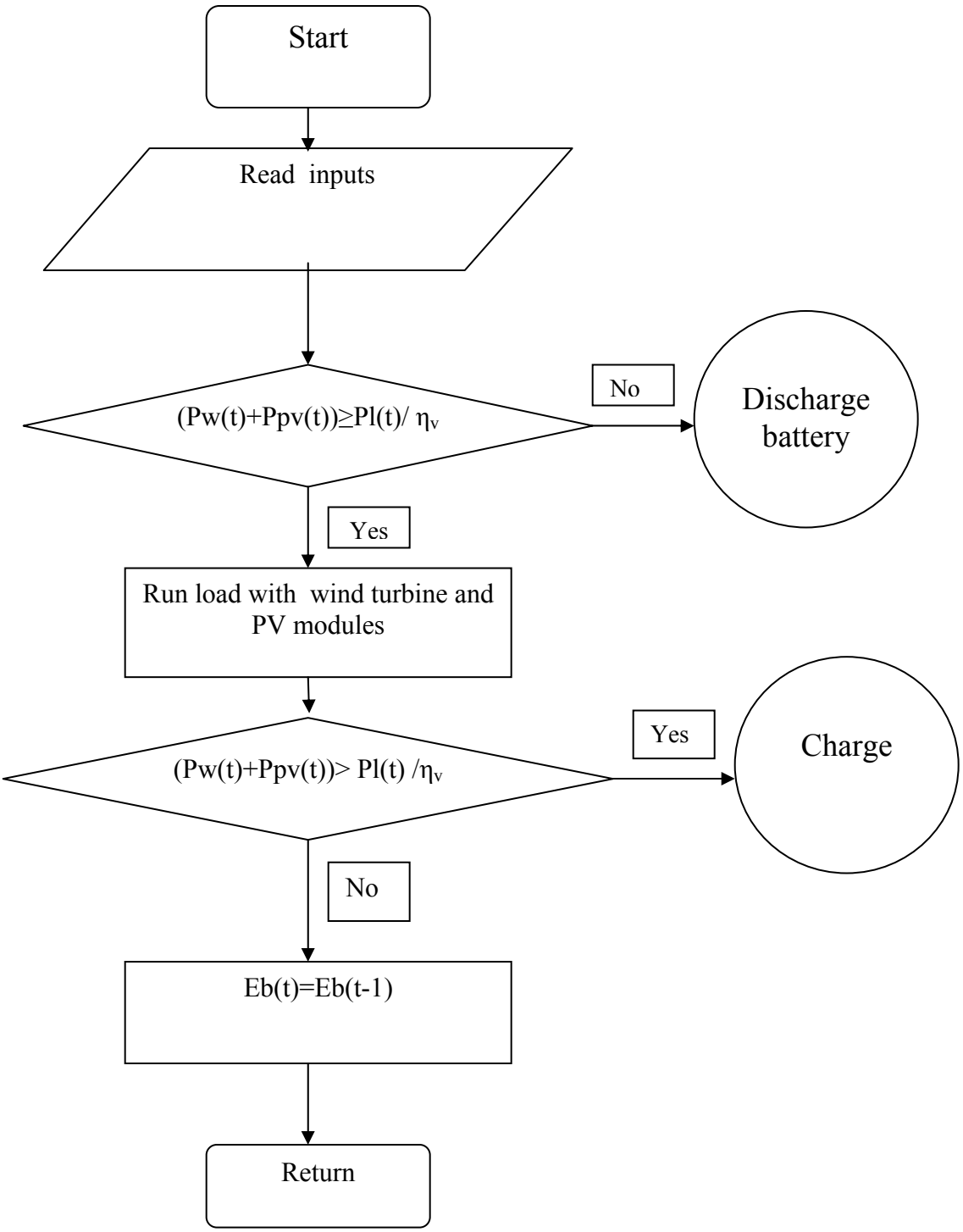

Figure (7.5): Main flow chart.

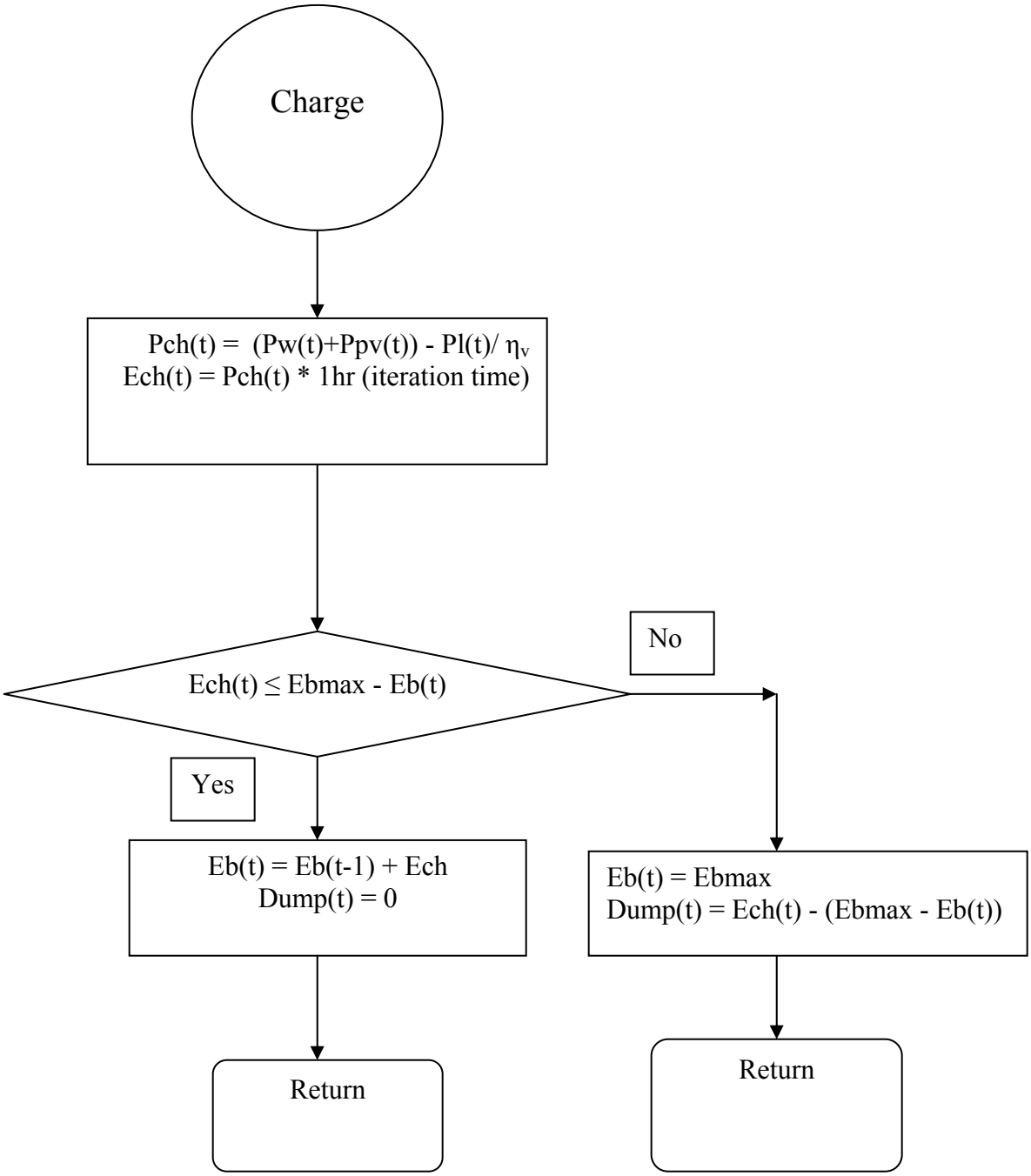

Figure (7.6): Charging mode flow chart.

.

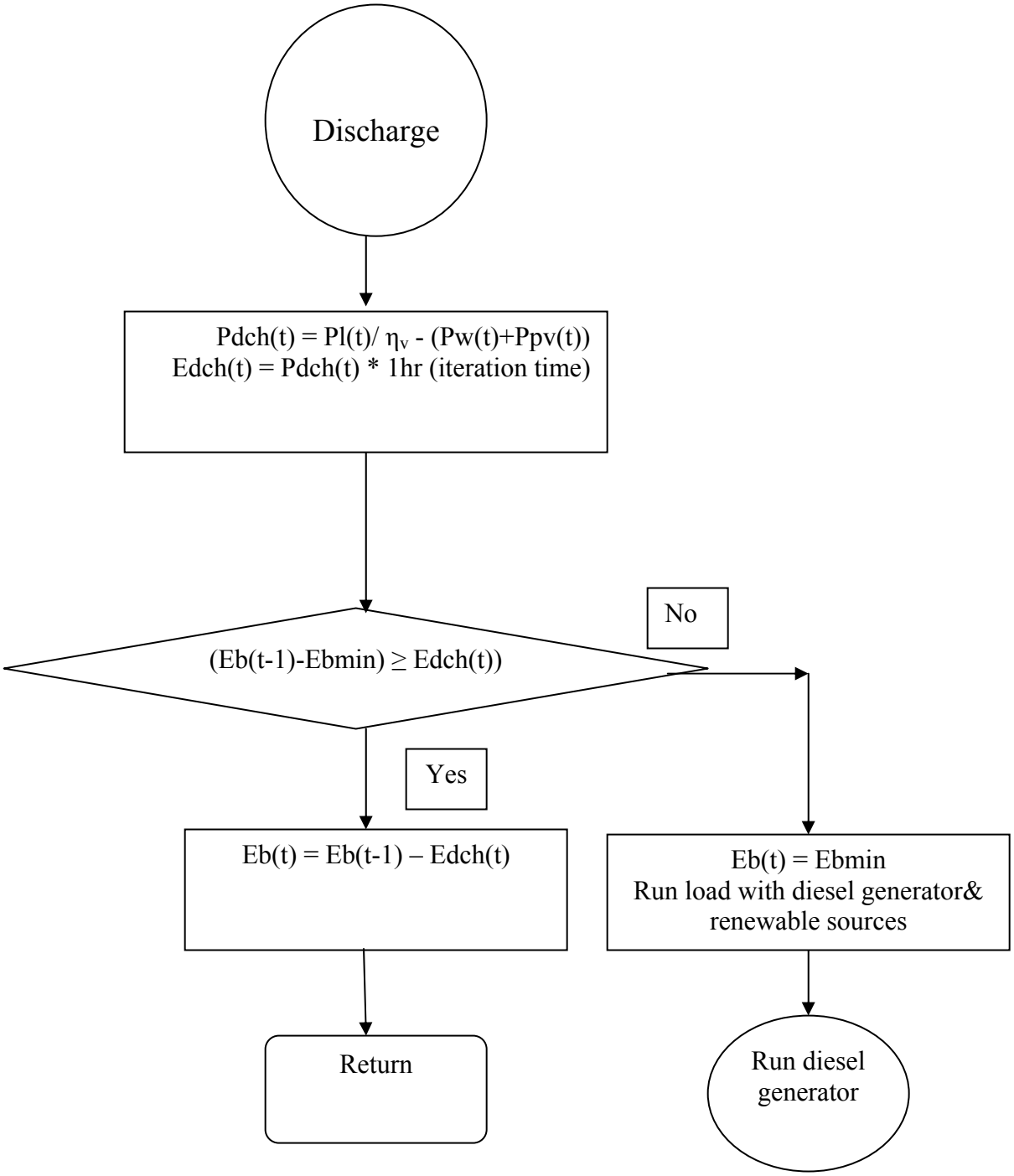

Figure(7.7): Discharge mode flow chart.

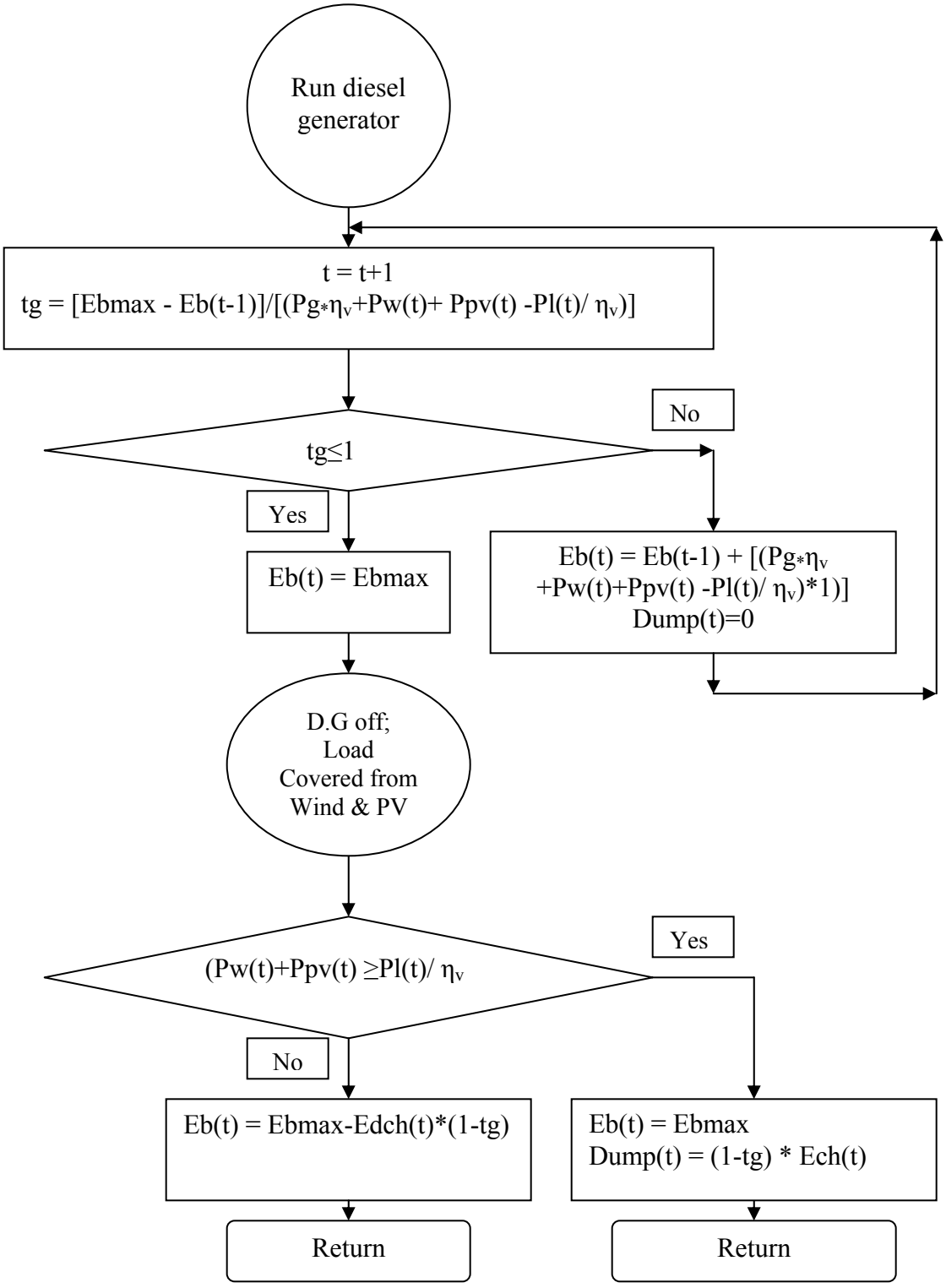

Figure(7.8): Diesel mode of operation flow chart.

CHAPTER EIGHT

CASE STUDY EVALUATION

Chapter 8

Case Study Evaluation

A case study is evaluated in this chapter where a load shall be supplied with its requirement of energy from a hybrid system with minimum life cycle cost for this hybrid system. The components of the hybrid system shall be sized to achieve this. The charge of the battery bank shall also be maintained within a range such that it doesn't reach the overcharge or the undercharge levels.

8.1 Special Inputs for the Case Study

The daily load curve of the group of consumers to be supplied by the hybrid system is shown in figure 5.1. This daily load curve is an input for the simulation program and synthesized on hourly basis since the analysis is performed using an iteration of hourly step. In this evaluation analysis, the daily load curve is considered identical for all days of the year. This is an assumption, it is considered here this way since no available measurements of a certain load during all days of the year, but the simulation program can deal with load changing during all hours of a year if data is available about this load. Total energy consumed daily by this load is 300 kWh. The maximum peak power of the load is 24 kW, but the minimum is 6 kW.

Tables 8.1, 8.2, 8.3 show all data and information of all components constituting the hybrid system.

Table (8.1): Wind turbine, PV, battery, regulators, and inverter data.

Wind turbine rated power (kW)	30
Wind turbine cut-in speed (m/s)	2
Wind turbine rated speed (m/s)	9.5
Wind turbine cut-off speed m/s)	40
Wind turbine tower height (m)	37
Wind turbine cost ($/kW), include installation cost	3000
PV cost($/kW)	5000
PV installation cost ($/kW)	800
Bi-directional inverter cost ($)	25000*
PV regulator cost ($)	10000*
Wind regulator cost ($)	10000*
Battery cost ($/kWh)	280
PV regulator efficiency (%)	95
Wind regulator efficiency (%)	95
Bi-directional inverter efficiency (%)	92
Battery Wh efficiency (%)	85
Wind turbine life (year)	24
PV life (year)	24
Battery life (year)	12

* These prices are real estimation prices. No exact prices are available for these components for the sizes required. The available prices are for different rating of these components.

Table (8.2): Technical data of the used diesel generator.

Diesel generator rated power (kW)	24
Diesel generator cost ($/kW)	500
Diesel fuel cost ($/liter)	1.5*
Oil change cost ($ each 250 hours)	5*
Oil filter replacement cost ($ each 500 hour)	10*
Air filter replacement cost ($ each 3000 hour)	35*
Fuel filter replacement cost ($ each 750 hour)	5*
Overhaul cost (% of initial cost each 6000 hour)	15%
Diesel generator salvage value ($)	1000*
Diesel engine life (hours)	24000
Technician labor cost ($/year)	1800*
* Local market prices	

Table (8.3): The considered factors in the economical analysis.

Interest (discount) rate (%)	8
General inflation rate (%)	4
Fuel inflation rate (%)	5
Project life cycle period (year)	24

8.2 Cost Analysis Results for the Wind-PV Hybrid System as Outputs from the Simulation Program

The following tables and graphs illustrate the cost results for the wind-PV hybrid system as an execution of the simulation program for different cases of operation:

8.2.1 COE, LCC and NPV results for Ramallah site

The cost of energy (COE) in (NIS/kWh) for ramallah site , life cycle cost (LCC) in(NIS) for Ramallah site , and net present value (NPV) in (NIS) for Ramallah site for different values of percentage of energy covered by PV (PV contribution) and different values for autonomy days (AD), are presented in tables 8-4,8-5, and 8-6.

Table (8.4): COE (NIS/kWh) for the wind-PV hybrid system for different values of PV contribution and autonomy days for Ramallah site.

AD	PV contribution (%)									
	10	20	30	40	50	60	70	80	90	100
0.1	1.4527	1.3688	1.3789	1.4191	1.4725	1.5348	1.6012	1.6703	1.7421	1.8153
0.2	1.4408	1.3555	1.3348	1.3659	1.4193	1.4824	1.5475	1.6210	1.6853	1.7623
0.3	1.4484	1.3849	1.3520	1.3445	1.3666	1.4107	1.4712	1.5377	1.6037	1.6754
0.4	1.4768	1.3753	1.3221	1.2971	1.2946	1.3043	1.3484	1.4160	1.4897	1.5625
0.5	1.4719	1.3869	1.3357	1.2880	**1.2809**	1.3016	1.3345	1.4060	1.4730	1.5433
0.6	1.4971	1.4248	1.3420	1.3153	1.2904	1.3081	1.3486	1.4191	1.4892	1.5591
0.7	1.5553	1.4442	1.3790	1.3251	1.2953	1.3224	1.3755	1.4448	1.5159	1.5920
0.8	1.5865	1.4547	1.4011	1.3308	1.3393	1.3532	1.4070	1.4757	1.5488	1.6229
0.9	1.6033	1.4978	1.4011	1.3632	1.3658	1.3800	1.4429	1.5153	1.5897	1.6666
1.0	1.6091	1.5220	1.4308	1.3802	1.3856	1.4241	1.4772	1.5523	1.6291	1.7008

The lowest cost of energy price is 1.28 NIS/kWh achieved at 50% PV contribution and 0.5 autonomy days.

Table(8.5): LCC (NIS) for the wind-PV hybrid system for different values of PV contribution and autonomy days for Ramallah site.

AD	PV contribution (%)									
	10	20	30	40	50	60	70	80	90	100
0.1	**2558748**	**2410979**	**2428789**	**2499621**	**2593732**	**2703415**	**2820301**	**2941983**	**3068557**	**3197367**
0.2	**2537865**	**2387536**	**2351124**	**2405855**	**2499927**	**2611051**	**2725750**	**2855128**	**2968461**	**3104180**
0.3	**2551147**	**2439326**	**2381463**	**2368140**	**2407041**	**2484778**	**2591341**	**2708481**	**2824819**	**2950954**
0.4	**2601218**	**2422373**	**2328799**	**2284662**	**2280362**	**2297352**	**2375077**	**2494046**	**2623941**	**2752243**
0.5	**2592668**	**2442908**	**2352717**	**2268695**	**2256180**	**2292547**	**2350641**	**2476534**	**2594482**	**2718390**
0.6	**2637019**	**2509677**	**2363741**	**2316729**	**2272873**	**2304115**	**2375392**	**2499629**	**2623031**	**2746119**
0.7	**2739469**	**2543725**	**2428999**	**2333951**	**2281540**	**2329220**	**2422814**	**2544792**	**2670167**	**2804059**
0.8	**2794399**	**2562336**	**2467876**	**2344045**	**2359018**	**2383550**	**2478242**	**2599314**	**2728064**	**2858547**
0.9	**2823971**	**2638199**	**2467801**	**2401145**	**2405695**	**2430724**	**2541537**	**2669026**	**2800143**	**2935457**
1.0	**2834300**	**2680821**	**2520139**	**2431154**	**2440601**	**2508341**	**2601899**	**2734188**	**2869398**	**2995807**

The lowest value of LCC is 2256180 NIS achieved at 50% PV contribution and 0.5 autonomy days.

Table (8.6) : NPV (NIS) for the wind-PV hybrid system for different values of PV contribution and autonomy days for Ramallah site.

AD	PV contribution (%)									
	10	20	30	40	50	60	70	80	90	100
0.1	83337	231106	213296	142464	48353	-61330	-178216	-299898	-426472	-555282
0.2	104220	254549	290961	236230	142158	31034	-83665	-213043	-326377	-462095
0.3	90938	202759	260622	273945	235044	157307	50744	-66396	-182734	-308869
0.4	40867	219712	313286	357423	361723	344733	267008	148039	18144	-110158
0.5	49417	199177	289368	373390	385905	349538	291444	165551	47603	-76305
0.6	5066	132408	278344	325356	369212	337970	266693	142456	19054	-104034
0.7	-97385	98360	213086	308134	360545	312864	219271	97293	-28082	-161974
0.8	-152314	79749	174209	298040	283067	258535	163843	42771	-85979	-216462
0.9	-181886	3886	174284	240940	236390	211361	100547	-26941	-158058	-293373
1.0	-192215	-38736	121946	210931	201484	133744	40185	-92103	-227313	-353722

The calculation is based on a sold price of each unit generated equals to 1.5 NIS/kWh.

The greatest NPV is 385905 NIS achieved at 50% PV contribution and 0.5 autonomy days.

8.2.2 Diesel generator operation data for Ramallah site

The operation time, fuel consumption and amount of CO_2 gas produced for the diesel generator for Ramallah site for different values of percentage of energy covered by PV (PV contribution) and different values for autonomy days (AD) are presented in tables 8.7, 8.8, and 8.9.

Table(8.7): Yearly operating hours of diesel generator for the wind-PV hybrid system for different values of PV contribution and autonomy days for Ramallah site.

AD	PV contribution (%)									
	10	20	30	40	50	60	70	80	90	100
0.1	2048	1682	1513	1412	1342	1292	1250	1216	1188	1163
0.2	1940	1551	1312	1191	1120	1072	1029	1005	979	962
0.3	1858	1519	1252	1043	920	828	773	732	690	660
0.4	1822	1397	1084	854	653	481	388	349	325	299
0.5	1711	1324	1016	732	**521**	373	255	225	185	153
0.6	1669	1311	950	694	442	288	187	155	122	89
0.7	1702	1256	935	616	352	220	148	113	83	64
0.8	1673	1180	885	528	353	190	120	84	58	35
0.9	1612	1179	784	502	313	151	102	74	52	35
1.0	1526	1135	752	440	258	152	80	59	42	13

It is obvious that yearly operating hours of diesel generator decrease as PV contribution or autonomy day increases. For 50% PV contribution and 0.5 autonomy days, the operating time is 521 hour.

Table(8.8): Yearly fuel consumption of diesel generator (liter) for the wind-PV hybrid system for different values of PV contribution and autonomy days for Ramallah site.

AD	PV contribution (%)									
	10	20	30	40	50	60	70	80	90	100
0.1	16225	13326	11985	11186	10630	10234	9907	9636	9409	9213
0.2	15370	12291	10393	9434	8876	8495	8152	7960	7757	7625
0.3	14718	12039	9917	8263	7292	6557	6122	5797	5464	5233
0.4	14440	11071	8591	6763	5175	3809	3074	2768	2575	2367
0.5	13560	10493	8053	5798	**4124**	2959	2020	1786	1470	1215
0.6	13222	10388	7530	5498	3498	2280	1478	1227	967	704
0.7	13488	9950	7409	4877	2789	1742	1172	897	658	507
0.8	13260	9351	7014	4183	2795	1507	949	665	461	274
0.9	12777	9341	6214	3977	2481	1198	808	590	411	275
1.0	12093	8991	5959	3490	2045	1206	636	468	331	103

The yearly fuel consumption of diesel generator decreases as PV contribution or autonomy day increases. For 50% PV contribution and 0.5 autonomy days, the amount of fuel consumption is 4124 liter.

Table(8.9):Yearly CO_2 produced from diesel generator (kg) for the wind-PV hybrid system for different values of PV contribution and autonomy days for Ramallah site.

AD	PV contribution (%)									
	10	20	30	40	50	60	70	80	90	100
0.1	40563	33314	29962	27966	26574	25586	24767	24091	23524	23032
0.2	38426	30728	25984	23586	22191	21239	20379	19900	19393	19064
0.3	36796	30096	24793	20657	18230	16393	15306	14493	13660	13081
0.4	36099	27677	21477	16908	12938	9522	7685	6920	6439	5916
0.5	33901	26232	20132	14494	**10311**	7398	5051	4466	3674	3038
0.6	33055	25969	18825	13744	8746	5700	3695	3067	2418	1760
0.7	33720	24875	18523	12193	6973	4354	2930	2243	1645	1268
0.8	33150	23378	17535	10457	6989	3768	2372	1662	1151	686
0.9	31942	23352	15534	9943	6203	2996	2019	1476	1027	687
1.0	30233	22479	14896	8725	5112	3016	1590	1171	829	257

The yearly CO_2 produced from diesel generator decreases as PV contribution or autonomy days increases. For 50% PV contribution and 0.5 autonomy days, the amount of CO_2 produced is 10311 kg.

8.2.3 Evaluation results for Nablus site

COE for Nablus site and for different values of percentage of energy covered by PV (PV contribution) and different values for autonomy days (AD), operating time of diesel generator, and fuel consumption of diesel generator are presented in tables 8.10, 8.11, and 8.12 respectively.

Table(8.10): COE (NIS/kWh) for the wind-PV hybrid system for different values of PV contribution and autonomy days for Nablus site.

AD	PV contribution (%)									
	10	20	30	40	50	60	70	80	90	100
0.1	1.8325	1.6985	1.6846	1.7001	1.7363	1.7815	1.8372	1.8990	1.9640	2.0327
0.2	1.8653	1.6951	1.6026	1.6105	1.6529	1.7081	1.7700	1.8360	1.9006	1.9689
0.3	1.8891	1.7581	1.6728	1.6354	1.6285	1.6511	1.6916	1.7416	1.7989	1.8616
0.4	1.9499	1.7826	1.6586	1.5863	1.4914	1.4405	1.4636	1.5207	1.5821	1.6456
0.5	1.9551	1.7998	1.6940	1.5599	1.4347	**1.3965**	1.4304	1.4634	1.5109	1.5837
0.6	1.9842	1.8318	1.6892	1.5645	1.4367	1.4075	1.4240	1.4592	1.5360	1.6065
0.7	2.0264	1.8635	1.7044	1.5801	1.4591	1.4336	1.4515	1.4999	1.5584	1.6317
0.8	2.0639	1.9039	1.7380	1.5970	1.4760	1.4560	1.4678	1.5317	1.5951	1.6683
0.9	2.0971	1.9380	1.7703	1.6304	1.5063	1.4963	1.5152	1.5660	1.6326	1.6993
1.0	2.1448	1.9902	1.8062	1.6681	1.5573	1.5387	1.5498	1.6053	1.6641	1.7366

The lowest price is 1.40 NIS/kWh and occurs at 60% PV contribution and 0.5 autonomy days. This price is greater than the price for Ramallah site , this is due to the lower wind speeds in Nablus site (yearly average wind speed for Ramallah site is 5.52 m/s while for Nablus site it is 4.35 m/s). As it is obvious from results more PV contribution and more yearly operating hours for diesel generator are required compared to Ramallah site.

Table(8.11) : Yearly operating hours of diesel generator for the wind-PV hybrid system for different values of PV contribution and autonomy days for Nablus site.

AD	PV contribution (%)									
	10	20	30	40	50	60	70	80	90	100
0.1	2913	2415	2192	2035	1945	1856	1790	1739	1694	1658
0.2	2888	2307	1924	1750	1654	1587	1537	1494	1450	1413
0.3	2842	2351	1986	1707	1498	1358	1258	1179	1118	1069
0.4	2882	2307	1853	1494	1086	795	654	592	539	491
0.5	2796	2249	1834	1335	876	**593**	477	358	273	247
0.6	2763	2222	1723	1245	780	517	361	248	230	198
0.7	2760	2194	1657	1181	731	477	324	241	181	156
0.8	2745	2187	1635	1120	669	428	260	213	165	139
0.9	2721	2165	1609	1098	638	420	269	192	151	110
1.0	2731	2185	1591	1084	655	417	248	182	123	96

For 60% PV contribution and 0.5 AD, the yearly operating hours is 593 hours.

Table(8.12): Yearly fuel consumption of diesel generator (liter) for the wind-PV hybrid system for different values of PV contribution and autonomy days for Nablus site.

AD	PV contribution (%)									
	10	20	30	40	50	60	70	80	90	100
0.1	23084	19138	17365	16128	15410	14703	14180	13778	13425	13141
0.2	22885	18277	15246	13868	13110	12578	12176	11841	11491	11197
0.3	22522	18630	15734	13524	11872	10758	9965	9344	8858	8470
0.4	22836	18281	14683	11841	8605	6303	5184	4687	4269	3887
0.5	22158	17821	14533	10574	6942	**4698**	3777	2838	2164	1955
0.6	21893	17607	13654	9867	6178	4100	2859	1962	1825	1572
0.7	21865	17388	13133	9360	5790	3779	2563	1908	1435	1234
0.8	21754	17329	12958	8877	5300	3390	2064	1690	1308	1105
0.9	21561	17154	12751	8698	5056	3329	2131	1519	1195	875
1.0	21636	17310	12609	8588	5190	3305	1967	1440	973	758

For 60% PV contribution and 0.5 autonomy days, the amount of fuel consumption is 4698 liters.

8.3 Performance Evaluation of Hybrid System for Ramallah Site at 50% PV Contribution and 0.5 Autonomy Days

Sizes of different components constructing the hybrid system and operation results of the system at 50% PV contribution and 0.5 AD for Ramallah site are presented in table 8.13.

Table (8.13): Design data results of wind-PV hybrid system components for 50% PV contribution and 0.5 AD for Ramallah site.

Wind turbine rated power (kW)	30
PV panel size (kW)	36.6
Battery capacity (kWh)	240
Diesel generator capacity (kW)	24
Yearly load demand (kWh)	109500
Yearly energy generated by wind turbine (kWh)	92331
Yearly energy generated by PV panel (kWh)	73179.9
Yearly energy generated by diesel generator (kWh)	12492.2
Yearly dump energy (kWh)	54002
Diesel generator operating hours (hour)	521
Yearly fuel consumption (liter)	4124
COE (NIS/kWh)	1.28
LCC (NIS)	2256180
NPV (NIS)	385905
Yearly CO_2 produced (kg)	10311

Figure 8.1 shows the yearly contribution of wind, PV, and diesel in supplying the load using a bar chart representation while figure 8.2 shows this contribution in a frequency polygon representation. It is obvious that diesel generator contribution is minimal in months June, July, and August where the solar insolation is high in these months and wind is available with considerable values.

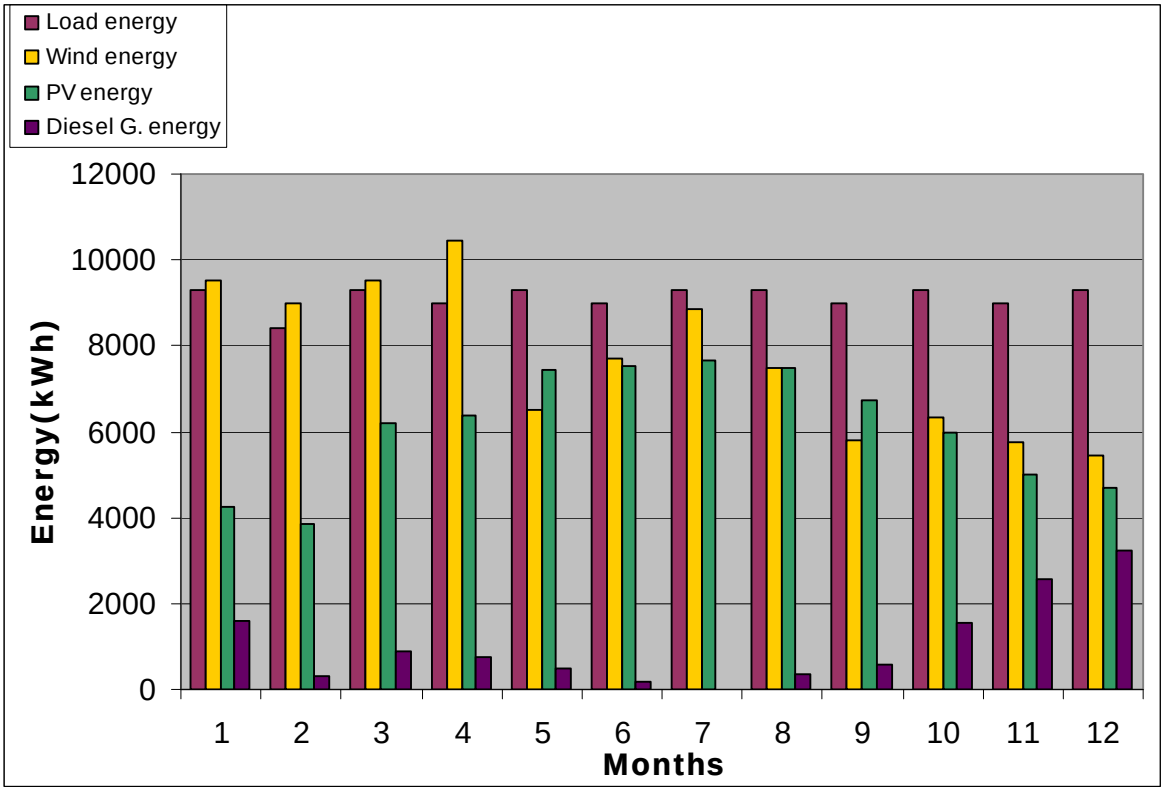

Figure (8.1) :A bar chart representation of energy contribution of wind, PV, and diesel generator for Ramallah site.

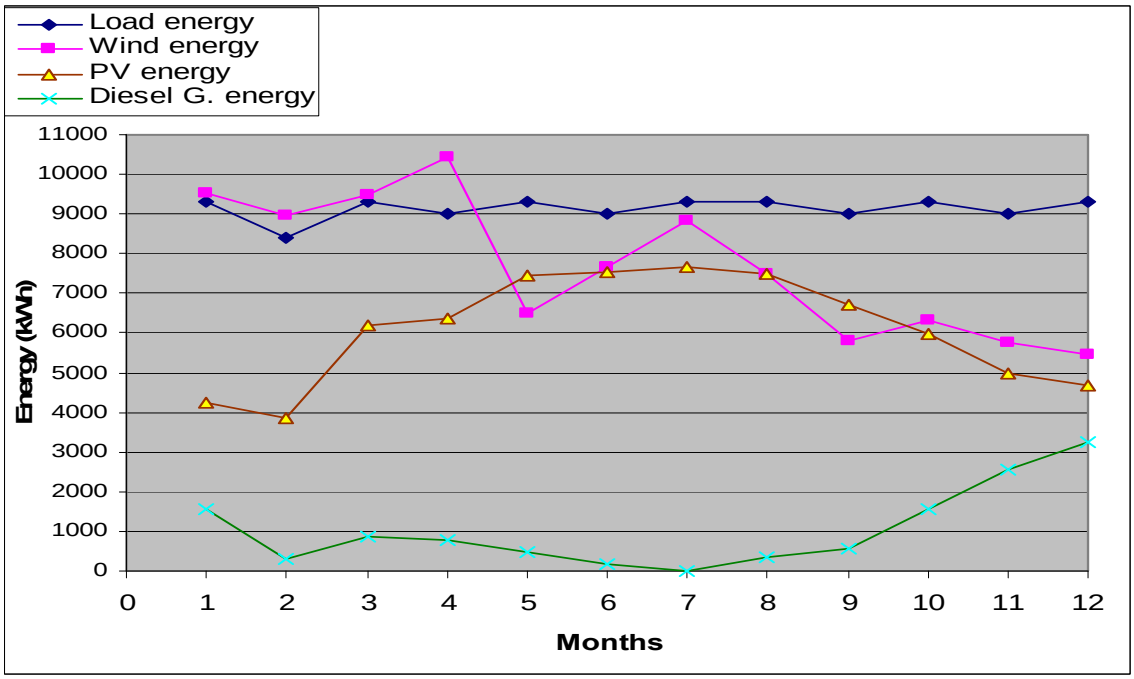

Figure (8.2): A frequency polygon representation of energy contribution of wind, PV, and diesel generator for Ramallah site..

For Ramallah site and 50% PV contribution, 0.5 AD, and for each month in a year, figures from 8.3 to 8.11 show graphical representation of: energy demand, energy generated by the wind turbine, energy generated by the PV panel, energy generated by the diesel generator, average battery SOC, dump energy, operating hours of the diesel generator, fuel consumption of the diesel generator, and amount of CO_2 produced by the diesel generator.

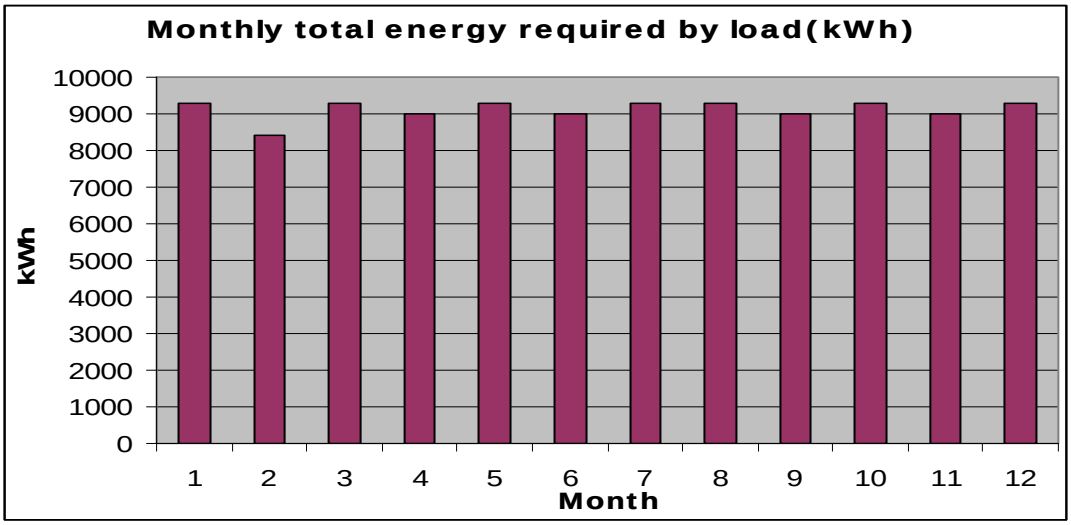

Figure (8.3): Monthly load demand.

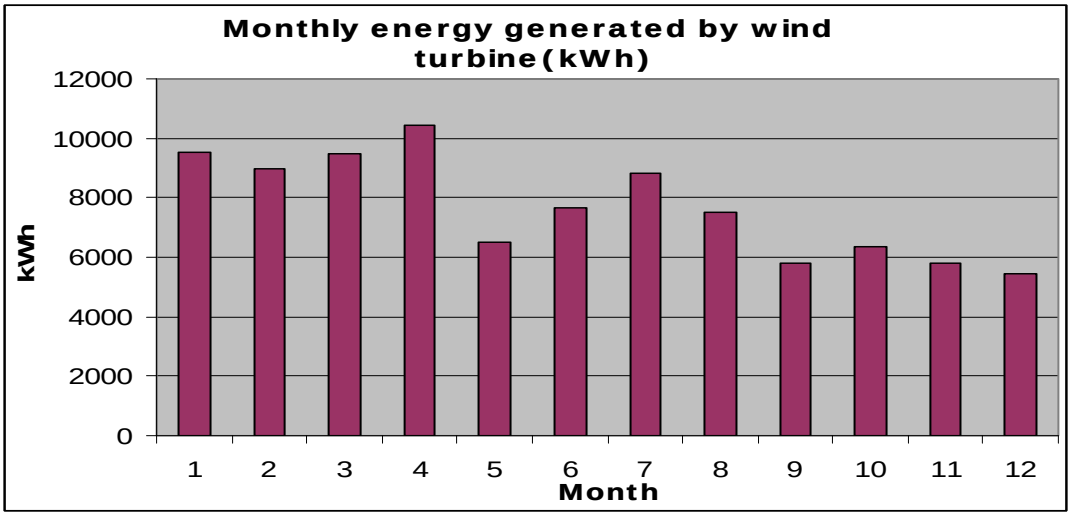

Figure (8.4): Monthly energy generated by the wind turbine for Ramallah site.

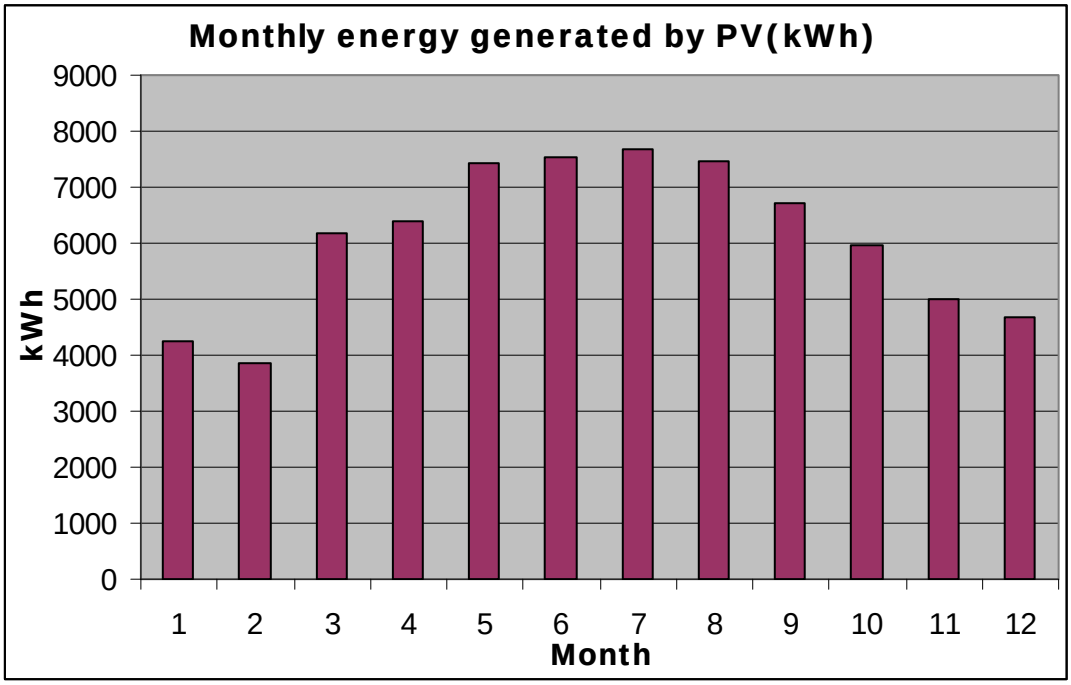

Figure (8.5): Monthly energy generated by the PV panel for Ramallah site.

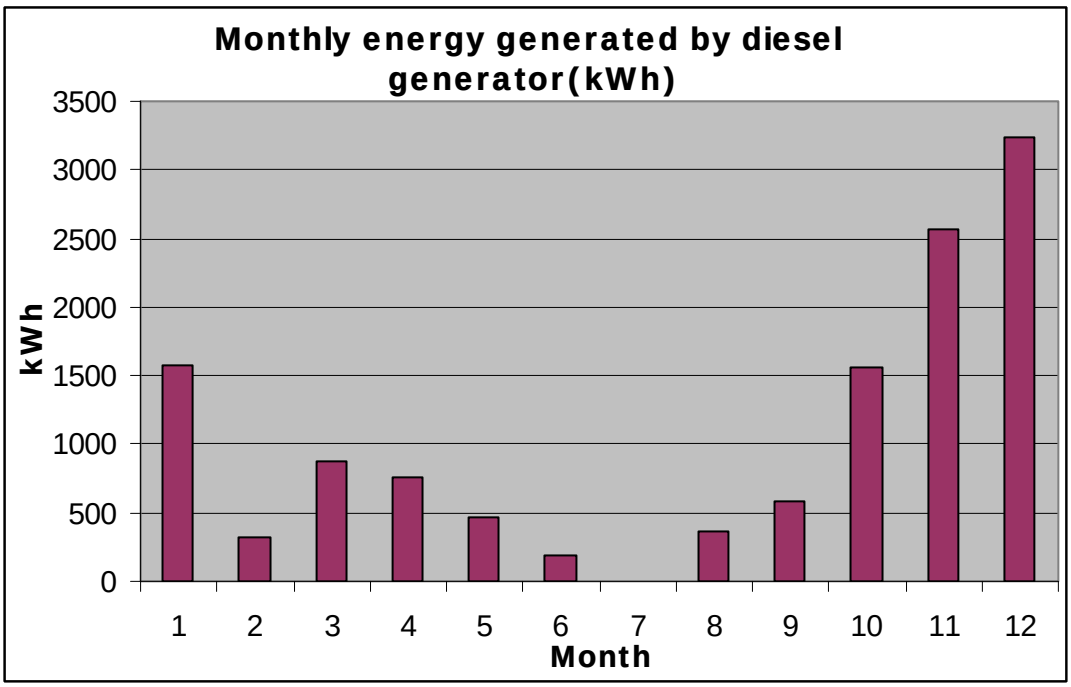

Figure (8.6): Monthly energy generated by the diesel generator for Ramallah site .

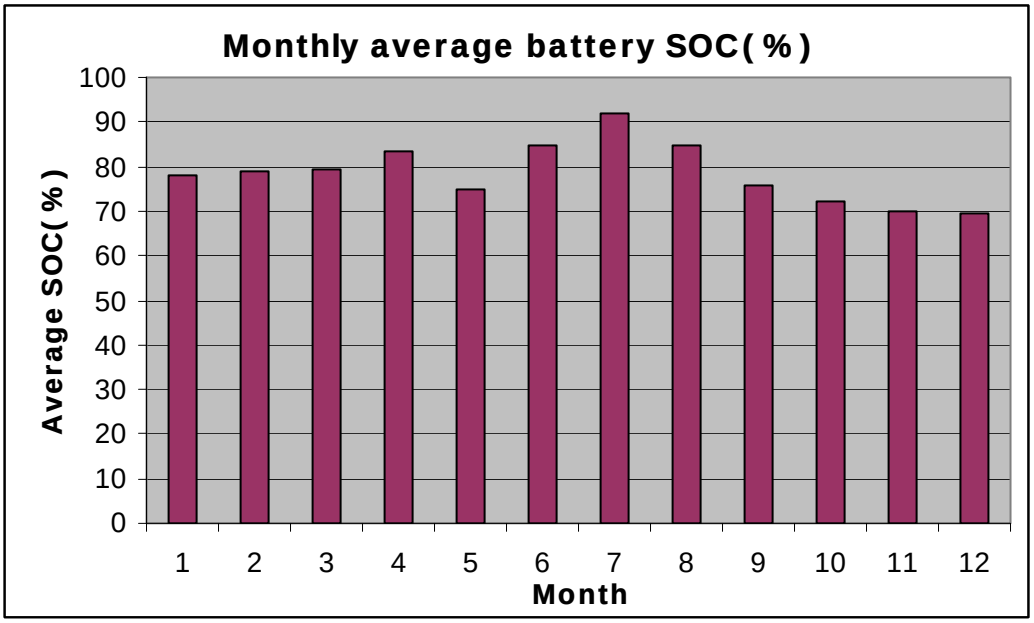

Figure (8.7): Monthly SOC of the battery bank for Ramallah site.

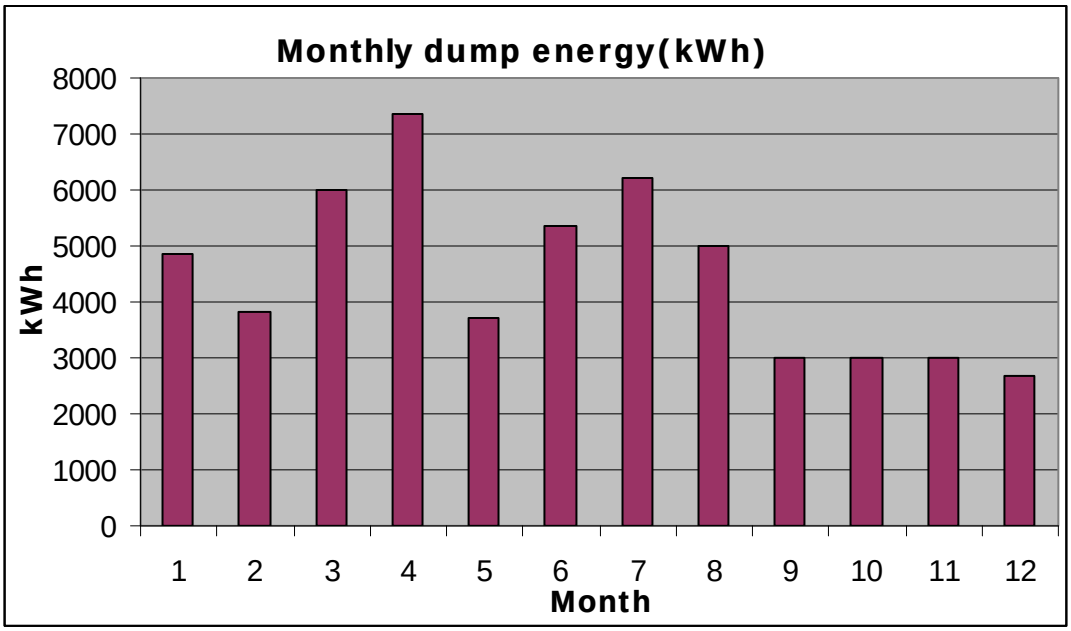

Figure (8.8): Monthly dump energy for Ramallah site.

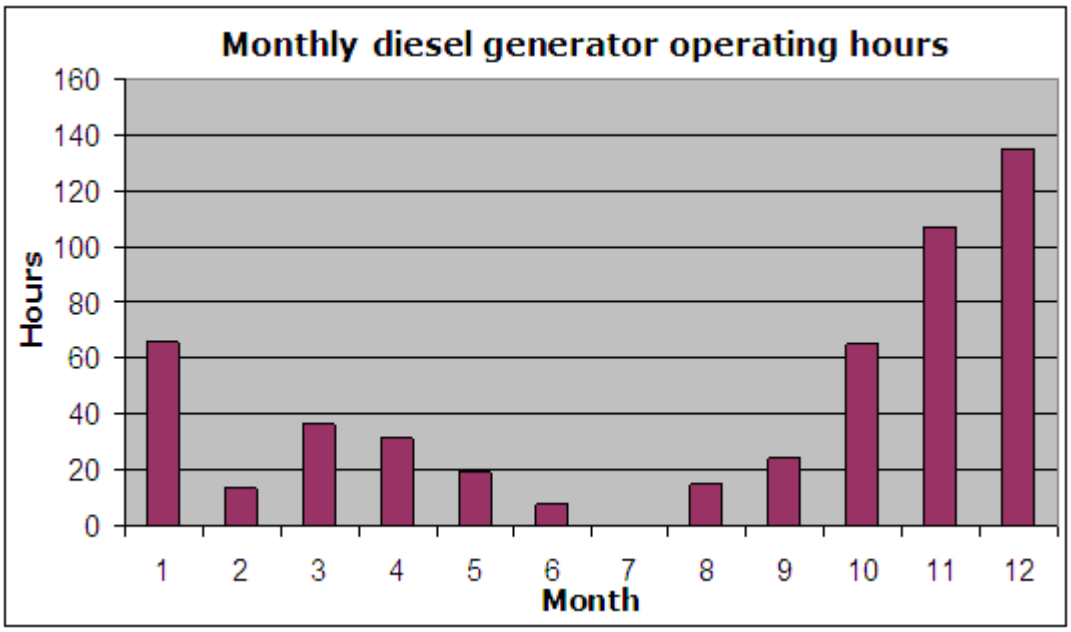

Figure (8.9): Monthly operating hours of the diesel generator for Ramallah site.

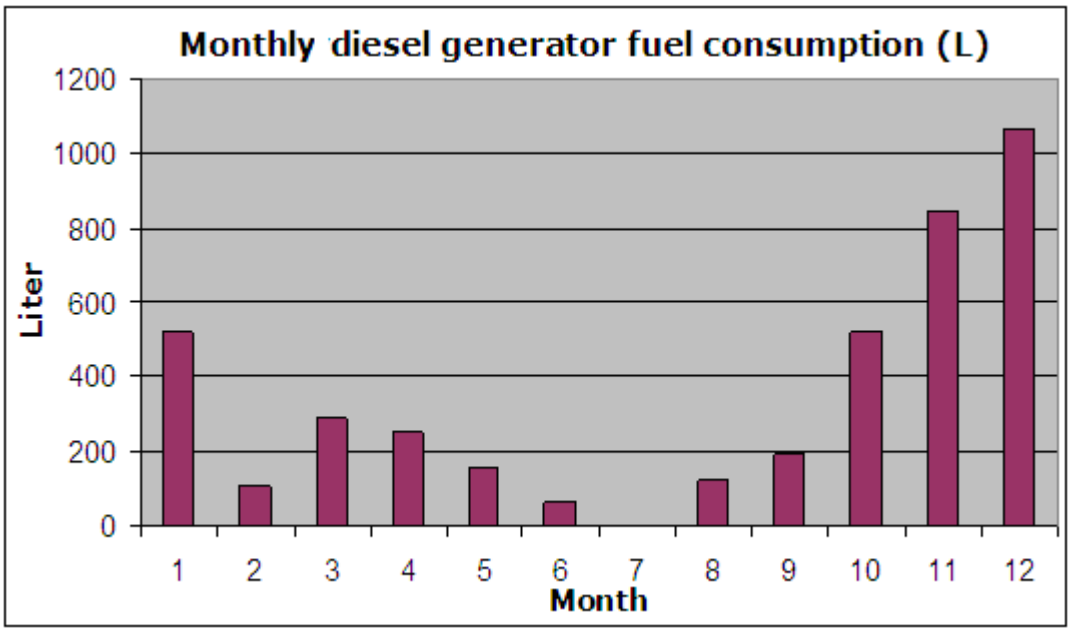

Figure (8.10): Monthly fuel consumption of the diesel generator for Ramallah site.

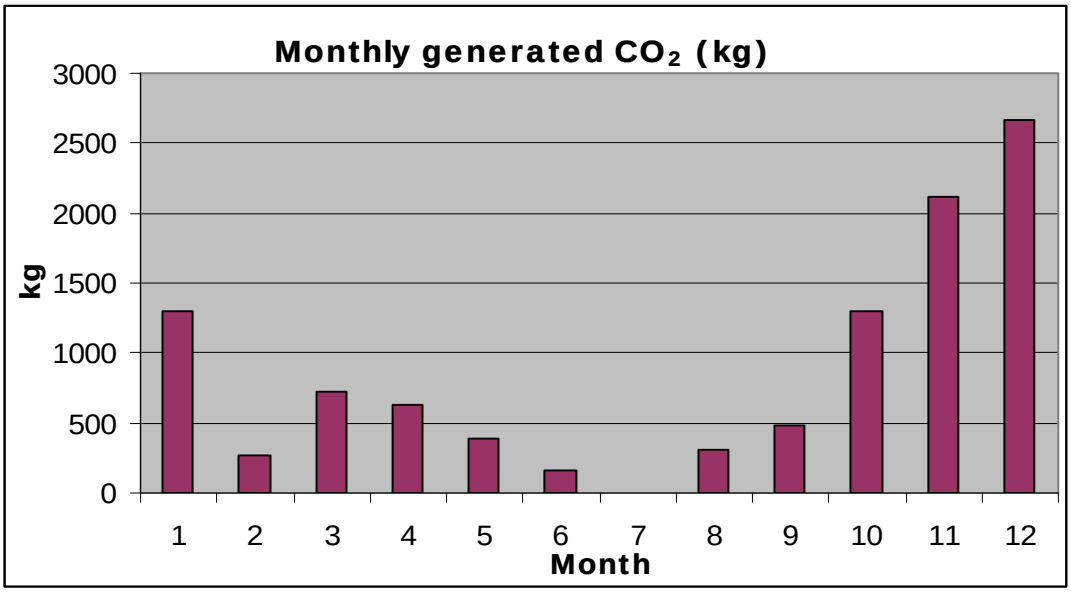

Figure (8.11): Monthly CO_2 produced by the diesel generator for Ramallah site.

For Ramallah site and 50% PV contribution,0.5 AD, figure 8.12 shows a pie graphical representation of the yearly energy contribution by wind, PV, and diesel, figure 8.13 shows a pie graphical representation of yearly load, dump, and losses energies in kWh, while figure 8.13 shows a pie graphical representation of these energies as percentages.

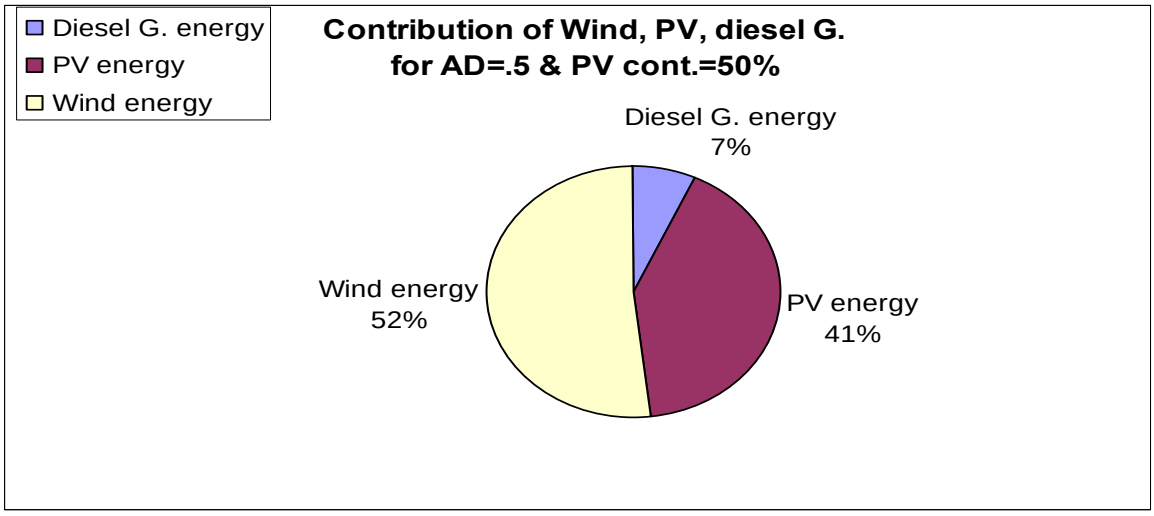

Figure (8.12): Yearly energy contribution of wind , PV, and diesel for Ramallah site.

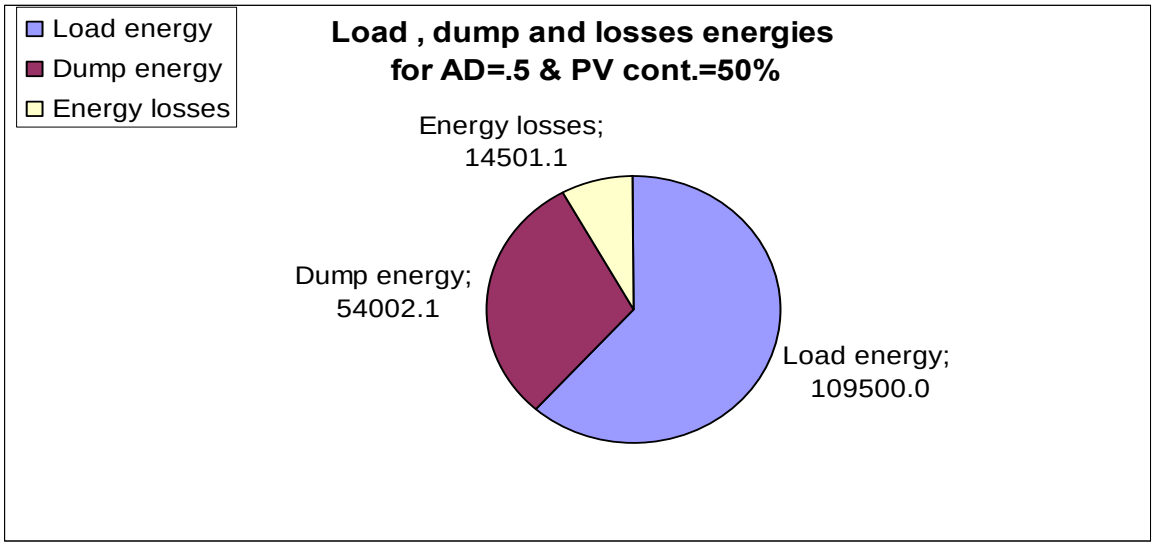

Figure(8.13): Yearly load, dump, and losses energies in kWh for Ramallah site.

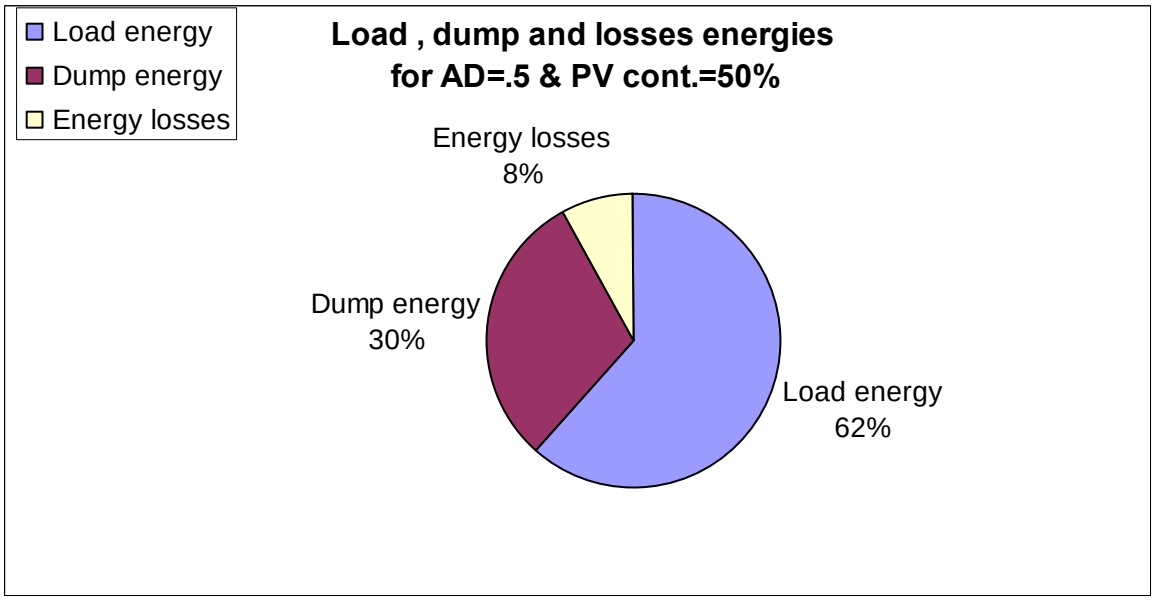

Figure(8.14): Yearly load, dump, and losses energies as percentages of total generated energy for Ramallah site.

For Ramallah site and 50% PV contribution,0.5 AD, Figure 8.15 shows graphical representation of the hourly SOC of the battery bank during a whole year, figure 8.16 shows a graphical representation of the hourly SOC during

July, while figure 8.17 shows a graphical representation of the hourly SOC during December. Figure 8.18 shows hourly dump energy during a year, figure 8.19 shows hourly dump energy during December, while figure 8.20 shows hourly dump energy during July.

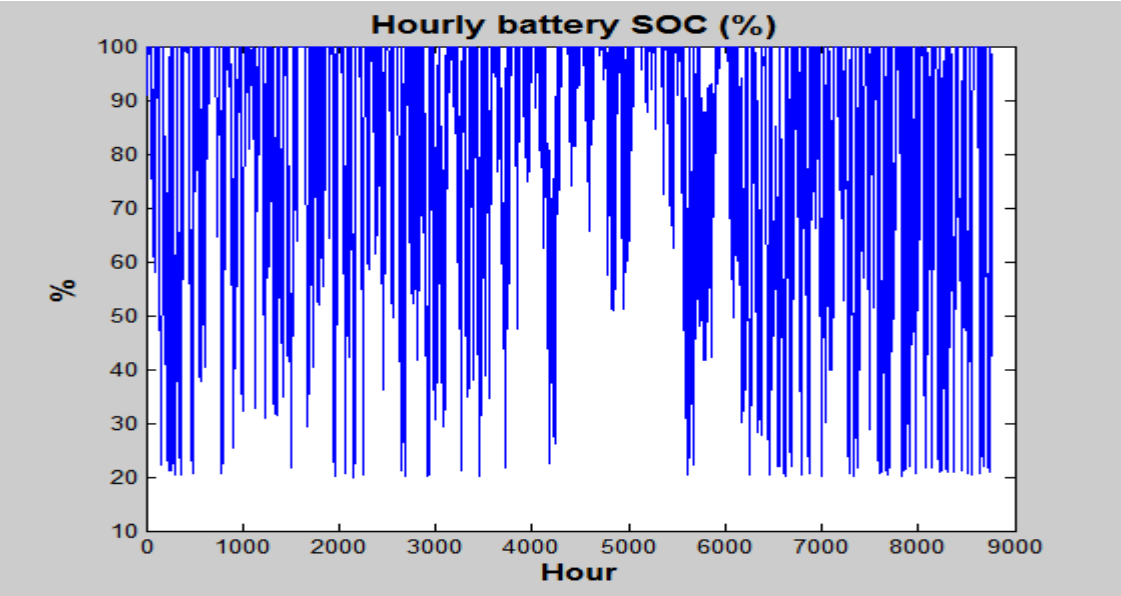

Figure (8.15) : Hourly battery SOC during a year for Ramallah site.

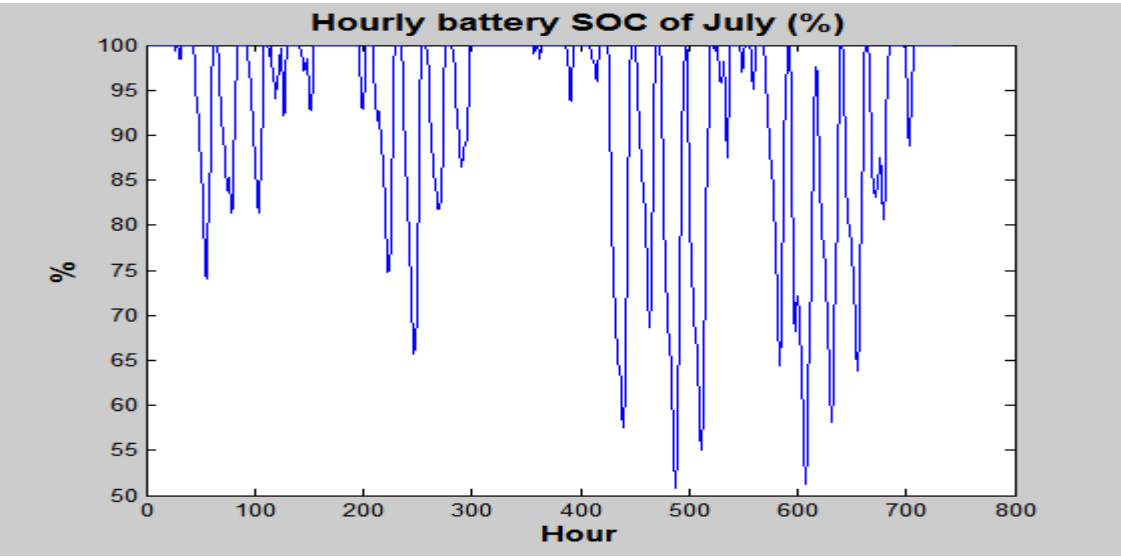

Figure (8.16): Hourly battery SOC through July for Ramallah site.

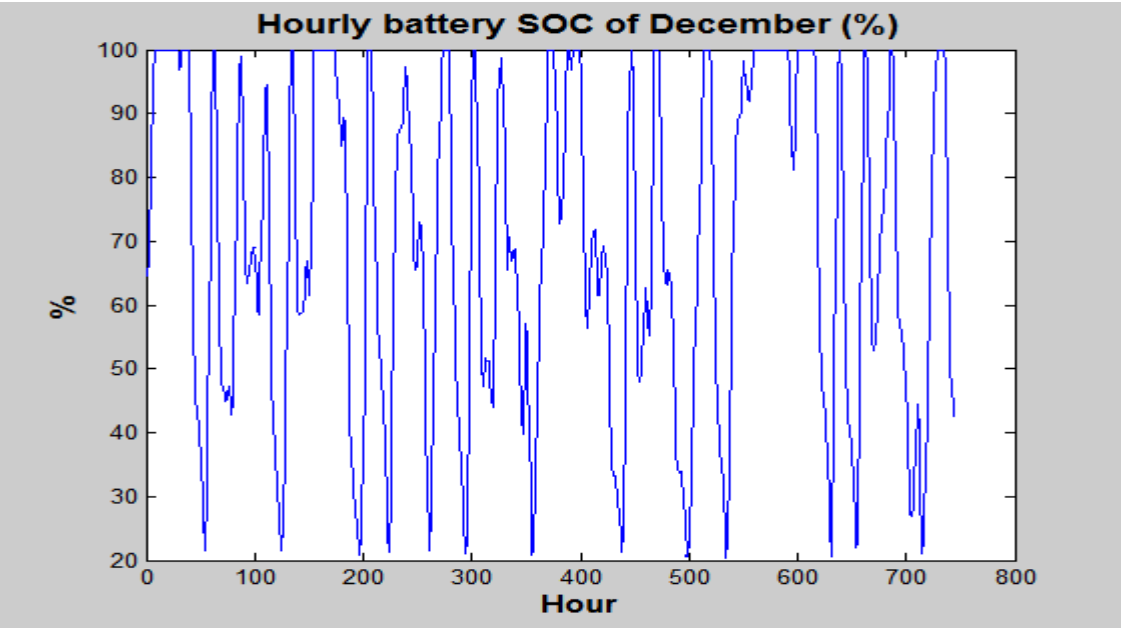

Figure (8.17): Hourly battery SOC through December for Ramallah site.

For December the SOC of the battery doesn't go below 20% of the battery capacity because it is specified that the DOD of the battery is 80% and this is the worst case, while for July it doesn't go below 50% of its capacity.

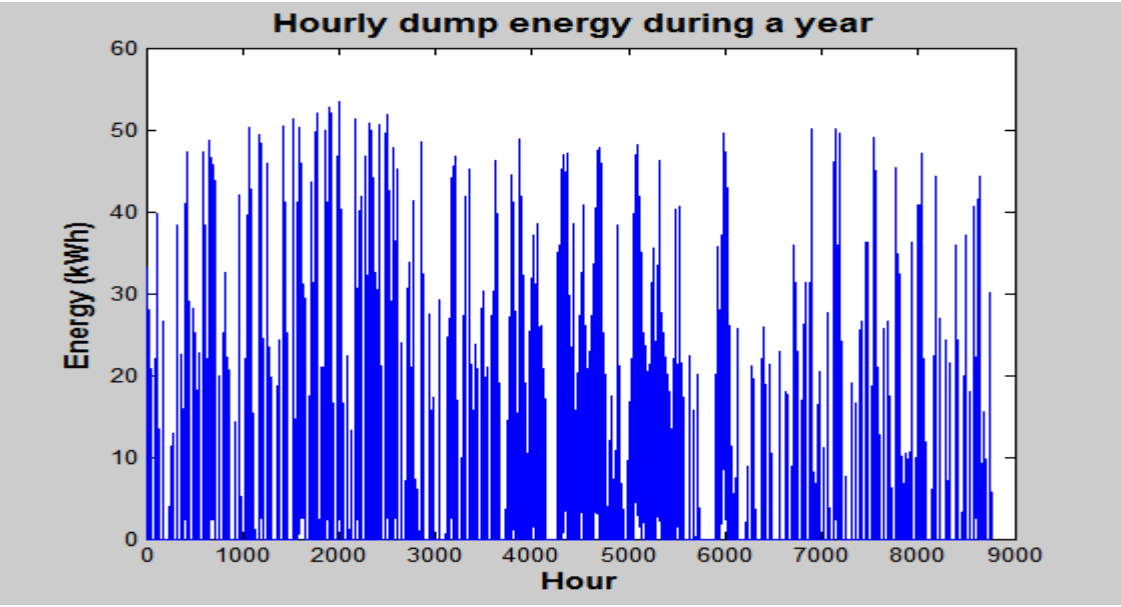

Figure(8.18): Hourly dump energy during a year for Ramallah site.

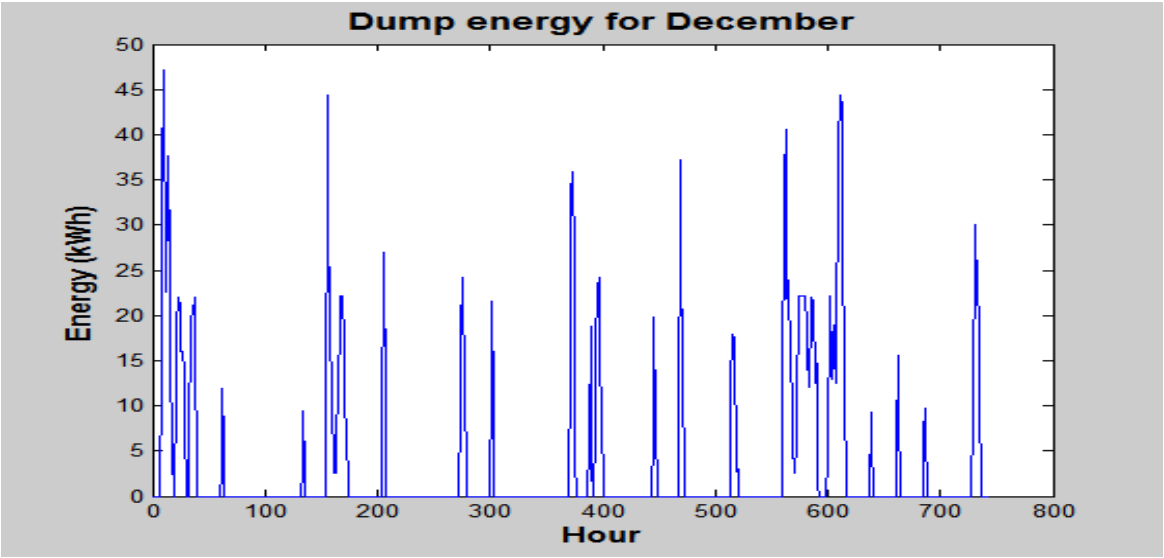

Figure(8.19): Hourly dump energy during December for Ramallah site.

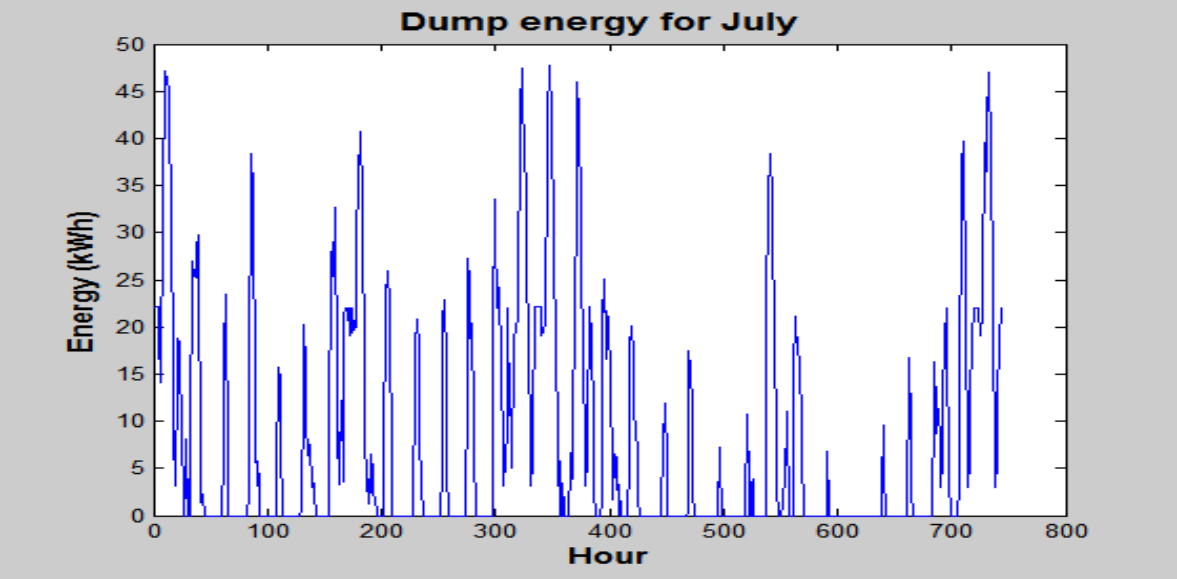

Figure(8.20): Dump energy during July for Ramallah site.

8.4 Hybrid System Cost Results

Table 8.14 summarizes different types of costs for different components constructing the hybrid system. Figure 8.21 shows a graphical representation of initial costs for these different components .

Table (8.14): Hybrid system costs.

Wind turbine initial cost(NIS)	315000
PV panel initial cost (NIS)	639620
Diesel generator initial cost (NIS)	42000
Battery bank initial cost (NIS)	234975
Bidirectional inverter cost(NIS)	87500
Charge controllers (wind&PV) (NIS)	87500
PV installation cost (NIS)	102340
Yearly wind turbine maintenance &operation cost (NIS)	6300
Yearly labor cost (NIS)	6300
Yearly diesel generator maintenance cost (NIS)	700
Total LCC (NIS)	2256180

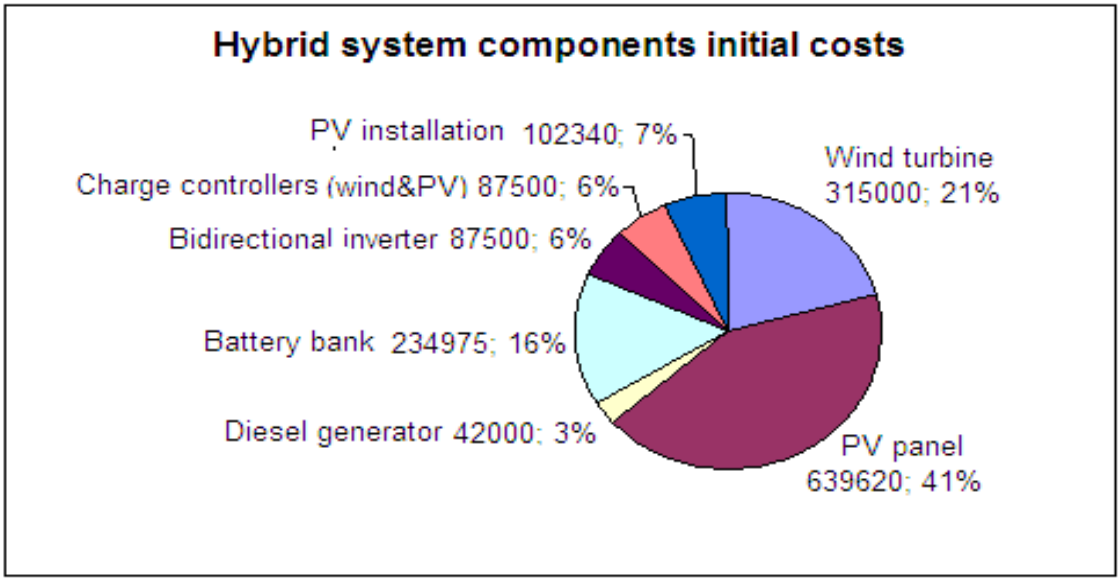

Figure (8.21): Hybrid system components initial costs for Ramallah site.

8.5 Sensitivity Analysis

The following cases are analyzed and the results are compared with the base case analyzed previously.

Case 1: Only wind, diesel, and battery hybrid system (i.e. no PV).

Table 8.15 presents the COE and LCC results for different values of AD for Ramallah site. The least COE is 1.57 NIS/kWh.

Table(8.15) : COE and LCC without PV contribution for Ramallah site .

AD	COE (NIS/kWh)	LCC (NIS)
0.1	1.5640	2754860
0.2	1.5741	2772604
0.3	**1.5694**	2764343
0.4	1.5935	2806700
0.5	1.6139	2842644
0.6	1.6305	2871901
0.7	1.6606	2924894
0.8	1.6868	2971072
0.9	1.7313	3049461
1.0	1.7710	3119467

Case 2 : Only PV, diesel, and battery hybrid system (i.e. no wind).

Table 8.16 presents the COE results for different values of PV contribution and AD for Ramallah site, while table (8.17) presents the LCC results. The least COE is 1.55 NIS/kWh. Comparing this value of COE with the value in case 1 , it is observed that using PV only is economically preferred on using wind only. But comparing these two cases with the base case where hybrid wind-PV system is analyzed , the base case is economically preferred.

Table (8.16): COE results without wind for Ramallah site (NIS/kWh).

AD	PV contribution (%)									
	10	20	30	40	50	60	70	80	90	100
0.1	2.4157	2.1871	2.0751	2.0721	2.0985	2.1323	2.1814	2.2326	2.2810	2.3422
0.2	2.5571	2.2612	2.0639	1.9202	1.9126	1.9515	2.0044	2.0622	2.1249	2.1898
0.3	2.4687	2.3314	2.1774	2.1567	2.1975	2.2416	2.2866	2.3356	2.3768	2.4312
0.4	2.6180	2.4230	2.2753	2.1886	2.1400	2.1067	2.0561	1.9978	1.9786	1.9965
0.5	2.6067	2.4056	2.2766	2.1155	2.0250	1.8833	1.6924	1.6325	1.6361	1.6576
0.6	2.6581	2.4558	2.2678	2.1543	2.0066	1.8425	1.6427	1.5642	**1.5502**	1.5838
0.7	2.6607	2.4988	2.3075	2.1605	2.0003	1.8128	1.6426	1.5686	1.5636	1.5959
0.8	2.6973	2.5141	2.3668	2.1556	2.0030	1.8354	1.6600	1.5943	1.5966	1.6228
0.9	2.7431	2.5378	2.3714	2.2047	2.0483	1.8717	1.7083	1.6269	1.6204	1.6606
1.0	2.7782	2.5991	2.4306	2.2567	2.0980	1.9245	1.7438	1.6702	1.6510	1.6982

Table (8.17): LCC results without wind for Ramallah site (NIS).

AD	PV contribution (%)									
	10	20	30	40	50	60	70	80	90	100
0.1	**4255011**	**3852305**	**3655088**	**3649818**	**3696261**	**3755803**	**3842256**	**3932519**	**4017644**	**4125519**
0.2	**4504085**	**3982769**	**3635355**	**3382134**	**3368787**	**3437422**	**3530504**	**3632313**	**3742703**	**3857010**
0.3	**4348316**	**4106487**	**3835286**	**3798805**	**3870603**	**3948285**	**4027675**	**4113856**	**4186481**	**4282248**
0.4	**4611260**	**4267867**	**4007740**	**3854958**	**3769301**	**3710683**	**3621523**	**3518892**	**3485052**	**3516674**
0.5	**4591367**	**4237144**	**4010022**	**3726266**	**3566839**	**3317221**	**2980986**	**2875412**	**2881800**	**2919718**
0.6	**4681944**	**4325688**	**3994473**	**3794511**	**3534352**	**3245401**	**2893513**	**2755092**	**2730550**	**2789616**
0.7	**4686592**	**4401318**	**4064409**	**3805454**	**3523264**	**3192979**	**2893292**	**2762978**	**2754093**	**2810934**
0.8	**4751078**	**4428360**	**4168889**	**3796909**	**3528117**	**3232794**	**2923841**	**2808272**	**2812285**	**2858320**
0.9	**4831653**	**4470032**	**4176951**	**3883292**	**3607908**	**3296809**	**3009007**	**2865537**	**2854234**	**2924936**
1.0	**4893519**	**4578049**	**4281170**	**3974913**	**3695426**	**3389707**	**3071511**	**2941827**	**2907994**	**2991267**

Case 3: Increase in fuel inflation rate to 7.5% rather than 5% and increase in discount rate to 12% rather than 8%.

Table 8.18 presents the values of COE for Ramallah site for different values of PV contribution and AD, taking into account the increase in fuel inflation and discount rate. As it is observed the value of COE increases for this case compared with the base case. It is 1.64 NIS/kWh.

Table (8.18) : COE results for fuel inflation rate = 7.5%, discount rate =12% for Ramallah site (NIS/kWh).

AD	PV contribution (%)									
	10	20	30	40	50	60	70	80	90	100
0.1	1.7905	1.7085	1.7349	1.7979	1.8770	1.9668	2.0616	2.1597	2.2611	2.3641
0.2	1.7809	1.6914	1.6805	1.7325	1.8116	1.9024	1.9957	2.0991	2.1971	2.3049
0.3	1.7890	1.7261	1.7005	1.7057	1.7525	1.8204	1.9082	2.0032	2.0976	2.1988
0.4	1.8226	1.7135	1.6634	1.6532	1.6647	1.6908	1.7587	1.8550	1.9587	2.0614
0.5	1.8157	1.7267	1.6791	**1.6414**	1.6473	1.6867	1.7411	1.8421	1.9377	2.0373
0.6	1.8454	1.7718	1.6914	1.6736	1.6579	1.6939	1.7574	1.8572	1.9565	2.0556
0.7	1.9150	1.7944	1.7355	1.6847	1.6631	1.7104	1.7892	1.8875	1.9881	2.0946
0.8	1.9520	1.8063	1.7614	1.6908	1.7156	1.7469	1.8265	1.9242	2.0271	2.1313
0.9	1.9713	1.8576	1.7606	1.7293	1.7469	1.7785	1.8692	1.9713	2.0759	2.1833
1.0	1.9775	1.8861	1.7958	1.7491	1.7701	1.8311	1.9099	2.0153	2.1227	2.2240
Diesel running hours @ (AD=.5 , PV con.=40%) =731 hr										

Case 4: Decrease in PV initial cost to a value 2.5 \$/W_p rather than 5\$/W_p .

Table 8.19 presents the values of COE for Ramallah site for different values of PV contribution and AD, taking into account the decrease in price of PV watt peak. As it is observed the value of COE decreases for this case compared with the base case. It is 1.08 NIS/kWh.

Table (8.19) : COE results considering decrease in price of PV watt peak (2.5 \$/W_p) for Ramallah site (NIS/kWh).

AD	PV contribution (%)									
	10	20	30	40	50	60	70	80	90	100
0.1	1.4164	1.2962	1.2700	1.2739	1.2910	1.3169	1.3470	1.3798	1.4153	1.4521
0.2	1.4045	1.2829	1.2259	1.2206	1.2377	1.2645	1.2933	1.3304	1.3585	1.3992
0.3	1.4121	1.3123	1.2431	1.1992	1.1850	1.1928	1.2170	1.2472	1.2769	1.3122
0.4	1.4405	1.3026	1.2132	1.1518	1.1131	1.0864	1.0942	1.1254	1.1629	1.1994
0.5	1.4356	1.3143	1.2268	1.1428	1.0993	1.0837	**1.0803**	1.1155	1.1462	1.1802
0.6	1.4608	1.3522	1.2330	1.1700	1.1088	1.0902	1.0944	1.1286	1.1624	1.1959
0.7	1.5190	1.3715	1.2701	1.1798	1.1137	1.1045	1.1213	1.1543	1.1891	1.2288
0.8	1.5502	1.3821	1.2922	1.1855	1.1577	1.1353	1.1528	1.1852	1.2220	1.2598
0.9	1.5669	1.4252	1.2921	1.2180	1.1842	1.1621	1.1887	1.2248	1.2629	1.3034
1.0	1.5728	1.4494	1.3218	1.2350	1.2040	1.2062	1.2230	1.2618	1.3022	1.3377

Case 5 : Increase in fuel cost to 2.25$/liter(50% increase) rather than 1.5 $/liter.

Table 8.20 presents the values of COE for Ramallah site for different values of PV contribution and AD, taking into account the increase in fuel cost. As it is observed the value of COE increases for this case compared with the base case. It is 1.37 NIS/kWh.

Table (8.20) : COE results considering increase in fuel cost to (2.25 $/liter) for Ramallah site (NIS/kWh).

AD	PV contribution (%)									
	10	20	30	40	50	60	70	80	90	100
0.1	1.8804	1.7201	1.6949	1.7140	1.7528	1.8046	1.8624	1.9243	1.9902	2.0581
0.2	1.8461	1.6795	1.6088	1.6146	1.6533	1.7064	1.7624	1.8308	1.8898	1.9634
0.3	1.8364	1.7023	1.6135	1.5623	1.5588	1.5836	1.6326	1.6905	1.7478	1.8133
0.4	1.8575	1.6671	1.5486	1.4754	1.4311	1.4047	1.4294	1.4889	1.5576	1.6249
0.5	1.8295	1.6636	1.5480	1.4409	1.3896	1.3796	1.3878	1.4531	1.5117	1.5754
0.6	1.8457	1.6987	1.5405	1.4602	1.3826	**1.3682**	1.3876	1.4515	1.5147	1.5776
0.7	1.9109	1.7065	1.5744	1.4537	1.3688	1.3683	1.4064	1.4684	1.5333	1.6053
0.8	1.9361	1.7013	1.5860	1.4411	1.4130	1.3930	1.4320	1.4932	1.5610	1.6301
0.9	1.9401	1.7441	1.5649	1.4681	1.4312	1.4116	1.4642	1.5309	1.6006	1.6738
1.0	1.9280	1.7590	1.5879	1.4723	1.4395	1.4559	1.4940	1.5646	1.6378	1.7035

Case 6 : Taking into account case 4 and case 5 at the same time.

Table 8.21 presents the values of COE for Ramallah site for different values of PV contribution and AD, taking into account the decrease in price of W_p and increase in fuel cost at the same time. As it is observed the value of COE decreases for this case compared with the base case. It is 1.13 NIS/kWh. Compared with case 4 and case 5, it is greater than case 4 but less than case 5.

Table (8.21) : COE results considering decrease in price of PV watt peak (2.5 \$/ W_p) and increase in fuel cost (2.25 \$/liter) for Ramallah site (NIS/kWh).

AD	PV contribution (%)									
	10	20	30	40	50	60	70	80	90	100
0.1	1.8441	1.6475	1.5859	1.5688	1.5712	1.5868	1.6082	1.6338	1.6634	1.6950
0.2	1.8097	1.6069	1.4999	1.4694	1.4717	1.4885	1.5082	1.5403	1.5630	1.6003
0.3	1.8001	1.6296	1.5046	1.4171	1.3772	1.3657	1.3784	1.4000	1.4210	1.4502
0.4	1.8212	1.5945	1.4397	1.3301	1.2495	1.1868	1.1753	1.1984	1.2308	1.2618
0.5	1.7931	1.5909	1.4391	1.2956	1.2081	1.1617	1.1336	1.1626	1.1849	1.2122
0.6	1.8094	1.6261	1.4316	1.3150	1.2011	1.1504	**1.1334**	1.1610	1.1879	1.2145
0.7	1.8746	1.6339	1.4654	1.3084	1.1873	1.1504	1.1522	1.1779	1.2065	1.2422
0.8	1.8997	1.6286	1.4771	1.2958	1.2314	1.1751	1.1778	1.2027	1.2341	1.2670
0.9	1.9038	1.6714	1.4559	1.3228	1.2496	1.1937	1.2100	1.2404	1.2737	1.3107
1.0	1.8916	1.6864	1.4789	1.3270	1.2580	1.2380	1.2398	1.2741	1.3110	1.3404

Case 7 : Decrease in diesel generator rating to be 15 kW rather than 24 kW.

Table 8.22 presents the values of COE for Ramallah site for different values of PV contribution and AD, but decreasing the diesel generator rating. As it is observed, the value of COE decreases for this case compared with the base case. It is 1.24 NIS/kWh. But for this case the state of charge of the battery goes below the 20% limit 6 times during a whole year as shown in figure 8.22. No problem occurs for this limited number of times goes below the DOD limit while decreasing the COE by .04 NIS compared with the base case.

Table(8.22): COE results considering decrease in diesel generator rating (15kW) for Ramallah site (NIS/kWh).

AD	PV contribution (%)									
	10	20	30	40	50	60	70	80	90	100
0.1	1.3677	1.3060	1.3143	1.3507	1.3999	1.4605	1.5239	1.5948	1.6676	1.7453
0.2	1.3617	1.3165	1.3171	1.3560	1.4106	1.4747	1.5398	1.6113	1.6819	1.7573
0.3	1.3744	1.3211	1.2971	1.2881	1.3170	1.3625	1.4177	1.4781	1.5450	1.6168
0.4	1.3871	1.3145	1.2626	1.2436	**1.2381**	1.2556	1.3061	1.3755	1.4471	1.5203
0.5	1.4134	1.3298	1.2823	1.2483	1.2383	1.2638	1.3056	1.3755	1.4459	1.5194
0.6	1.4492	1.3735	1.3060	1.2654	1.2536	1.2760	1.3276	1.3971	1.4681	1.5414
0.7	1.4730	1.3877	1.3299	1.2816	1.2745	1.3002	1.3568	1.4256	1.5000	1.5780
0.8	1.5132	1.4070	1.3600	1.3022	1.3115	1.3303	1.3926	1.4583	1.5347	1.6117
0.9	1.5361	1.4331	1.3780	1.3414	1.3381	1.3674	1.4305	1.4994	1.5747	1.6531
1.0	1.5279	1.4533	1.4008	1.3662	1.3663	1.4076	1.4678	1.5367	1.6152	1.6903

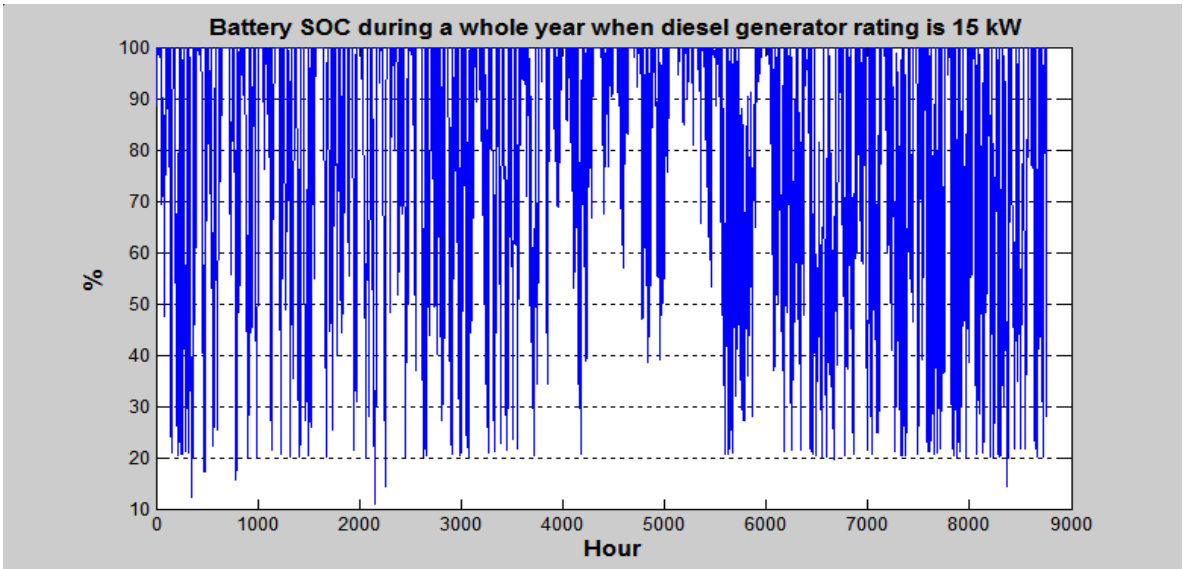

Figure (8.22): Hourly battery SOC during a year when diesel generator rating is 15 kW for Ramallah site.

Case 8: Diesel generator only (without renewable, without battery)

In this case two similar diesel generators each has 24 kW rated power are required to supply the load for the 24 hours each operates for 12 hours per

day. Table (8.23) summarizes different costs and operation data. It is observed that the COE increases for this case compared with the base case and all other previous cases.

Table(8.23): Only operation diesel generator data.

Number of diesel generators	2
Rated power for each (kW)	24
Yearly fuel consumption for the two generators (liter)	34393
Replacement period for each (year)	5
Initial cost for each (NIS)	42000
Daily operating hours for each (hour)	12
Annual fuel cost for the two (NIS)	180563
Annual maintenance including labor cost (NIS)	18104
Total LCC (NIS)	3763100
COE (NIS/kWh)	2.14

Case 9 : PV stand alone system (i.e. without wind, without diesel).

Analyzing this case using the simulation program yields the following results:

- For PSH=5.4 hour , the least COE occurs at 150% PV contribution and 2.0 AD. The COE is 2.71 NIS/kWh and the LCC is 4780293 NIS.

- For PSH= 2.8 hour- the worst case for winter season-, the PV standalone system shall be designed to deal with case. For this case the least COE occurs at 100% PV contribution and 3.0 AD. The COE is 3.09 NIS/kWh and the LCC is 5442983 NIS.

Case 10 : Wind stand alone system (i.e. without PV, without diesel). Analyzing this case yields the following results:

- For 30 kW wind turbine, it is found that the least COE occurs at 55.0 AD. The COE is 24.40 NIS/kWh and the LCC is 42969821 NIS. This case is not practicable.

- For 45 kW wind turbine, it is found that the least COE occurs at 6.0 AD. The COE is 3.13 NIS/kWh and the LCC is 5507366 NIS. This case is a practicable one if it is the only choice.

Case 11 : Changing the tilt angle of the PV array.

Table 8.24 presents different values for the tilt angle of the PV array and the corresponding COE. As it is observed the effect is so small compared with the base case where the tilt angle is 30 degrees. The least COE occurs at 25 degree tilt angle. It is 1.275 NIS/kWh.

Table(8.24) : Effect of tilt angle change on the COE for ramallah site.

Tilt angle (β) (degree)	Cost of energy production (NIS/kWh)
20	1.282
22	1.279
24	1.277
25	**1.275**
26	1.280
28	1.282
30	1.281
32	1.278
34	1.275
36	1.278
38	1.278
40	1.278
42	1.279
44	1.279
46	1.286

Case 12: Changing the height of the wind turbine.

Table 8.25 presents different values of the tower of the wind turbine and the corresponding COE and the yearly energy generated by the wind turbine. It is observed that as tower height increases the energy generated increases while COE decreases. The effect is obvious for this case.

Table (8.25) : Effect of height of wind tower on COE for Ramallah site.

Height of wind turbine tower (m)	Cost of energy production (NIS/kWh)	Yearly energy generated by wind turbine (kWh)
15	1.383	72366
20	1.346	78585
25	1.322	83536
30	1.304	87614
35	1.285	91073
37	1.281	92331
40	1.271	94097
45	1.260	96783

Case13: Choosing different wind turbines from different manufacturers at the same rated power but with different specifications concerning cut- in speed, rated speed, and height.

Table 8.26 presents different wind turbine specifications but at the same rated power and the corresponding COE and the yearly generated energy by the wind turbine. The effect can obviously be observed. Comparing the turbine with 3.5 m/s cut-in speed , 12 m/s rated speed, and 35 m tower height with the turbine chosen for the base case with 2 m/s cut-in speed, 9.5 m/s rated speed, and 37 m tower height. While the height of the two turbines are approximately equal, the increase in the COE can't be neglected. This increase is about 0.265 NIS/kWh.

This emphasizes on the importance of choosing the wind turbine with the suitable specifications that appropriate the wind speed variations in the site to install this turbine.

Table(8.26): Effect of changed characteristics of different wind turbine on COE for Ramallah site.

Cut-in & rated speed of wind turbine(resp.) (m/s)	Cost of energy production (NIS/kWh)	Yearly energy generated by wind turbine (kWh)
2.0 , 9.5 @ 37 m height	1.281	92331
3.0 , 12.0@ 32 m height	1.539	53982
3.5 , 12.0@ 35 m height	1.546	54227
2.5 , 12.0@ 27 m height	1.549	52058
4.0 , 13.0@ 25 m height	1.687	38564
2.0 , 15.0@ 62 m height	1.623	41654

8.6 Comparison between Simulation Results & Wind Data Analysis Results

Results of wind data analysis performed in chapter 3 in this thesis illustrate that the energy available in the wind for Ramallah site is 2008 kWh/m^2 –year, while it is 927 kWh/m^2 –year for Nablus site. For the 30 kW, 15 m rotor diameter wind turbine that selected for the analysis, the energy available in the wind for this wind turbine for Ramallah site is 354663 kWh/year while it is 163731 kWh/year for Nablus site.

For Ramallah site but using the wind power curve of the wind turbine and as a result of simulation, the wind energy generated by this wind turbine is 92331 kWh/year while it is 51904 kWh/year for Nablus site.

To compare results, the following cases can be considered: The first is considered if the coefficient of performance (COP) of the wind turbine- that relates the output energy of the wind turbine to the energy available in wind-

is known from the manufacturer, for this case and if the energy available in wind is known by wind data analysis, the output of the wind turbine can be found by simply multiplying this energy by the COP. The second case is considered if the COP in not known but the values of energies (output energy and the available energy in wind) are known -as in this case study-, the COP of the wind turbine can be calculated. The third case is considered if the COP is known and both the output energy and the available energy in wind are known, for this case a comparison can be done.

If no hourly wind speed data are available, only yearly average wind speed is known then equation (3.7) can be used to calculate an approximate estimate of annual energy generated by a wind turbine. For Ramallah site where annual average wind speed is 5. 52 m/s and using equation (3.7), annual wind energy production is 95065 kWh, while for Nablus site where the annual average wind speed is 4.35 m/s , the annual wind energy production is 46523 kWh. The values obtained using this equation are not far from the values obtained using the simulation program or the values obtained using the Weibull distribution analysis.

8.7 Design Considerations of the Hybrid System

As stated in table 8.13, rated power of wind turbine is 30 kW, rated power of the PV generator is 36.6 kW, rated capacity of the diesel generator is 24 kW, and the rated capacity of the battery bank is 240 kWh.

A 220 V DC is recommended for the DC bus voltage where the battery bank is connected. So the output of charge controllers shall be rated at this level of voltage and the bidirectional inverter shall also be rated at this level of voltage.

110*2 V cell lead acid batteries shall be connected in series to obtain this level of DC voltage at the DC bus. At 25 ^{o}C, this cell has a charging open circuit voltage equals to 2.4 V, so the maximum open circuit voltage for the bank is 264 V. The output of the charge controllers and the DC voltage of the bidirectional converter shall be chosen to deal with this voltage. The Ampere-hour capacity (C_{Ah}) of the battery block, necessary to cover the load demand for a period of 0.5 AD is C_{Ah}= 240*1000/220 = 1090 Ah. The battery cells shall be selected with this Ah rating.

A 2 V lead acid battery of capacity of 648 Ah – the nearest capacity that found after searching products of battery manufacturers - can be used instead. In this case a two parallel strings, each has 110 cell batteries connected in series each cell has 2V * 648 Ah.

Mono-crystalline or poly-crystalline PV modules can be used to supply the load. If poly-crystalline PV modules of 54 W peak power are selected, the number of the necessary PV modules is obtained as N_{PV} = 36.6*1000/ 54 = 678 PV modules.

Each 16 modules will be connected in series to build 43 parallel strings. The open circuit voltage for this PV array at standard conditions is V_{oc} = 21.7*16 = 347.2 V, while the voltage at the maximum power point of this

array is 17.4*16=278.4 V. The input of PV charge controller shall sustain this level of input voltage.

The input/output ratings of the PV charge controller are determined by the output of the PV array and the battery nominal voltage. The rated power of the PV charge controller is 37 kW. In this power range it is recommended that the charge controller should have a maximum power control unit[1] .

The wind turbine has a 30 kW rated power, 3ph-400V , 50 Hz output voltage, it has 2 blades, its rotor is 15 m , and has a 37 m tower height. It uses a permanent magnet synchronous generator.

The wind charge controller comes after a rectifier circuit that rectifies the 3-phase variable AC voltage output from the wind turbine. The rated power of rectifier circuit is 30 kW. The rectifier circuit can be selected to have a 220 V DC rated voltage at its output. For this case a wind charge controller is selected with a voltage ratings similar to the PV charge controller except that the rated power of it is 30 kW. Some companies manufacture a special wind charge controller to satisfy the two goals (rectify & charge control) in the same product.

The bidirectional inverter side voltages have to be matched with the battery bank voltage (220 V DC) and the 3-phase, 3*380V, 50Hz output voltage from the diesel generator. The rated power of the bidirectional inverter is selected at 30 kW rating.

Detailed specifications for bidirectional inverter, PV module, battery cell, wind turbine and diesel generator, are included in the appendices.

CHAPTER NINE

CONCLUSIONS AND RECOMMENDATIONS

Chapter 9

Conclusions and Recommendations

Conclusions

Based on the simulation program results previously presented, the following conclusions can be demonstrated:

- AS a result of analyzing wind, PV, diesel with a storage battery bank hybrid system to supply a load, a combination of them with wind as a main source, 50% PV contribution, 0.5 battery autonomy days, with limited operation of diesel generator (521 hour/year) forms the optimum case with a COE equals to 1.28 NIS/kWh.

- For wind-only hybrid system, the COE is 1.57 NIS/kWh and occurs at 0.3 battery bank AD.

- For PV-only hybrid system, the COE is 1.55 NIS/kWh and occurs at 90% PV contribution and 0.6 battery bank AD. So using PV-only hybrid system is more economical than using wind-only hybrid system but the difference is so small. The most economical scenario is using wind-PV hybrid system as stated before.

- Using wind as a stand alone system to supply load is not economical or practical choice because of low availability of wind during different times in a year (months from September to December have low average wind speeds). Higher rating is required for the wind turbine required to supply a load with a certain power, also higher

battery capacity (higher autonomy days) are required to supply the this load. For Ramallah site a 45 kW wind turbine with a 6 AD batteries required to supply the load that has a maximum power equals to 24 kW. The COE is also high, it is 3.13 NIS/kWh.

- Using PV as a stand alone system to supply the load isn't also economical or practical one. Different times through a year have low solar insolation especially during winter months (Months December, January, and February). High capacity battery bank is required to meet the load demand (higher autonomy days). For Ramallah site a 3 AD battery bank is required. The COE is also high, it is 3.09 NIS/kWh.

- Using diesel generator only to supply the load requires two units to supply this load, each works for 12 hours daily. More fuel, so more CO_2 is produced, also more maintenance and operational costs is needed. The COE is high, it is 2.14 NIS/kWh. Amount of CO_2 produced is about 86 ton/year, it is too high compared with the hybrid system where amount of CO_2 produced is 10.3 Ton/year.

- High quantities of dump energy (about 54000 kWh/year) generated due to operation of the hybrid system is due to the fact that the size of the components constructing the hybrid system shall be to meet the worst cases during the year, so during the months of high level availability of wind and solar radiation, excess (dump) energy will be produced. It can be managed to use this dump energy to supply

auxiliary loads such as streets lighting, water pumping, heating, and refrigeration. This will benefit the performance of the hybrid system.

Recommendations

The following recommendations are drawn out of this research, some of them are directed to the researchers while the others are directed to decision makers.

- Similar wind analysis can be conducted for other sites in Palestine that have strong wind speeds (as Hebron) .

- An implementation for this hybrid system as a pilot system in Palestine can be done if a subsidy is available for this project, this will make it possible for more research , study and analysis.

- As far as the environmental aspects are concerned, this kind of hybrid systems have to be wide spread in order to cover the energy demands, and in that way to help reduce the green house gases and the pollution of the environment. This is an important point to be taken into consideration.

- In addition to all these, there is another aspect of effective use of this system in the residential sector. A hybrid system like the one analyzed, can be used very effectively and efficiently as well, in rural areas, where the connection from the grid is not possible. In this case an installation of a system like this, in these kind of areas usually is an economically and cost saving viable idea.

References

References

[1] Mahmoud M.M. , Ibrik H.I. . **Techno-economic feasibility of energy supply of remote villages in Palestine by PV- systems, diesel generators and electric grid.** Renewable & Sustainable Energy Reviews. 10(2006) 128-138.

[2] Energy Research Center (ERC) , **Meteorological measurements in West Bank / Nablus & Ramallah**. An-Najah National University.

[3] B. Ai, H. Yang, H. Shen, X. Liao . **Computer-aided design of PV / wind hybrid system**. Renewable Energy 28 (2003) 1491–1512.

[4] **Wind energy: our wind farms**. Available at: http://www.Stable windenergy.net/windenergy/wind_enrgy20.html [access date 3 December 2007]

[5] Boyle G., 2004 , **Renewable Energy**, OXFORD university press.

[6] **Wind and Hydro Power Technologies Program.** Available at : http:// www . eere .energy.gov/windandhydro/wind_how.html [access date 3 December 2007]

[7] **Basic Wind Turbine Configurations**. Available at: http:// www.awea. org/ faq/ basiccf.html [access date 7 December 2007]

[8] Marwan Mahmoud. **Lecture notes**: **Renewable Energy Technology 1 &2** . An-Najah National University. 2006-2007.

[9] Roger A. Messenger, Jerry Ventre, 2004, **Photovoltaic Systems Engineering**, 2nd edition, CRC press.

[10] Marwan Mahmoud, Ismail Nabhan. **Determination of optimum tilt angle of single and multi rows of photovoltaic arrays for selected sites in Jordan**. Solar & Wind technology Vol.7 , No. 6 , pp. 739-745,1990 .

[11] Iakovos Tzanakis. **Combining Wind and Solar Energy to Meet Demands in the Built Environment** (thesis report). Energy Systems Research Unit. University of Strathclyde. 2005-2006 .

[12] **Research and markets Brochure**. Available at: http:// www .research andmarkets.com/reports/328418/ [access date 4 February 2008]

[13] **Technical Status of Thin Film Solar Cells**. Available at : http:// www . udel.edu/iec/status.html [access date 10 February]

[14] **Solar cell-Wikipedia, the free encyclopedia**. Available at : http:// en.wikipedia.org/wiki/Solar_cell [access date 10 February]

[15] **EV World Blogs: Personal Perspectives on the Future In Motion**. Available at http://www.evworld.com/blogs/index.cfm?page= blogentry &blogid=497&authorid=183&archive=0 [access date 10 April 2008]

[16] **PV payback** .Available at :http://www.gosolarnow.com/pdf%20files / pvpaybackHP.pdf [access date10 April 2008]

[17] **Energy Payback: Clean Energy from PV**. Available at :http:// www.nrel.gov /docs/fy99osti/24619.pdf [access date 12 April 2008]

[18] **Environmental Impact of Photovoltaic. Electrification in Rural Areas**. Available at : http:// www.tiedekirjasto.helsinki.fi:8080 /bitstream /1975/295/1 [Access date 12 April 2008]

[19] **A Decision Support Technique for the Design of Hybrid Solar Power**. Available at : http:// www.ceage.vt.edu /2DOC /IEEE_ cov1998 _v13_no1 _76-83.pdf [access date 20 April 2008]

[20] Mahmoud M.M. **On the Storage Batteries Used in Solar Electric Power Systems and Development of an Algorithm for Determining their Ampere-Hour Capacity**. Electric Power Systems Research 2004. 71(85-89)

[21] Panichar P.S., Islam S.M. and PryorT.L. **Effect of Load Management and Optimal Sizing on the Economics of a Wind-Diesel Hybrid power System.** Murdoch University Energy Institute. Available at: http:/ www.itee.uq.edu.au/~aupec/aupec99/paper_index.html.

[22] Omar M.A. **Computer-Aided Design and Performance Evaluation of PV-Diesel Hybrid System.** Thesis report at An-Najah University.2007.

[23] **EnergyAtlasFinal2006.pdf Coastal zone management**. Available at : http ://www.akenergyauthority.org/Reports%20and%20Presentations /Analysis %20of%20Loads%20and%20Wind-Disel%20Option [access date 22 April 2008]

[24] **Optimization of Hybrid Energy Systems. Sizing and Operation control**. Available at : http:// www.upress.uni-kassel. de/ online/inhalt / 978-3-933146-19-9.[access date 4 may 2008]

APPENDICES

Appendix 1 **Bidirectional inverter technical specifications**

Appendix 2 **Solar PV module technical specifications**

Appendix 3 **Battery cell technical specifications**

Appendix 4 **Wind turbine technical specifications**

Appendix 5 **Diesel generator technical specifications**

Appendix 1 : Bidirectional inverter technical specifications

LEONICS®
ADVANCED POWER TECHNOLOGY

APOLLO MTP-410

THREE PHASE BIDIRECTIONAL DUAL MODE INVERTER FOR MINI-GRID SYSTEM

- Three phase configuration
- Low harmonic distortion (less than 4%)
- High efficiency more than 94%
- Capable to use with multiple renewable energy sources in both DC coupling and AC coupling such as solar panel, wind turbine generator and micro hydro generator
- Seperate DC Bus for multiple source charging
- Monitor energy available from the renewable energy (DC) sources and minimize the charging current from the diesel generator.
- Automatic battery equalization (14 days or 30 days) to prevent battery capacity loss and prolong battery life.
- Preset time schedule by System Command Unit (SCU) for automatic controlling the auxiliary power sources such as generators in mini-grid system (option)
- Battery temperature compensation (option)
- Dual control, bi-directional inverter operate in two modes; VCVSI –Voltage Control Voltage Source Inverter and CCVSI – Current Control Voltage Source Inverter.
- Automatic / Manual generator control
- DC external charge control

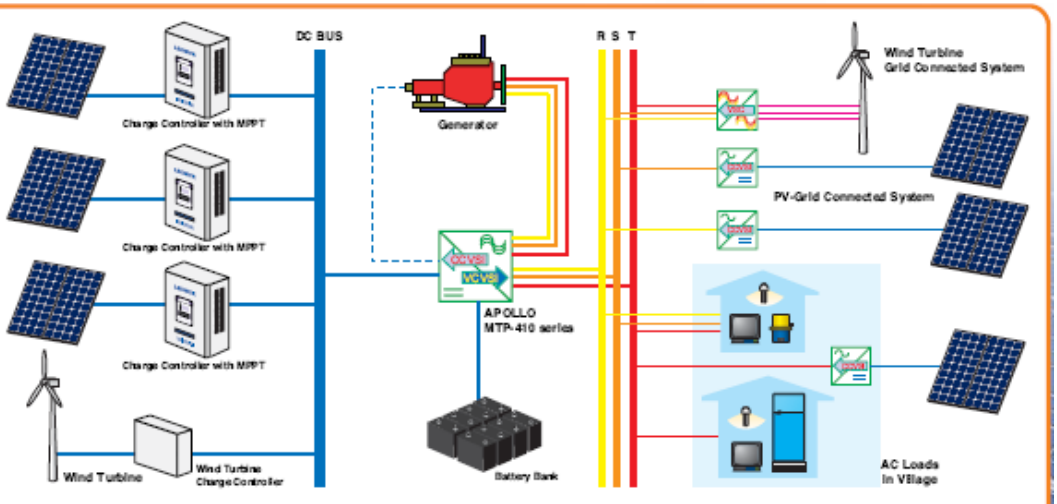

The APOLLO MTP-410 Series is a three phase bidirectional dual mode inverter capable of functioning as a main supply source as well as providing automatic control and management of a generator and a battery bank. The inverter features very high efficiency in both charging and inverting modes with maximum efficiency of 94% for 120 kW model.

MINI-GRID SYSTEM WITH MTP-410 SERIES

Appendix 1 : Bidirectional inverter technical specifications (cont…)

LEONICS

APOLLO MTP-410 series

THREE PHASE BIDIRECTIONAL DUAL-MODE INVERTER FOR MINI-GRID SYSTEM

SPECIFICATIONS

MODEL		MTP-412E	MTP-413E	MTP-414F	MTP-415F	MTP-416F	MTP-417G	MTP-418G	MTP-419G	MTP-4110G
RATED POWER		15 kW	24 kW	30 kW	45 kW	60 kW	75 kW	90 kW	100 kW	120 kW
DC INPUT	Nominal voltage	120 Vdc			240 Vdc		360 Vdc			
	Maximum current	100 A	200 A	100 A	200 A	200 A	200 A	250 A	250 A	300 A
DC OUTPUT	Battery Voltage	120 Vdc			240 Vdc		360 Vdc			
	Maximum charging current	84 A	130 A	84 A	125 A	168 A	140 A	168 A	186 A	220 A
DC CHARGE CONTROL		Relay dry contact 10 A (for over external charge protection)								
AC INPUT FROM GENERATOR	Recommended generator power rating	> 30 kW	> 50 kW	> 60 kW	> 90 kW	> 120 kW	> 150 kW	> 180 kW	> 200 kW	> 240 kW
	Voltage	380 / 415 Vac (L-L), 220 / 240 Vac (L-N) ± 10%								
	Phase	Three phase								
	Frequency	50 / 60 Hz ± 3%								
	Automatic start/stop	Relay dry contact 10 A (ACC on and start pluse)								
AC OUTPUT	Voltage	380 / 415 Vac (L-L), 220 / 240 Vac (L-N)								
	Voltage regulation	± 1% (steady load), < 4% at 100% step load within 0.1 sec.								
	Phase	Three phase								
	Frequency	50 / 60 Hz ± 0.1% (auto sensing)								
	Wave form	Pure sine wave								
	Total harmonic distortion	total < 4%, each < 3 %								
	Current limiting	110 %								
	Maximum surge current	200%								
ISOLATION	Galvanic isolation	yes								
EFFICIENCY	Inverter peak efficiency	94%								
PROTECTION		Over current, Over load, Short circuit, Over temperature, Over voltage, Under voltage								
INDICATOR	LED	Generator Running, Generator Failure, Stand by/Run, Inverter, Charging, Load on Inverter, Overload, Low Battery, High temperature, Fault								
	LCD display	Inverter voltage, Inverter current, Inverter frequency, Generator voltage, Generator current, Generator frequency, Battery voltage, Battery current, Battery temperature, Load voltage, Load current, Heat sink temperature								
AUDIABLE ALARM		Low battery, Inverter fault, High temperature								
COOLING		Fan								
ENVIRONMENT	Temperature	0 - 45°C								
	Relative humidity	0 - 95 % (Non - condensing)								
DESIGN STANDARD		AS/NZ 3100:2002								
DIMENSION	W x H x D (approx. in cm.)	53.4 x 123 x 60	70 x 165 x 100			110 x 180 x 90		120 x 80 x 100		
WEIGHT	Approximate in kg.	218	250	380	470	745	850	945	1,000	1,250

Appendix 2 Solar PV module technical specifications

THE NEW VALUE FRONTIER

KYOCERA

KC50T

HIGH EFFICIENCY MULTICRYSTAL
PHOTOVOLTAIC MODULE

UL LISTED

HIGHLIGHTS OF KYOCERA PHOTOVOLTAIC MODULES

Kyocera's advanced cell processing technology and automated production facilities produce a highly efficient multicrystal photovoltaic modules.
The conversion efficiency of the Kyocera solar cell is over 16%.
These cells are encapsulated between a tempered glass cover and a pottant with back sheet to provide efficient protection from the severest environmental conditions.
The entire laminate is installed in an anodized aluminum frame to provide structural strength and ease of installation.

APPLICATIONS

- Microwave / Radio repeater stations
- Electrification of villages in remote areas
- Medical facilities in rural areas
- Power source for summer vacation homes
- Emergency communication systems
- Water quality and environmental data monitoring systems
- Navigation lighthouses, and ocean buoys
- Pumping systems for irrigation, rural water supplies and livestock watering
- Aviation obstruction lights
- Cathodic protection systems
- Desalination systems
- Recreational vehicles
- Railroad signals
- Sailboat charging systems
- etc.

QUALIFICATIONS

- **MODULE** : UL 1703 certified
  Hazardous Locations Class I, Div 2, Groups A, B, C and D
- **FACTORY** : ISO9001 and ISO 14001

QUALITY ASSURANCE

Kyocera multicrystal photovoltaic modules have passed the following tests.

- Thermal cycling test
- Thermal shock test
- Thermal / Freezing and high humidity cycling test
- Electrical isolation test
- Hail impact test
- Mechanical, wind and twist loading test
- Salt mist test
- Light and water-exposure test
- Field exposure test

LIMITED WARRANTY

※1 year limited warranty on material and workmanship
※20 years limited warranty on power output: For detail, please refer to "category IV" in Warranty issued by Kyocera

(Long term output warranty shall warrant if PV Module(s) exhibits power output of less than 90% of the original minimum rated power specified at the time of sale within 10 years and less than 80% within 20 years after the date of sale to the Customer. The power output values shall be those measured under Kyocera's standard measurement conditions. Regarding the warranty conditions in detail, please refer to Warranty issued by Kyocera)

Appendix 2 Solar PV module technical specifications (cont…)

MODEL KC50T

ELECTRICAL CHARACTERISTICS

Current-Voltage characteristics of Photovoltaic Module KC50T at various cell temperatures

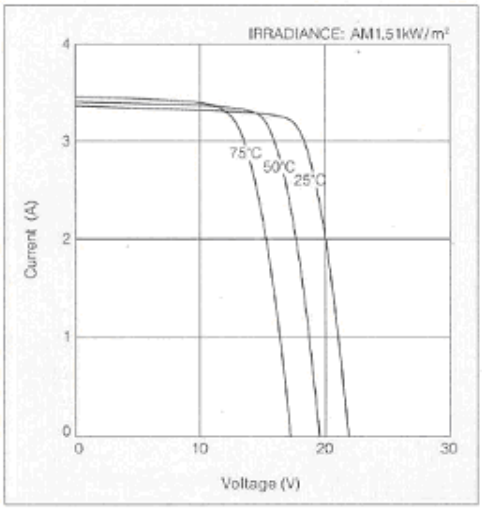

Current-Voltage characteristics of Photovoltaic Module KC50T at various irradiance levels

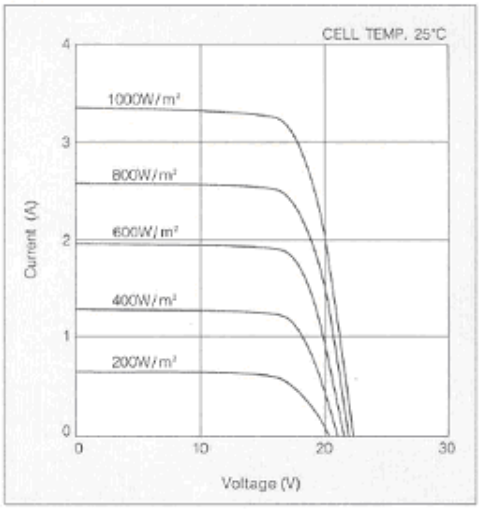

SPECIFICATIONS KC50T

Physical Specifications

Unit : mm (in.)

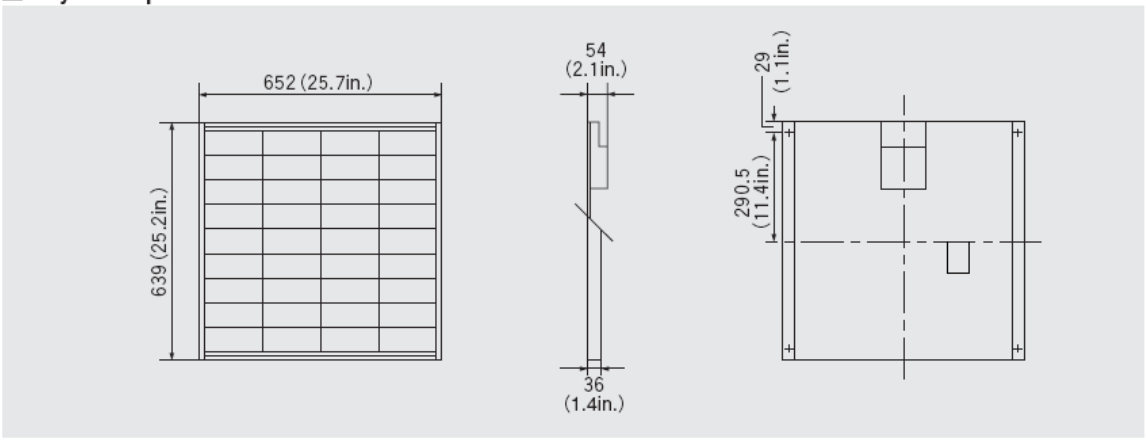

Specifications

Electrical Performance under Standard Test Conditions (*STC)	
Maximum Power (Pmax)	54W (+10%/−5%)
Maximum Power Voltage (Vmpp)	17.4V
Maximum Power Current (Impp)	3.11A
Open Circuit Voltage (Voc)	21.7V
Short Circuit Current (Isc)	3.31A
Max System Voltage	600V
Temperature Coefficient of Voc	-8.21×10^{-2} V/℃
Temperature Coefficient of Isc	1.33×10^{-3} A/℃

*STC : Irradiance 1000W/m², AM1.5 spectrum, module temperture 25℃

Electrical Performance at 800W/m², NOCT, AM1.5	
Maximum Power (Pmax)	38W
Maximum Power Voltage (Vmpp)	15.3V
Maximum Power Current (Impp)	2.49A
Open Circuit Voltage (Voc)	19.7V
Short Circuit Current (Isc)	2.67A

NOCT (Nominal Operating Cell Temperature) : 47℃

Cells	
Number per Module	36

Module Characteristics	
Length × Width × Depth	639mm(25.2in)×652mm(25.7in)×54mm(2.1in)
Weight	5.0kg(11.0lbs.)

Junction Box Characteristics	
Length × Width × Depth	120mm(4.7in)×160mm(7.1in)×46mm(1.8in)
IP Code	IP65

Reduction of Efficiency under Low Irradiance	
Reduction	6.2%

Reduction of efficiency from an irrandiance of 1000W/m² to 200W/m² (module temperature 25℃)

Appendix 2 Solar PV module technical specifications (cont…)

Please contact our office for further information

KYOCERA

KYOCERA Corporation

■ KYOCERA Corporation Headquarters
CORPORATE SOLAR ENERGY DIVISION
6 Takeda Tobadono-cho
Fushimi-ku, Kyoto
612-8501, Japan
TEL:(81)75-604-3476 FAX:(81)75-604-3475
http://www.kyocera.com

● KYOCERA Solar, Inc.
7812 East Acoma Drive
Scottsdale, AZ 85260, USA
TEL:(1)480-948-8003 or (800)223-9580 FAX:(1)480-483-6431
http://www.kyocerasolar.com

● KYOCERA Solar do Brasil Ltda.
Av. Guignard 661, Loja A
22790-200, Recreio dos Bandeirantes, Rio de Janeiro, Brazil
TEL:(55)21-2437-8525 FAX:(55)21-2437-2338
http://www.kyocerasolar.com.br

● KYOCERA Solar Pty Ltd.
Level 3, 6-10 Talavera Road, North Ryde
N.S.W. 2113, Australia
TEL:(61)2-9870-3948 FAX:(61)2-9888-9588
http://www.kyocerasolar.com.au/

● KYOCERA Fineceramics GmbH
Fritz-Mueller-Strasse 107, 73730 Esslingen, Germany
TEL:(49)711-93934-999 FAX:(49)711-93934-950
http://www.kyocerasolar.eu

● KYOCERA Asia Pacific Pte. Ltd.
298 Tiong Bahru Road, #13-03/05
Central Plaza, Singapore 168730
TEL:(65)6271-0500 FAX:(65)6271-0600

● KYOCERA Asia Pacific Ltd.
Room 801-802, Tower 1 South Seas Centre, 75 Mody Road,
Tsimshatsui East, Kowloon, Hong Kong
TEL:(852)2-7237183 FAX:(852)2-7244501

● KYOCERA Asia Pacific Ltd. Taipei Office
10 Fl., No.66, Nanking West Road, Taipei, Taiwan
TEL:(886)2-2555-3609 FAX:(886)2-2559-4131

● KYOCERA(Tianjin) Sales & Trading Corporation
19F, Tower C HeQiao Building 8A GuangHua Rd.,
Chao Yang District, Beijing 100026, China
TEL:(86)10-6583-2270 FAX:(86)10-6583-2250

Kyocera reserves the right to modify these specifications without notice

LIE/109F0709-SAGKM

Appendix 3 Battery cell technical specifications

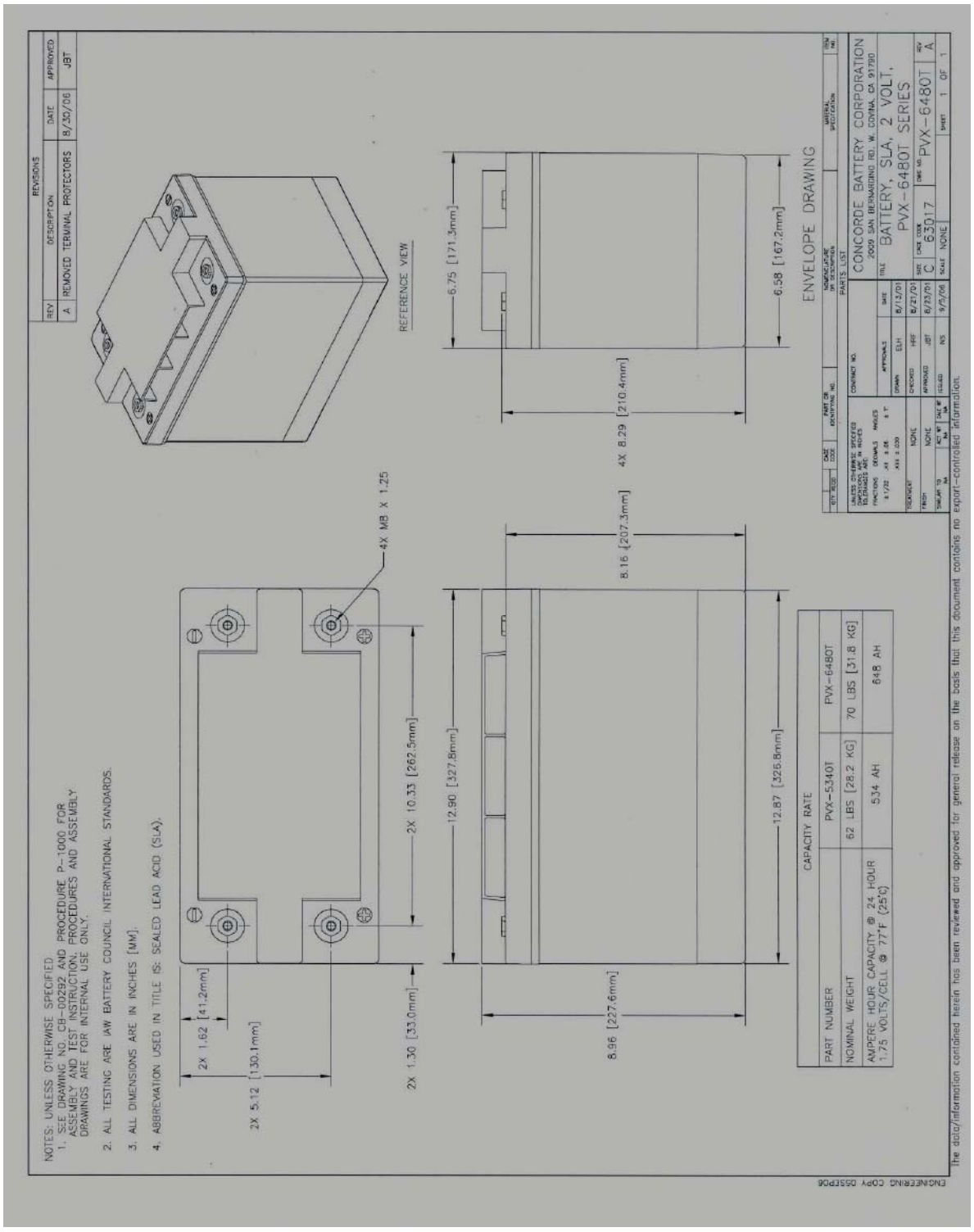

Appendix 3 Battery cell technical specifications (cont…)

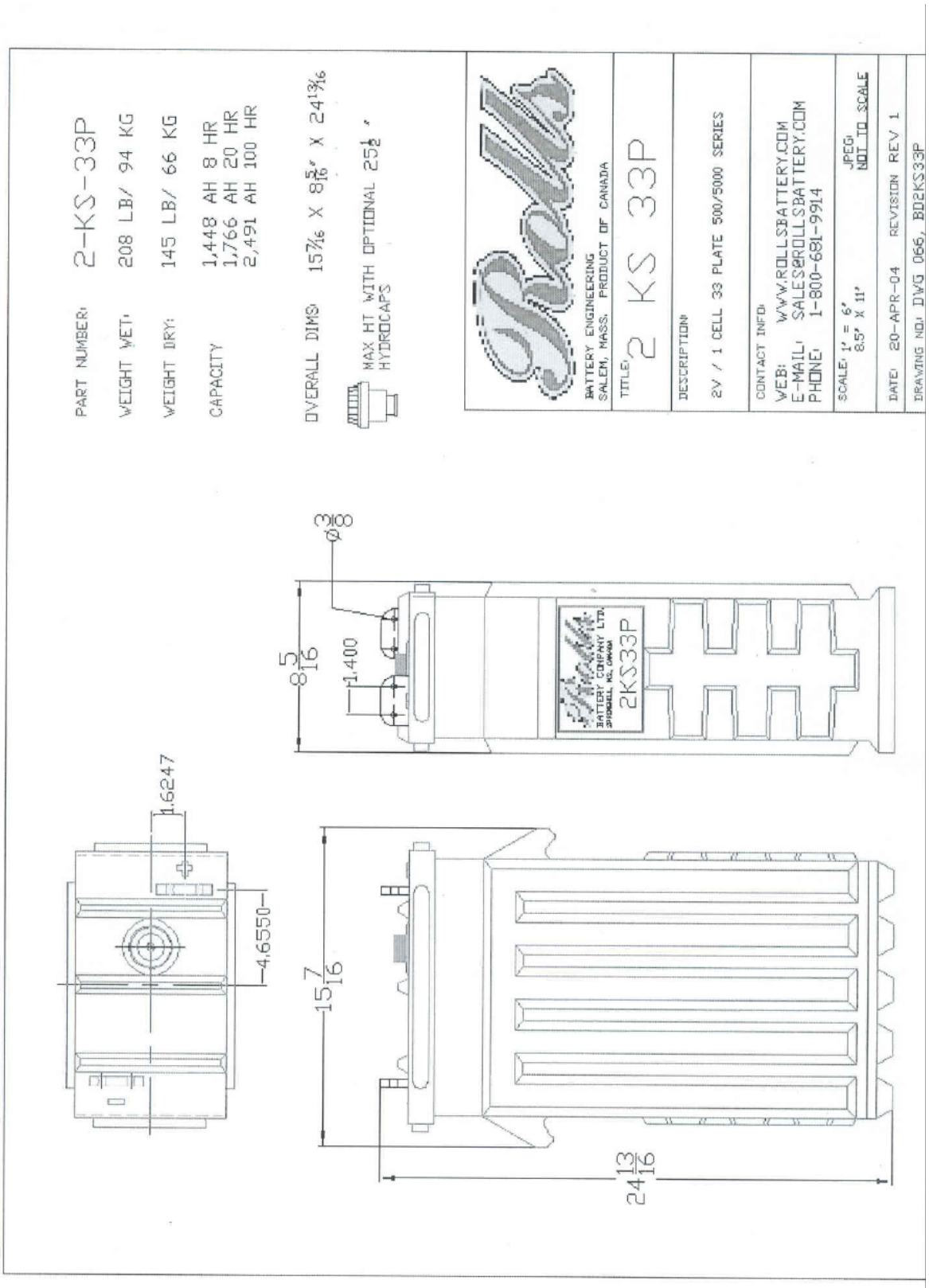

Appendix 3 Battery cell technical specifications (cont…)

Rolls

DEEP CYCLE-SOLAR

SERIES 5000

BATTERY TYPE VOLTS 2 — **2 KS 33PS**

DIMENSIONS

LENGTH	392	MM	15 4/9	INCHES
WIDTH	211	MM	8 1/3	INCHES
HEIGHT	630	MM	24 4/5	INCHES
WEIGHT DRY	66	KG	145	LBS.
WEIGHT WET	95	KG	208	LBS.

CONTAINER CONSTRUCTION

INNER CONTAINER	POLYPROPYLENE
INNER COVER	POLYPROPYLENE - HEAT SEALED TO INNER CONTAINER
OUTER CONTAINER	HIGH DENSITY POLYETHYLENE
OUTER COVER	HIGH DENSITY POLYETHYLENE SNAP FIT TO OUTER CONTAINER
HANDLES	MOLDED

PLATES PER CELL 33

ELECTROLYTE RESERVE ABOVE PLATES 76 MM 3 INCHES

DESIGN CRITREA 10 YEAR WARRANTY 3300 CYCLES 15 YEAR LIFE

POSITIVE PLATE DIMENSION

HEIGHT	432	MM	17.0	INCHES
WIDTH	143	MM	5.625	INCHES
THICKNESS	6.99	MM	0.275	INCHES

NEGATIVE PLATE DIMENSION

HEIGHT	432	MM	17.0	INCHES
WIDTH	143	MM	5.625	INCHES
THICKNESS	4.57	MM	0.180	INCHES

SEPARATOR SEPARATOR THICKNESS 0.105 INCH

INSULATION POSITIVE PLATE DOUBLE WRAPPED WITH SLYVER 0.020 HEAVY GLASS MAT AND ENVELOPED WITH HEAVY DUTY SEPARATOR

TERMINALS FLAG WITH STAINLESS STEEL NUTS AND BOLTS

COLD CRANK CCA 0°F / -17.8°C 4952 — **RESERVE MINUTES AT 25A** 4915

MCA 32°F / 0°C 6190

CAPACITY 20 HR RATE 1766

		CAP / AH	CURRENT / AMPS
CAPACITY AT THE 100 HOUR RATE	1.265 SP. GR.	2349	23.49
CAPACITY AT THE 72 HOUR RATE	1.265 SP. GR.	2225	30.91
CAPACITY AT THE 50 HOUR RATE	1.265 SP. GR.	2102	42.03
CAPACITY AT THE 24 HOUR RATE	1.265 SP. GR.	1819	75.8
CAPACITY AT THE 20 HOUR RATE	**1.265 SP. GR.**	**1766**	**88.3**
CAPACITY AT THE 15 HOUR RATE	1.265 SP. GR.	1660	110.7
CAPACITY AT THE 12 HOUR RATE	1.265 SP. GR.	1572	131.0
CAPACITY AT THE 10 HOUR RATE	1.265 SP. GR.	1501	150.1
CAPACITY AT THE 8 HOUR RATE	1.265 SP. GR.	1413	176.6
CAPACITY AT THE 6 HOUR RATE	1.265 SP. GR.	1307	217.8
CAPACITY AT THE 5 HOUR RATE	1.265 SP. GR.	1236	247
CAPACITY AT THE 4 HOUR RATE	1.265 SP. GR.	1148	287
CAPACITY AT THE 3 HOUR RATE	1.265 SP. GR.	1042	347
CAPACITY AT THE 2 HOUR RATE	1.265 SP. GR.	901	450
CAPACITY AT THE 1 HOUR RATE	1.265 SP. GR.	636	636

Rev. 0 April - 04 RDSPECS 94

Appendix 4 Wind turbine technical specifications

PitchWind Systems AB
(Sweden)

PO Box 89,
SE-443 22 Lerum

www.pitchwind.se
Tel: +46 (0)302 519 10
Fax: +46 (0)302 519 11
E-mail: info@pitchwind.se

Model	P 14-30
Rated Output (W)	30 000
Generator Type	PMG
Controller Type	PitchWind Hybrid Control System
Overspeed Protection	Self regulating passive pitch to feather
# of Blades	2
Rotor Diameter (m)	14
Swept Area (m^2)	154
Tower Type	Hot-dip galvanised welded lattice with guy wires
Tower Height (m)	20 to 40
Additional Info	PitchWind Systems AB specializes in providing Industrial Wind Hybrid Power Systems for average power loads ranging from 10 kVA and upwards for autonomous and unattended operation in off-grid applications. This system can consist of one or several Wind Turbines, one or several Diesel GenSets, Battery Banks and Chargers of varying capacities. These components are all interconnected via the pivotal PitchWind Hybrid Control System that automatically controlls Gen Set operation and Battery Managment allowing the diesel generators to be completely shut off when the wind power exceeds the load power demand. The turbine rotor design concept allows for an oversizing of the swept area of the rotor relative to the rated power, resulting in excellent wind capture capabilities particularly in moderate winds.

Appendix 4 Wind turbine technical specifications (cont…)

Wind speed Threshold

This PITCHWIND speed-control solution is unique and allows for convenient integration in weak grids and wind-diesel systems. A two-bladed turbine is also more cost-efficient than the familiar three-bladed turbine (except on very small wind turbines).This allows for survival in wind speeds up to 75 meters per second or 270 km/hour.

PITCHWIND is a variable-speed turbine, extracting more energy as the wind speed increases. When the rated wind speed of 9.5 meters per second is reached, the blade pitches to hold the speed constant up to a wind speed of 30 meters per second. From 30 to 40 meters per second, the blades speed drops, with the blade coming to a halt at 40 meters per second.

The blade is coupled directly to the permanent magnet ring generator eliminating the need for a gearbox, effectively reducing noise, maintenance and cost. The variable AC/DC/AC inversion system controls the electrical output and is available as 240 volt 50 cycle or 400 volt 3 phase supply. The IGBT inverter can also draw from batteries connected directly to the DC rail.

Installation

Installation and erection of the PITCHWIND is relatively inexpensive. The tubular tower and turbine are assembled on the ground. The whole structure is assembled as a complete unit, and is then ready for commissioning. The process can be completed using a relatively small crane.

Foundation Requirements

Because of the size of the turbine, foundation engineering and soil type requirements are relatively modest. Foundations for soil and sand locations require excavation. Setting of concrete footings is completed with an easily assembled base structure.

Rock locations are also suitable for tower sites. These require circular drilling and blasting, and concrete requirements are minimal.

Lattice Tower for Remote Locations

The lattice tower is cheaper to purchase and install than the tubular tower and is often used in remote locations. The lattice tower does not need a mobile crane. All that is needed is a large tractor to position a climbing crane. This device raises itself up by its own bootstraps and is used to build the tower. The crane is assembled on location and lifted into position. The lattice tower components and the climbing crane fit into the same shipping container as the PITCHWIND turbine.

Appendix 4 Wind turbine technical specifications (cont…)

Site Suitability

The PITCHWIND turbine is suitable for remote resorts and communities, islands, cattle stations, working properties and developing countries for water pumping and electricity generation. The unit can run in tandem with a diesel generator which it can control. It can be with or without batteries and can accept solar input. As well, it can be connected to a grid situation. This inherent flexibility and economy of the PITCHWIND turbine makes it suitable for a wide range of applications

Direct-driven generator .

The generator is direct-driven and permanently magnetized, eliminating the need for a clutch and transmission and thus improving the unit's efficiency rating. The generator features a three-point mounting so it does not affect the machine bed in the event of temperature fluctuations.

Generator maintenance is minimal-virtually non-existent- which is naturally a major benefit. The absence of clutch and transmission frees plenty of space in the nacelle for service operations.

The machine bed consists of a fully-welded, torsionally rigid box-section construction which stretches forwards from the tower towards the wind direction . This construction reduces the load on both the tower and the turbine blades, not least because the blades are routed far ahead of the tower to avoid "impacts" caused by the cushion of air which is always found in front of the tower.

In the machine bed's front end-panel, the generator is installed with three cylindrical studs in such way that the generator's thermal expansion does not apply a load on the machine bed with any resulting constriction forces. The nacelle has two fold-down side-hatches which, when opened, extend the machine bed's floor surface during service operations. This device has been patented

Appendix 4 Wind turbine technical specifications (cont…)

The Turbine

Type:	2-blade, flap-suspended in the hub.
Control:	Passive pitch (outer blade section).
Max rotating speed:	75 vpm at 8<1/oo <30 m/s.
Rotor diameter	15 m
Turbine tilt angle	6°
Turbine weight	500 kg

The turbine is 2-bladed, self adjusting (regulated by the laws of nature) and has a rotor diameter of 15 m. The turbine blades features an articulated attachment at the hub (flap control). The blades pitch function offers increased energy extraction. Variable speed means that the turbine operates at peak efficiency at any given wind speed, providing an energy supplement at even low rotational speeds (in other words at low wind speeds).

Owing to this feature, the turbine is extremely quiet in operation. The turbine is patented. Pitch Wind's patented 2-blade turbine together with the direct-driven generator and frequency converter operate in the O - 75 vpm range in such a way that the stated output at each speed corresponds to the turbine's performance at its highest efficiency rating.

This method produces higher energy output and lower noise emissions than the more conventional constant-speed system. At wind speeds between 9.5 and 30 m/s, the turbine's rotational speed is 75 vpm and the rated power is 30 kW.

Rotational speed is limited to 75 vpm in this area by means of the pitch of the outer half of the blade adjusting to the appropriate angle for every increment in wind speed, thus keeping the rotational speed at a constant level.

Appendix 4 Wind turbine technical specifications (cont…)

The Blades	
Inner blade section:	Blade profile of self-supporting steel plate with flap bearing at the root end.
Blade profile,inner section:	Root end, NACA 4424 switching to Pitch 11 Wind Mod. at the coupling with the pitch-regulated section.
Blade profile, pitch blade:	Mod II switching to KTH F1 53. The turbine blade has a built-in lightning protector.
Main shaft:	Shared with the generator. The pitch rod for vane activation is located in the shaft. At vane activation in excess of 90°, a mechanical drum brake in the generator is activated.
Generator:	Direct-drive, permanent-magnetised. Synchronous 66-magnetic poles 3-phase. Make: Pitch Wind, 3-point attachment to the machine bed.
Rated output:	30 kW at 75 vpm. Efficiency rating: 0.92 sinus.
Rotating speed :	O to 75 vpm
Weight:	610 kg

The pitch angle is determined by the outer half of the blade which generates a degree of torsional moment in the airflow owing to its profile. At wind speeds above the rated 9.5 m/s, this torsional moment begins to overcome the torsional spring which is fitted in the blade.

As wind speed increases, the blade increases its pitch accordingly and more air is simply "drained off', with the turbine dumping the excessive air. At wind speeds in excess of 30 m/s the pitch moment increases so much that the turbine's drive torque drops and thus also its speed.

At 40 m/s, the turbine and blades come to a standstill.

The operation of the turbine is thus regulated by the laws of nature, without necessitating any manual interference. However, the turbine can be stopped manually by using the manual winch at the base of the tower to pitch the blades to 90ê via the connecting wire. If the pitch is increased somewhat over this limit, an extremely powerful mechanical brake is activated.

The turbine blades are individually suspended in their own flap-regulation shaft joint, so that the turbine blades can move freely back and forth to permit flap activation while in operation, whereupon the wind-imposed load on the turbine blades is balanced by centrifugal force. With this design, the peak blade-root moment which is found on conventional turbines is reduced to zero, so the all-too-common turbine breakdowns which afflict conventional turbine systems are avoided.

Yet another advantage from the viewpoint of load avoidance is the so-called "flap-pitch feedback", whereby a flap movement on one blade owing to a gust of wind causes the blade to pitch out of the way to avoid major load application. This has been achieved by placing the pitch axle's crankshaft outside the flap shaft. Owing not least to the efficient flap joints, the turbine offers excellent aerodynamic damping.

Appendix 5 Diesel generator technical specifications

GeneratorJoe: 30 kW 60 Hz or 25 kW 50 Hz

- Admiral™ Series, 30 kW (38 kVA) 60 Hz, or 25 kW (31.7 kVA) 50 Hz.
- SKU GJAD-030D325, Model 30 AD3,
- (Open, No Enclosure) or sound enclosed
- Isuzu 4JGI,
- Three phase,
- Diesel fueled,
- Liquid cooled,
- 1800 rpm or 1500 rpm ,
- Electric start

جامعة النجاح الوطنية
كلية الدراسات العليا

محاكاة نظام قدرة مهجن مكون من مولد طاقة رياح,خلايا شمسية,بطارية تخزين ومولد ديزل مع شبكة تعويض:تصميم,تحقيق النظام الأمثل و تقييم اقتصادي

إعداد
محمود صلاح إسماعيل عبد القادر

إشراف
أ.د. مروان محمود

قدمت هذه الأطروحة استكمالا لمتطلبات نيل درجة الماجستير في هندسة الطاقة النظيفة وإستراتيجية الترشيد بكلية الدراسات العليا في جامعة النجاح الوطنية, نابلس – فلسطين.
2008

محاكاة نظام قدرة مهجن مكون من مولد طاقة رياح,خلايا شمسية,بطارية تخزين و مولد ديزل مع شبكة تعويض:تصميم,تحقيق النظام الأمثل و تقييم اقتصادي

إعداد

محمود صلاح إسماعيل

إشراف

أ.د. مروان محمود

الملخص

أنظمة القدرة المهجنة التي تعتمد على الطاقة المتجددة, خاصة الطاقة الشمسية و طاقة الرياح, هي خيار فاعل لحل مشاكل تزويد الطاقة للمناطق المعزولة و البعيدة عن شبكات التغذية.

حزمة برمجيات (ميكروسوفت اكسل) استخدمت لتحليل البيانات المقاسة لكل من سرعة الرياح و شدة الإشعاع الشمسي لمنطقتين في فلسطين (رام الله و نابلس). نتائج تحليل البيانات أظهرت أن كثافة الطاقة المتوفرة في الرياح لموقع رام الله تساوي 2008 كيلووات ساعة/م^2 /سنة بينما تساوي 927 كيلووات ساعة/م^2 /سنة لموقع نابلس و المعدل اليومي لشدة الإشعاع الشمسي على سطح أفقي تساوي 5.4 كيلووات ساعة/م^2 /يوم.

استخدمت حزمة برمجيات (مات لاب) لتصميم برنامج محاكاة لمحاكاة سيناريوهات مختلفة لتشغيل نظام القدرة المهجن و ذلك بعمل حسابات توازن طاقة لكل ساعة من 8760 ساعة خلال عام كامل, و من ثم لاختيار السعات المناسبة للأجزاء المختلفة المكونة للسيناريو الذي يحقق اقل تكلفة حيث أن المعيار المستخدم للمقارنة هو تكلفة إنتاج الطاقة.

نتائج برنامج المحاكاة بين أن أفضل سيناريو اقتصاديا هو السيناريو الذي يستخدم نظام مهجن يعتمد بشكل أساسي على طاقة الرياح . تكلفة إنتاج الطاقة في هذا السيناريو تساوي 1.28 شيكل/كيلو وات ساعة. سيناريوهات أخرى تعتمد على الرياح لوحدها في النظام المهجن أو على الخلايا الشمسية لوحدها في النظام المهجن أو على الرياح كمصدر طاقة مستقل أو على الخلايا

الشمسية كمصدر طاقة مستقل أو على مولد الديزل لوحده أظهرت قيم أعلى لتكلفة إنتاج الطاقة. كمية غاز CO_2 المتولد نتيجة تشغيل النظام المهجن تعتبر قليلة جدا بالمقارنة مع كميـــة الغـــاز المتولدة نتيجة تشغيل مولد الديزل لوحده لتغذية الحمل. يعتبر ذلك من القضايا البيئية المهمة جدا التي لا يمكن اهمالها.

لقد تم الاستنتاج انه لم يحقق في هذه الآونة أي من الأنظمة المهجنة التي تم تحليلها سعر لإنتاج الطاقة اقل من سعر الطاقة التي يتم شراؤها من الشبكات المغذية حيث أن ســـعر الطاقـــة يساوي 0.7 شيكل/كيلو وات ساعة. باعتبار المناطق التي ينوى تغذيتها مناطق معزولة و بعيدة عن الشبكات أو تغيرات قد تطرأ على سعر الكهرباء أو توفر مساعدات و منح أو تغيرفي أسعار تجهيزات أنظمة الطاقة المتجددة,كذلك الأخذ بعين الاعتبار القضايا البيئية قـــد يغيـــر الوضـــع مستقبلا.